RESEDA

ASSIMILATION OF MULTISENSOR & MULTITEMPORAL REMOTE SENSING DATA TO MONITOR SOIL & VEGETATION FUNCTIONING

An EC research project
co-funded by the Environment and Climate Programme within the topic
'*Space Techniques Applied to Environmental Monitoring and Research – Methodological Research*'.

FINAL REPORT

F. BARET

June, 2000

Contract number **ENV4CT960326**

Foreword

The ReSeDA project was originally initiated by Daniel Vidal-Madjar within the Programme National de télédétection Spatiale in France. Because of the importance of the experiment and the large scope covered by its objectives, it was extended to the European level to organise a collaborative effort. The start of the ReSeDA project was somewhat difficult because of delays in final acceptation of the project by the Commission. We thank very much Alan Cross for the effort spent to speed up the process. We thank also very kindly Michel Schouppe from the European commission for his interest in the project, for his patience and for his positive comments made along the life time of the project.

After the Launch of the project, the experiment started and required intensive efforts of all the partners. The processing of the large data set collected took more time than expected and delayed the actual scientific processing by few months. It provides now a unique data base as well as improved models and concepts that have been presented at the final meeting during the ReSeDA special session that took place within the European Geophysical Society General Assembly in Nice. These investigations are already or will be soon published in refereed journals.

Besides the scientific results obtained, the ReSeDA project contributed significantly to organise both the French and the European scientific community concerned by application of remote sensing to the continental biosphere. Further, it initiated a momentum around remote sensing data assimilation that is still growing through a range of projects ranging from very local applications such as precision farming up to global applications linked with human impacts on climatic change.

This report is an attempt to present the main results obtained within the ReSeDA project, as well as the limitations associated. It provides recommendations for future investigations to carry on for setting the concepts, models, algorithms, methods and techniques up to a level allowing operational applications. It is organised as along nine chapters:

1. Highlights: the ReSeDA objective, approach and results are presented in a synthetic way,
2. Partners: the ReSeDA partners are briefly presented,
3. Rationale: the background is analysed in detail with due attention to applications to conclude on the required investigations,
4. Objectives and timeframe: The objectives of the ReSeDA project are clearly stated and decomposed into three work-packages,
5. Achievements. For each work-packages, the results are presented with enough details to understand the progress achieved within ReSeDA. Problems and limitations of the results are also discussed,
6. Evaluation-user component. The ReSeDA results are evaluated with emphasis on actual and potential applications for users,
7. Exploitation. The results are evaluated in terms of their exploitation both for the scientific and user communities. Perspectives for future studies are proposed,
8. List of deliverables and publications,
9. Conclusion. The conclusion reviewed the main achievements and provides clues for future investigations.

Additionally, a more detailed description of the studies and results gathered during the ReSeDA project are presented in annexe.

The reader who wants to get a rapid flavour of the project should read chapters 1 and 9.
The one who wants to evaluate the achievements will have to browse through all chapters.

Frédéric Baret
Happy PI of the ReSeDA project

PLAN

1. Highlights

Awareness by the governments and the population is increasing on Climatic changes at the global scale and environmental issues at the local to regional scales. In order to better understand the underlying mechanisms, and propose solutions to mitigate these effects mainly due to human activity, proper models have to be developed and exploited. They could then be used to predict the consequences on the environment at a range of scales under possible scenarios of human activity and practices. Such models are describing the processes occurring at the surface of our planet, with emphasis on the dynamics of the exchanges of mass (mainly carbon and water) and energy (heat, radiation, momentum) between the soil and the atmosphere. Obviously, the vegetation, at the interface between the soil and the atmosphere plays a major role in the regulation of these exchanges.

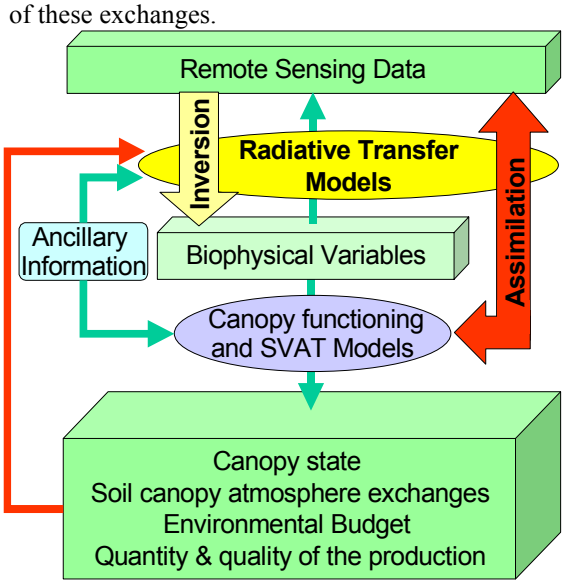

Figure 1. Flow chart diagram showing how to infer variables of interest such as canopy state, fluxes, environmental budget, production in quantity and quality from remote sensing data and ancillary information. The small green arrows indicate the direct way the models actually run.

Beside the above environmental issues, the estimation of crop production in quantity and quality is also very important, both at the local to regional scales for optimisation of the harvest process, and at the national, continental or global scales for food security issues and the regulation of the market of the main crop production. Here again, canopy functioning models, called in this context crop models, can be used to understand the main driving factors, and to get estimates and forecasts of the quantity, quality and timeliness of the production.
The soil and vegetation functioning, models, require a large set of parameters and variables to run. These parameters and variables may vary strongly with space and time, and only few of them are well known. Therefore, remote sensing techniques, with the ability to cover rapidly and frequently large areas, constitute a very promising tool that provides pertinent inputs and controls to the process models.
The main objective of the **ReSeDA** (**Re**mote **Se**nsing **D**ata **A**ssimilation) project is to develop and test remote sensing data interpretation methods for a better description and understanding of the soil and vegetation functioning through dedicated process models.
The signal recorded by remote sensing sensors aboard satellites is determined by canopy and soil characteristics, i.e. the biophysical variables, through physical processes of the interaction of electromagnetic radiation with vegetation and soil, i.e. the radiative transfer. Some of these biophysical variables can be used as inputs to the process models, i.e. soil vegetation atmosphere transfer models (SVAT) and canopy functioning models. (Figure 1).
Two main approaches could be used to exploit remote sensing data, depending on the degree of integration of interpretation scheme.

- The first one consists in deriving the canopy or soil biophysical variables from remote sensing data in an independent step. This step could exploit our knowledge on the physical processes put in the radiative transfer models. This corresponds to **radiative transfer model inversion**. It could also exploit few ancillary information, mainly the a priori knowledge of the distribution of canopy and soil variables. The biophysical variables estimated from remote sensing techniques could then be used as inputs to the process models to derive the variables of interest such as canopy state, fluxes, crop production, …).
- The second approach is the most integrated one and corresponds to the **assimilation of remote sensing data into radiative transfer and canopy or soil functioning coupled models**. It allows to explicitly account for the temporal dimension. It allows also to use concurrently and in synergy the data provided by different sensors. Further, it permits to directly access the variables of interest, while exploiting ancillary data such as climate and soil variables. Assimilation consists in tuning some parameters of the coupled radiative transfer and canopy functioning models so that the simulations matches the closest possible the radiometric measurements. This technique is potentially the most promising one because it uses the largest amount of information, both on the physical or biological processes and on ancillary data. We note (Figure 1) that canopy or soil functioning models could provide useful information on canopy or soil attributes that will increase the performances and the accuracy of radiative transfer model simulations.

Both approaches have already been investigated for other applications such as ocean or atmosphere problems. However it is relatively new for the continental biosphere. Therefore, the ReSeDA project will emphasise on the development and test of such approaches.

The ReSeDA project was decomposed into three main tasks:

1- The experiment and the corresponding data base
2- Estimation of canopy biophysical variables from radiative model inversion
3- Assimilation of remote sensing data into process models

1.1 The experiment over the Alpilles site.

A consistent and comprehensive data set has been acquired during a whole growth season over the Alpilles site located in the south east of France, close to Avignon. The site is about 25km² size, flat, and corresponds to an agricultural landscape, with relatively large fields for the region.

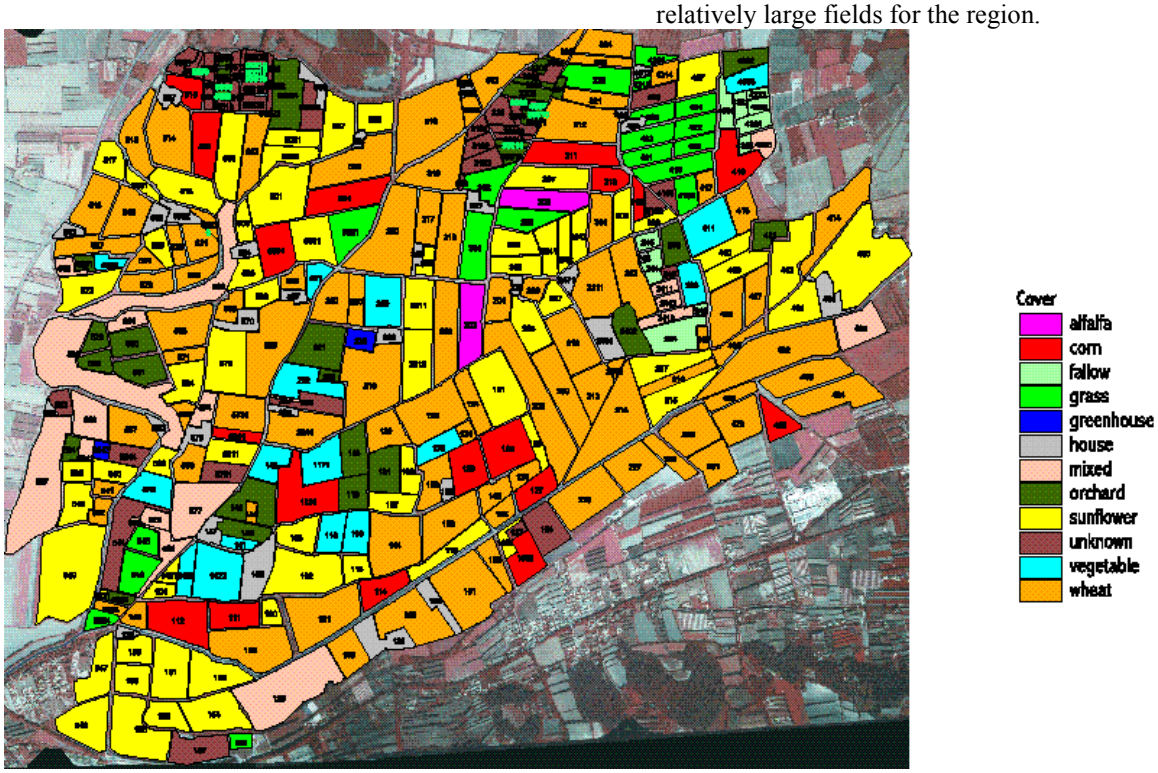

Figure 2. The Alpilles site. Land use map overlayed on a SPOT image.

The data correspond both to remote sensing and ground measurements. All these data are included in the data base that is available on the web (www.avignon.inra.fr/reseda).

1.1.1 Remote sensing data

Remote sensing systems have been operated in a variety of spectral ranges (optical, thermal infrared and microwave) and configurations from October 1996 up to October 1997. They include

1.1.1.1 airborne sensors

such as POLDER (4 bands in the visible and near infrared with directional and polarisation observations), INFRAMETRICS thermal infrared camera (directional observations in a single broad band), ERASME (C and X bands, in VV and HH polarisation) and RENE (S band, in HH polarisation) which are scatterometric profilers. All these sensors were flown several times during the growth cycle, allowing to get a good monitoring of the vegetation and soil dynamics. Additionally, single flights of particular instruments were performed. These instruments were either imaging spectro-radiometers (DAIS visible, near infrared, short-wave infrared and thermal infrared) and IROE passive microwave radiometer (6.8 GHz and 10 GHz). All the data were calibrated, the atmospheric effects corrected, and registered over a single reference image.

1.1.1.2 Satellite data

The images available during the experiment were acquired. This includes 6 SPOT, 1 TM, 10 ERS images and 12 Radarsat images. The data were calibrated and corrected from the atmospheric effects. Further, a geometric correction was applied using the single reference image. Additionally, the whole series of NOAA/AVHRR was acquired as well.

1.1.2 Ground measurements

The ground measurements were performed on a selection of fields, mainly wheat, sunflower, maize and alfalfa. They include soil, canopy and atmosphere characteristics. Additionally, a meteorological station provided the routine climatic data.

1.1.2.1 Soil measurements

The soil measurements included the permanent characteristics of the soils such as texture, chemical properties, thermal and hydraulic resistance and capacity, as well as dynamic characteristics such as moisture, water potential and roughness.

1.1.2.2 Canopy characterisation

The main structural variables such as the organ area index including *LAI*, the height and the gap fraction were measured during the whole growth cycle. Additionally, biomass amount and partitioning into organs were also measured concurrently. Particular attention was paid to the water content for exploitation of µ-wave data.

1.1.2.3 Microclimatic data

Micro climatic measurements were implemented over a selection of fields to characterise the fluxes in the soil-vegetation-atmosphere system. They include radiation, temperature, humidity and wind speed sensors, and soil heat flux devices. The sensors were placed in conditions allowing to compute the fluxes from the aerodynamic and Bowen ratio methods. These measurements span over the whole growth cycle. Additionally, Eddy correlation measurements were acquired for shorter periods. Finally, during an intensive campaign, scintillometer measurements and unmanned plane acquiring temperature and moisture measurements were implemented to analyse the spatial variability of fluxes.

1.1.2.4 Meteorological data and atmosphere characterisation

A meteorological station was installed in the centre of the site, with all the classical variables measured at a 20 minute time step during the whole experiment. Radiosoundings were performed close to the site every day, and additionally, some balloons were launched during intensive campaigns from the site itself –at a higher frequency. Finally, an automatic CIMEL station was measuring routinely the atmospheric aerosol and water vapour optical depths for correction of remote sensing data.

1.1.3 The data base

A data base with all the measurements and images and the associated documentation files was developed. It is a hierarchic data base hosted by an INRA web server (www.avignon.inra.fr/reseda). It is accessible to the whole scientific community.

1.2 Estimation of canopy and soil characteristics from remote sensing data

This will be reviewed as a function of the wavelength domain.

1.2.1 Solar domain

The ***atmospheric correction*** was simply applied to images based on sun-photometer measurements. However, the atmospheric correction based on the image data itself is a main issue of investigation when using remote sensing within surface radiative transfer models to get estimates of canopy or soil biophysical variables. This is certainly one avenue of research to develop. The Alpilles data base can be used only partly for this purpose, because this required more than the few bands provided by SPOT or POLDER. The DAIS data itself, because of their poor radiometric calibration stability are not very pertinent to investigate this problem.

The ***directionality of reflectance*** was investigated both for ***data normalisation***, and for the estimation of ***hemispherical reflectance*** and thus ***albedo*** derivation. Models with 2 to 4 parameters (MRPV, GEN, Walthall, FLIK) allow to get a robust and accurate estimates of the BRDF from a subsampling of directions available from POLDER data. However, when estimating albedo values in the whole solar domain (300-3000µm) from hemispherical reflectance observed in few bands, a systematic bias appears and should be corrected for. We showed also that hemispherical reflectance and albedo estimation is little sensitive to ***scaling effects***.

The ***amount of information*** contained in the directional dimension appears to be limited. However, we also showed the interest of particular configurations for estimation of some biophysical variables such as *LAI* and chlorophyll content. However, these results should be validated from the POLDER data available in the ReSeDA data base. A tentative was made for height estimation using an hybrid geometric-turbid medium model applied on the POLDER data. However, poor performances were obtained. This should be re-conducted over more simple biophysical variables such as *LAI* and chlorophyll content.

The ***spectral dimension*** was the one mostly exploited. However, no particular investigation was focusing on the optimal spectral sampling problem from the experimental point of view, because of the lack of appropriate data.

Investigation about the ***model inversion problem*** shows that:

- Little differences are observed between the 3 versions of turbid medium radiative transfer models used.
- Techniques based on minimisation over the biophysical variables (neural nets, vegetation indices) appear performing better than those based on the minimisation over the reflectance (Look up tables, optimisation).
- However, the, main factor to pay attention at is the ***amount of information*** actually used in the inverse problem.
- Flux variables such as ***fCover*** and ***fAPAR*** are better estimated than primary variables such as ***LAI*** and ***chlorophyll content***.
- *fCover* and *fAPAR* are little sensitive to ***scaling*** as opposed to *LAI*

1.2.2 Thermal infrared domain

The ***atmospheric correction*** problem was investigated using a range of techniques. They gave quite consistent results. The importance of applying atmospheric corrections was clearly demonstrated.

The ***spectral dimension*** was exploited for emissivity estimation from the DAIS data. However, the poor calibration stability of DAIS limited the results.
The ***directional dimension*** was investigated thanks to the INFRAMETRICS camera. Important directional effects ranging from 2° to 4° were observed. However, the variation between the acquisition of the directions over a single pixel due to the temporal dynamics has to be carefully removed.

1.2.3 µ-wave domain

The first issue investigated is ***classification***. This was achieved using the series of ERS and Radarsat images along the growth season. It appears critical to filter the speckle prior to the classification when made on the pixel basis. The ***Gamma map filter appears the most efficient***. The ***dual angle classification*** provided by the combination of ERS and Radarsat did not always provide improved performances. However, for a single date, ***the potential of the combination of active and passive µ-waves*** was clearly shown for classification purposes.

One of the main problem in ***retrieving soil moisture*** from µ-wave data is the ***confounding effect of soil roughness***. Several attempts were developed to solve this problem.

- A new radiative transfer model was developed based on a ***fractal description of soil roughness***. Confrontation with experimental results appears quite satisfactory.
- The ***IEM model*** is based on a description of soil roughness through the correlation length. However, it appears that it does not perform satisfactorily when using the actual correlation length. An ***effective correlation length*** was adjusted over a set of experimental data. A strong correlation was observed between the effective correlation length and the actual root mean square of height. Application on the ReSeDA data base shows that this approach is quite robust.
- A simple ***linear relationship relates the soil moisture to the backscattering coefficient***. However, ***the slope appears to be almost constant***, the intercept depending on the roughness and soil type. However, when investigating the relationship at a larger scale, the variation in roughness is smoothed out, and the slope and intercept are much better defined.
- ***In the passive µ-wave domain the roughness appears to have little influence*** as compared to the active domain (at least band C, 20° incidence). This results in a strong linear relationship between the brightness temperature in band X, 20° incidence, and the first top centimetre soil surface moisture.

Further work is to be conducted on the comparison of the retrieval performances of the different approaches and models listed above. The ReSeDA data base is well suited for this purpose amongst other data sets.

Concerning ***canopy biophysical variables retrieval***, focus was mostly on ***LAI and canopy water content***. Several approaches were investigated:
A new discrete model was developed that shows the drastic differences of the response between small leaves (wheat) and large leaves (sunflower) canopies. Further, the model, when inverted on actual ERS data during the ReSeDA experiment appears performing satisfactorily.
The ***cloud model was calibrated and then inverted over several canopies*** (wheat and sunflower). It appears performing quite satisfactorily, with an uncertainty (RMSE) associated to the estimation close to 0.5 $kg.m^{-2}$ for water content and 1.0 for *LAI*. For the retrieval of soil and canopy characteristics, the use of simultaneous observations in two different configurations appears mandatory. Optimal configurations were discussed based on this data set for wheat crops. Here again, one of the main limit is the unknown surface roughness and its possible variation along time.

1.3 Assimilation of remote sensing data into process models

The assimilation of remote sensing data was investigated in two separate parts corresponding to the two categories of process models: soil vegetation atmosphere transfer and canopy functioning models.

1.3.1 Assimilation into SVAT models

- The ***SVAT models were first compared*** and evaluated. For this purpose, a strategy for comparison was developed, based on the evaluation of three main criteria: (i) the accuracy of processes description; (ii) the portability of the models;(iii) the robustness of the calibration. In the comparison process, the calibration and validation phases were as independent as possible. Results show that despite the large range of complexity amongst the models considered, they were performing similarly. However, the ***simplest models (ISBA, MAGRET) were performing generally better*** than complex models such as SISPAT for which the calibration appears not very robust, particularly for the turbulent heat fluxes. This was later investigated by a sensitivity analysis for this SISPAT version considering a single homogeneous soil layer. It shows that water content and land surface water and energy fluxes are very sensitive to soil hydraulic properties for medium to low moisture levels. It was therefore concluded that ***SISPAT has to be implemented with more than a single layer*** to describe accurately surface soil water moisture.
- The ***aerodynamic resistance scheme*** used in the two-layer SVAT model, affects strongly the surface fluxes and temperature simulation. Six parameterisation scheme implemented in the

SISPAT model have been compared. Results show that the total surface fluxes were marginally affected. However, the main ***difference lies in the simulation of the soil and vegetation temperature*** because of the change in the partition of energy between the soil and vegetation. These differences are critical for the description of the radiative temperature as observed by remote sensing in the thermal infrared.

- The ***SEBAL algorithm exploiting the spatial variation in the optical domain*** was evaluated. The several assumptions in the algorithm were evaluated experimentally. Then the estimates of fluxes were compared to measurements and show good results for the net radiation, but poorer results for soil, latent and sensible heat fluxes. This was mainly explained by the ***poor parameterisation of the aerodynamic resistance***.
- The ***spatial variability of fluxes*** was investigated over contrasted neighbour fields using an unmanned plane. The structure of the lower atmosphere layers described this way confirms the contrasts at the borders, and sets the ***blending height above 30m***. Scintillometer measurements set up over similar field boundaries between contrasted crops show the ***importance of the aggregation scheme***.

1.3.2 Assimilation into Canopy functioning models

- Similarly to SVAT models, the first task was directed to the ***calibration of the several models*** considered. This was achieved over the calibration fields, or over data sets independent from the ReSeDA experiment. The calibration was mainly consisting in tuning the parameters related to the phenology, the biomass partitioning and the water balance. In Addition, to use more realistic radiative transfer models, a ***more detailed canopy – structure and optical properties of elements was implemented*** for the STICS model.
- Several assimilation schemes were used.
  - The ***ROTASK canopy functioning model was forced by estimates of LAI*** using vegetation indices. The use of remote sensing data (SPOT and TM data) ***shows significant improvement of yield estimation*** at the field scale, although absolute accuracy could be improved. The same scheme was implemented at the regional scale over MARS segments and shows that it could be operational.
  – The ***STICS-RT model was used to assimilate POLDER and ERS/Radarsat*** data over the growing season. A preliminary sensitivity analysis was used to identify the variables to tune during the assimilation process. They mainly corresponds to phenology, stand density and top layer soil characterisation. ***The assimilation of POLDER improved significantly estimates of total biomass production***. Concurrent use of µ-wave data did not contribute much to improve the dry biomass estimation, nor the water balance.

2. The partners

2.1 List of partners

The ReSeDA project is a collaborative effort of 10 partners. They are listed above, with the name of the main investigators:

INRA: Coordinator
Frédéric Baret, INRA Bioclimatologie,
Site Agroparc, 84 914 cedex 9 FRANCE
tel: (33) 4 90 31 60 82; fax: (33) 4 90 89 98 10
Email: baret@avignon.inra.fr
CESB
IO
Marc Leroy,
CESBIO, 18 Avenue Edouard Belin,
31 055 Cedex, FRANCE
Tel: (33) 5 61 55 85 14; fax: (33) 5 61 55 85 00
Email: marc.leroy@cesbio.cnes.fr
CETP
Catherine Ottlé,
10-12, avenue de l'Europe,
78 140 Velizy, FRANCE
Tel: (33) 1 39 25 49 18; fax: (33) 1 39 25 49 22
Email: ottlé@cetp.ipsl.fr
BRGM
Christine King,
BRGM, BP 6009, Avenue de Concyr,
45 060 Orléans, Cedex 2, FRANCE
Tel: (33) 2 38 64 33 92; fax: (33) 2 38 64 33 61
Email: king@brgm.fr
WAU
Jan Clevers,
Department of Landsurveying and Remote Sensing,
Hesselink Van suchtelenweg 6,
P.O.Box 339, 6700 AH Wageningen, THE NETHERLANDS
Tel: (31) 317 482902; fax: (31) 317 484643
Email: jan.clevers@staff.girs.wau.nl
SYNOPTICS
Hans van Leeuween,
SYNOPTICS Integrated Remote Sensing & GIS Applications, P.O. Box 117,
6700 AC, Wageningen
The Netherlands
Tel: (31) 317 42 69 36; fax: (31) 317 42 57 05
Email: main@synoptics.nl
AB-DLO
Raymond Jongschaap,
DLO Research Institute for Agrobiology and Soil Fertility,
P.O. Box 14,
6700 AA, Wageningen,
The Netherlands
Tel: (31) 8370 75972; fax: (31) 8370 23110
Email: r.e.e.jongschaap@ab.dlo.nl
IROE
Paolo Pampaloni,
IROE, Via Pancuatichi, 64, Firenze 50 127, ITALY
Tel: (39) 55 4235 205; fax: (39) 55 4235 290

Email: pampa@iroe.fi.cnr
UV
Vicente Caselles,
Departament de Termodinamica, Facultat de Fisica,
Universitat de Valencia,
Dr. Moliner, 50. Burjassot 46100 SPAIN
Tel: (34) 6 386 43 50; fax: (34) 6 364 23 45
Email: cesar.coll@uv.es

UC
Stephen Hobbs,
Space systems and Applications Group,
College of Aeronautics,
Cranfield University, Bedford MK43 0AL, GB
Tel: (44) 1234 750111; fax: (44) 1234 752149
Email: s.e.hobbs@cranfield.ac.uk

2.2 Role of partners

Each partner has a well identified responsibility according to the following chart:

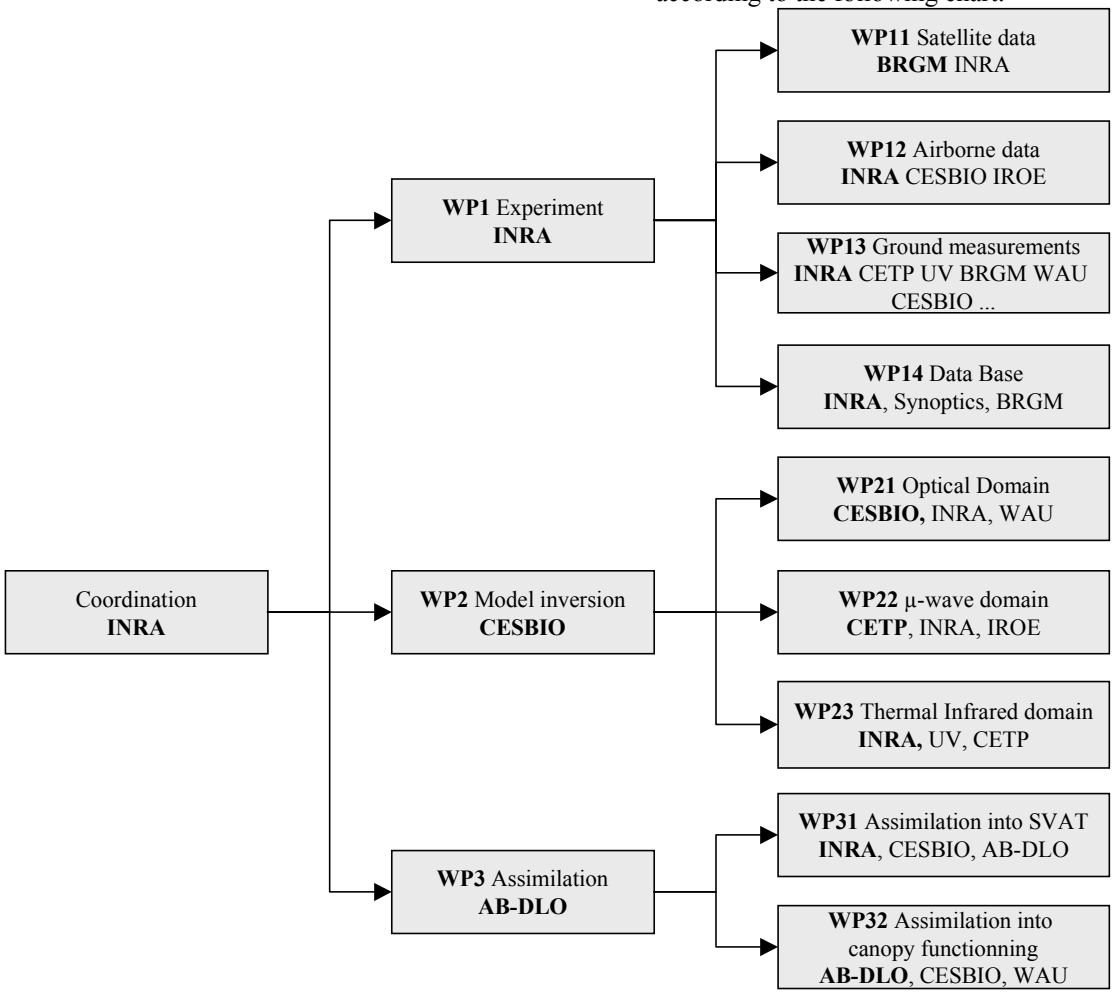

Figure 3 Chart showing the structure of the project. Each Working Package is under the responsibility of one partner (in bold). Other partners participating actively are also indicated.

3. Rationale

3.1 Main issues of concern

Two main issues of concern are considered within the ReSeDA project which are related to human activity at two different scales:

3.1.1 Global scale issues.

Since the last decades, evidence of significant global climate change due to the constantly growing human activity have been accumulated. This is obviously a main concern for governments because this climatic change directly impacts human's conditions of life. Strong warning were already issued by recent international initiatives organised within the United Nations. A large part of the scientific community is now investigating these key questions through international programmes such as WCRP (World Climate Research Programme) and IGBP (International Geosphere-Biosphere Programme). They need to be

answered to forecast climate change for the next decades according to scenarios of human activity, and therefore to propose recommendations for governments to minimise the impact on human beings. This was recognised during the last International conferences (Kyoto, Rio) on climate change (IPCC), and actions were taken in order to mitigate the effects of human activity. Vegetation constitutes the interface between the atmosphere and the soil, and therefore plays a key role in energy and mass transfers. Water and carbon cycles are obviously the main processes of concern. Although the objective is to understand the climate at the global scale, many processes take place at the local to regional scales as we will see later. Therefore, investigations about the global issues should be addressed also at the local to regional scales.

3.1.2 Local to regional scale issues

Apart from the understanding of the processes of interest for global change issues, great attention is also paid to the environmental problems that occur at the local to regional scales. In particular, intensive agriculture practices induce strong constraints to the quality of the environment. The European community has taken actions to promote sustainable agriculture practices in order to reduce the impact of agriculture on the environment.
Additionally, estimation and forecast of the production of crops, its year to year variation, as well as its spatial distribution is a highly valuable information for the organisation of the harvest and the management of the market for the main crops. This issue concerns a range of users, from the local scale such as farmers and local traders, to the global scale for the biggest traders, the transformation industry, as well as governments and non governmental organisation for the food security problem.

3.2 The need in modelling vegetation and soil processes

3.2.1 Processes and models

The evolution of the global climate and its consequence on ecosystems has been intensively investigated. Global Circulation Models (GCMs) were developed to simulate the climate change both at short time periods (weather forecast) and at longer time periods (global change). They require the surface to be accurately described in order to properly model its interaction with the atmosphere, and particularly energy, water, and carbon fluxes.
Environmental issues that take place at the local to regional scales could be also described by vegetation and soil models. Vegetation (canopy functioning) models will describe the dynamics of the vegetation over the growing season as well as the energy, water, carbon, and sometimes nitrogen and other mineral fluxes. Soil Vegetation Atmosphere Transfer models (SVAT) provide also a physical description of energy and mass fluxes (mainly water and carbon) at the instantaneous time scale.
All these models could be used both as a way to formalise our understanding of the processes, but also as tools for diagnostics as well prognostics in order to correct or remedy negative effects on the environment.
All those processes are complex and are still lacking adequate modelling as well as inputs. They need to be coupled together to get a comprehensive and consistent view of the system.

3.2.2 The range of spatial and temporal scales

Processes occur mainly at the very elementary time scale, but with a range of time constant. Therefore, in order to be able to measure significant trends, a range of typical time scales have to be considered. It goes from the instantaneous time scale for energy and mass fluxes within the atmosphere, up to the growth season for yield production, and several decades for impact of climate change on vegetation dynamics.
The typical spatial scale where many processes can be described is the local scale corresponding to few tenths of meters. However, vegetation and soils are constrained by the atmospheric boundary conditions for energy or mass fluxes at short time periods, as well as for their evolution over longer time periods. Conversely, the atmosphere dynamics depends on the boundary conditions determined by the soil or vegetation characteristics (Figure 4). Furthermore, hydrological processes, and atmospheric advection constrain the local processes at the regional scale. The processes are therefore intimately coupled at a range of scales. The high spatial and temporal variability observed at the local to the regional scales have to be accounted for when using process models. The same applies for measurements or estimates of the state variables and the fluxes over scales with significant spatial heterogeneity.

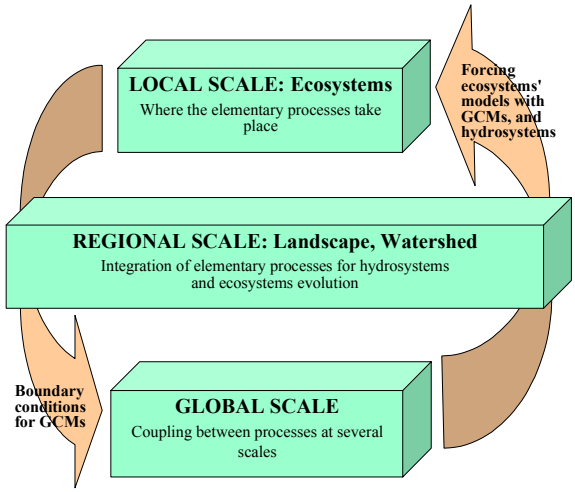

Figure 4. Processes are coupled over a range of scales.

3.2.3 The limits of process models: number and accuracy of the inputs

Canopy functioning models will be used as paradigm. Canopy functioning models describe the elementary processes such as photosynthesis, respiration, biomass partitioning, water and nitrogen transfers. They use within a deterministic scheme, climate variables and soil characteristics. These models allow to estimate directly variables of interest such as the biomass production, water and nitrogen balance, as well as the yield. However, they require a lot of parameters and variables as inputs. Some of them are poorly known and should be calibrated for the particular conditions where the canopy is subjected. An example of the poor performances of such canopy functioning models when run mainly over meteorological and soil data was demonstrated by Cramer and Field (1999). They showed a wide range of variation between the simulation of net primary production (NPP) models in these conditions (Figure 5).

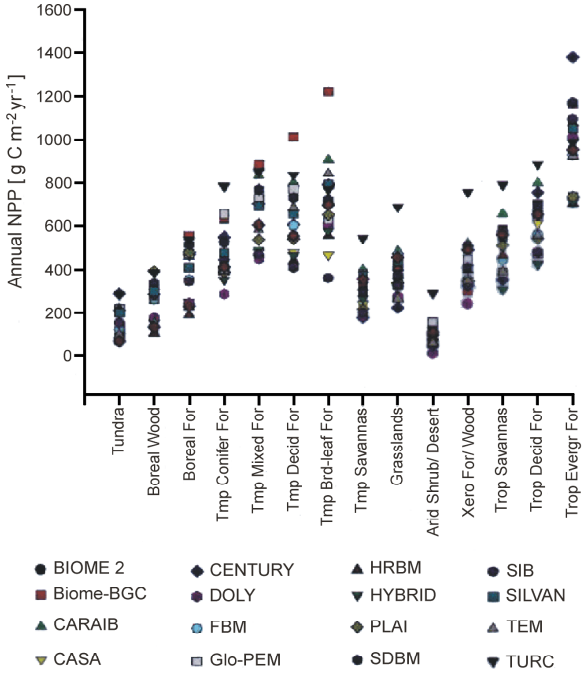

Figure 5. Comparison between a range of canopy functioning models for the simulation of the net primary productivity (NPP) when mainly driven by soil and climate variables From Cramer and Field (1999).

Franks and Beven (1997) proposed a fundamental explanation apart from the simple differences between models. Complex models use a rather large number of variables and parameters to describe biophysical processes. The accuracy of estimates of such variables is sometime very poor, leading to large uncertainties in the model simulations. Although information is put in the models within the knowledge about physiological processes, it is still too limited to get good enough performances. Therefore, additional sources of information is required either to directly estimate input variables to the process model, or to control the behaviour of the model by checking on few outputs of the model. Remote sensing techniques could play a very important role at this level as we will see in the following.

3.3 The need in remote sensing observations

3.3.1 Role and diversity of remote sensing systems

Remote sensing techniques have been widely developed and used in the past years for several application domains including the continental biosphere. However, for natural and cultivated areas, satellite data were mostly dedicated to the mapping and the inventory of crops and natural resources. Earth observation sensors (Landsat TM, SPOT), large swath satellites (NOAA/AVHRR, METEOSAT, VEGETATION) and radar systems (ERS, Radarsat, JERS) were the most important sources of images. These sensors were mainly used in qualitative and relative ways that were nevertheless very useful. However, their potentials is under-exploited, particularly regarding the combination with the models that can be used for a better understanding, diagnosis and prognosis of the processes of interest. Emphasis is currently put on quantitative approaches that could provide estimates of surface characteristics from remote sensing data.

The signal that is recorded by remote sensing instruments is driven by physical processes governing the radiative transfer within the soil, canopy and the atmosphere. The interaction of radiation with canopies and soils depends on the optical thermal or dielectric properties of the elements as well as on their number, area, orientation and position in space which constitute the primary biophysical variables. Therefore remote sensing allows to derive directly only canopy or soil primary biophysical variables. Additionally, secondary variables that are combinations of the primary biophysical variables could be also estimated generally with a quite good accuracy. The main primary and secondary variables are listed in **Table 1**. Each spectral domain is sensitive to particular canopy or soil characteristics. The reflective optical domain (400-2500nm) will provide estimates of canopy structural variables such as *LAI* (leaf area index) and biochemical composition (pigment, water, ...). Thermal infrared domain and passive µ-wave will depend on the surface temperature and canopy structural variables. The active microwave domain will provide information on soil roughness, moisture, as well as canopy structure and water content. Therefore, the combined use of several spectral domains is likely to be the only way to extract the maximum amount of information on canopy or soil biophysical characteristics.

	Biophysical Variables	Spectral domains				
		Visible Near Infrared	Near Infrared Short Wave Infrared	Thermal Infrared	Active µ-wave (radar)	Passives µ-wave
Canopy structure	*LAI*	+++	+++	+	++	+
	Leaf orientation	+++	+++	+	+	+
	Leaf size and shape	+	+	+	+	+
	Canopy height	-	-	-	++	-
	Canopy water mass				+++	+++
Leaf characteristics	Chlorophyll content	+++	-	-	-	-
	Water content	-	+++	-	+++	+++
	Temperature	-	-	++++	-	++
Soil characteristics	Surface soil moisture	-	+	+	+++	+++
	Roughness	+	+	-	++	+
	residues	+++	++	-		-
	Organic matter	++	++	-	-	-
	Soil type	++	++	+		
Secondary variables	*fCover*	++++	++++	++	++	+
	fAPAR	++++	++++			
	albedo	++++	+++			
	Long wave flux	-	-	++++	-	-

Table 1. Estimation of canopy, leaf or soil biophysical variables as a function of the spectral domain used. The level of accuracy and robustness of the estimation is indicated by the "+" ("++++" accurate and robust; "-" no estimates possible). Secondary biophysical variables are also indicated.

We note that the number of biophysical variables potentially accessible by remote sensing techniques is rather large. However, their estimation from the radiometric data is not always very accurate because of the number of biophysical variables that drive the radiative transfer and the limited information content in the spectra variation of the radiometric signal. The only way to improve these estimates is to exploit other dimensions than the **spectral dimension**, as well as ancillary information.

Current and future Earth observation sensors aboard satellites will almost cover the whole electromagnetic spectrum, from the optical domain to the microwave (SPOT, TM, AVHRR, VEGETATION, POLDER, AATSR, RADARSAT, ERS, JERS, MERIS, MODIS, ASAR, MISR, MSG, LSPIM, SMOS ...). This situation is new and forces to investigate the combined use of these various data sources. This will therefore also implies to explicitly account for other dimensions than the spectral one:

- **Temporal dimension**. All the sensors are not borne on the same platform. They will thus provide observations of the same target at different dates or hours in the day. We need interpolation techniques to use concurrently those multi-sensor data. The vegetation or soil are dynamic targets. Their time course brings in itself a lot of information that can be used to characterise their functioning. This requires to have robust methods to infer surface parameters from remote sensing over the entire range of surface conditions encountered over a whole growth cycle.
- **Directional dimension.** Many systems will be able to provide observations of the same target under different view and sun geometrical configurations. Algorithms dedicated to correct or normalise from these directional effects are required. Furthermore, this can be also used to get more information on the structural characteristics of the vegetation or soil. Polarisation features in the visible and the microwave domains may also provide important information on the properties of the surface and the atmosphere.
- **Spatial dimension**. The spatial resolution is often closely related to the temporal repetitivity of observations. For example, large swath satellite that are able to acquire frequent images have a low spatial resolution (NOAA/AVHRR, METEOSAT). Conversely, high spatial resolution (SPOT, TM) have poor revisit capability. Further, to address climate issues by providing to global circulation models surface variables such as albedo, roughness and moisture, the large scale is the one to be considered. The several sensors that can be used may have different spatial resolution. Thus, the up-scaling and down-scaling problems are intimately associated to the scientific issues addressed (environment and climate monitoring) as well as the tools available (the several satellite systems available in the future).

To be able to concurrently use data provided by all the current and future satellite systems with their spectral/temporal/directional/spatial characteristics, vegetation and soil models provide a convenient way to assimilate this complex information. Further, the use of the temporal variation observed throughout the growth cycle is likely to provide pertinent information on the mechanisms underlying changes in the functioning of soil and vegetation.

3.3.2 From radiative transfer model inversion to assimilation into process models.

Retrieval of information on canopies or soils from remote sensing observations can be achieved using two approaches.

3.3.2.1 Inverse methods: exploitation of instantaneous measurements.

Radiative transfer and surface reflectivity models describe the interaction between vegetation soil or atmosphere and the electromagnetic radiation. The ***inversion*** of these models can provide estimates of canopy or soil biophysical characteristics from their spectral/directional/polarisation variation acquired instantaneously, or at least under the assumption of a steady state for soil and vegetation. Several inversion methods have been developed by the geophysical scientific community. However, they are generally limited by the amount of information exploited, and have difficulties in solving problems such as uniqueness of the solution, ambiguities or the effect of confounding variables. Therefore, improvement of the retrieval performances could only come from the exploitation of additional information such as more detailed canopy structure description, knowledge on uncertainties on measurements and models, and a priori information on the distribution of the variables. Nevertheless, these methods will provide only estimates of primary and secondary variables which have to be ingested into canopy and soil functioning models to get the full description of the processes of interest (Figure 6). All these limitations of inverse methods will be largely attenuated when using assimilation methods as we will see in the following.

3.3.2.2 Assimilation methods.

Vegetation and soil process models have been developed to describe our current understanding of the physical and biophysical processes that occur between the atmosphere, vegetation and soil. These models describe the energy and mass budget at the instantaneous time scale and provide also estimates of the time course of soil and vegetation state variables over the growing season. Two types of models are generally distinguished at this local scale:

- **Canopy functioning models.** The biophysical processes that govern canopy functioning and dynamics are described in these models,. They control plant phenological development, photosynthesis, respiration, water, carbon and nitrogen balance, and allocation of resources between the several parts of the canopy (leaves, stems, roots, fruits, ...).
- **Soil Vegetation Atmosphere Transfer models.** (SVAT models) describe the physical processes that control the transfer of energy and mass (mainly water) in the soil vegetation atmosphere continuum. They generally require information on canopy structure and climatic variables such as the incoming radiation, air temperature and humidity and wind speed. In addition to the fluxes, they may be used to estimate the surface temperature and moisture distribution within the soil or the canopy. SVAT models may be coupled with canopy functioning models to be able to describe the energy and mass transfer along a whole growth cycle.

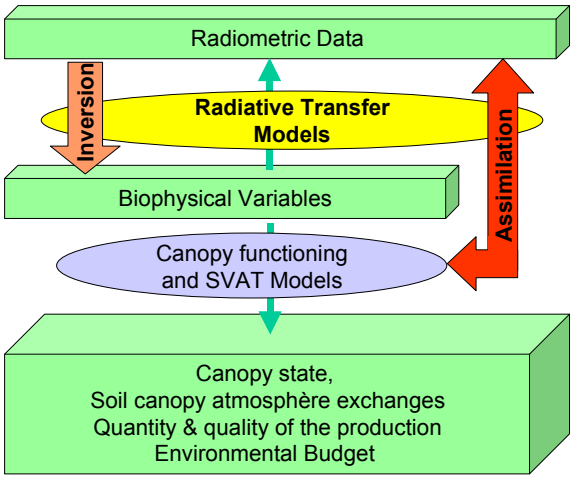

Figure 6. Flow chart diagram showing how to infer end variables such as canopy net primary production (NPP), yield or water fluxes from assimilation of remote sensing data into canopy and soil models. The inversion is restricted to the retrieval of canopy biophysical variables using radiative transfer models in the inverse mode. The green arrows indicate the way models work in the forward direction.

SVAT and canopy functioning models contain a description of the biophysical characteristics such as canopy structure and optical/dielectric properties of the soil or vegetation elements that govern the radiative transfer. They thus can be coupled to radiative transfer or surface reflectivity models to simulate what remote sensing systems actually observe, i.e. the temporal time course of the spectral/directional/polarisation signature of soil and canopies. They thus may be used to "assimilate" remote sensing data. The assimilation process will consists in tuning SVAT and soil or canopy functioning model parameters so that model outputs such as the time course of reflectance, brightness temperature or backscattering coefficient, agree with actual remote sensing observations. Thus the assimilation will provide deeper characterisation of the surface processes as opposed to the state variables provided by the inverse methods (Figure 6). Assimilation techniques can be used to set initial conditions to SVAT or canopy functioning models as

well as define the optimal values of parameters describing particular processes. Once calibrated and initialised, these models can be used later in a predictive mode that does not require necessarily remote sensing information. This use of process models is quite interesting in the perspective of the evaluation of median to long term effects of environmental or climatic changes.

4. Objectives & time frame of the project

4.1 Objectives of ReSeDA

The main objective of the ReSeDA project is ***the use of multi-sensor and multi-temporal observations for monitoring soil and vegetation processes, in relation with the atmospheric boundary layer at local and regional scales by assimilation of remote sensing data into canopy and soil functioning models***. This study aims at developing and evaluating methods to estimate net primary productivity, water and energy fluxes over cultivated vegetation. It will provide recommendations useful to:

- improve information retrieval from the multiplicity of sensors that are or will be available within few years,
- deliver improved methodologies for the interpretation of multi-temporal/multi-sensor remote sensing data,
- drive the policy of technological developments of space observations.

The project is decomposed into three main tasks corresponding to the three work packages:

WP1-The experiment.
A consistent and comprehensive data set has been acquired during a whole growth season allowing calibration and evaluation of the algorithms proposed, both at the field scale (10-100m) and the 1km scale corresponding to large swath satellite observations. Remote sensing systems will be operated to collect data in a variety of spectral ranges and configurations (optical, thermal infrared and microwave). Measurements span over a whole year long with emphasis on the multi-temporal aspect. This data set was exploited in the later tasks for scientific purposes. Further, it is now available to the whole scientific community via the web site: www.avignon.inra.fr/reseda.

WP2-Evaluation of inverse methods.
Canopy or soil biophysical variables (structure, temperature, moisture, ...) have been be retrieved from remote sensing observations using mainly the spectral, directional and polarisation signatures. Analytical approaches using radiative transfer and surface reflectivity models as well as semi-empirical approaches have been used. Biophysical variables retrieved through these inverse methods have been compared to the values measured in the fields. The concurrent use of large scale systems providing frequent observations and local scale sensors have been investigated and the scaling issue discussed. This work package was decomposed into three subpackages corresponding to the spectral domains considered: solar, thermal infrared, and μ-wave.

WP3-Evaluation of assimilation methods.
Canopy functioning models and SVAT models have been tuned so that the temporal, spectral, directional and polarisation signature simulated matches the observed remote sensing signals as close as possible. Several approaches of data assimilation have been evaluated with emphasis on the use of the whole remote sensing data available and knowledge of the physical and physiological processes governing soil and vegetation functioning. They have been mainly studied at the field scale.

4.2 Time frame

The ReSeDA project was planned for a three year duration. According to the original schedule, the data processing phase was largely underestimated, which resulted in delays for the two last working packages. These delays were mainly due to several problems observed in the measurements and that took a lot of time to be sorted out and corrected for. These problems were associated mostly to the airborne instruments which were prototype systems that had not the degree of operationallity expected. The delay was partly compensated by a two months extension.
A General co-ordination meeting was organised at the end of each year, followed by the annual report. Additionally, meetings in subgroups were also organised in order to have deeper discussion around a particular topic

Year	1				2				3			
Term (3 months)	1	2	3	4	5	6	7	8	9	10	11	12
WP1:Data acquisition												
Details of the experimental plan and preparation												
Definition of the data base format,												
Satellite data acquisition and processing												
Airborne data acquisition and processing												
Ground level data acquisition and processing												
Constitution and validation of the data base												
Access to the whole scientific community												
WP2: Inversion												
Solar domain.												
Thermal infrared domain												
µ-wave domain												
WP3: Assimilation												
Calibration of SVAT and canopy functioning models												
Assimilation in SVAT models												
Assimilation in canopy functioning models												
Assimilation in coupled SVAT/canopy models												
Milestones												
Main Co-ordination Meeting	●			●				●				●
annual report				■				■				
Final/Mid term report												■

Table 2. Flowchart showing the main milestones along this 3 year project.

5. Achievements

The achievements will be described according to the three main work packages identified previously.

5.1 The experiment and the data base.

5.1.1 Description of the Alpilles test site.

The ReSeDA site is located near Avignon (SE of France) in the Rhone valley (
Figure 7). Its maximum dimension is approximately 5km*5km. It is a very flat area. Fields are large enough (200 m x 200 m) to extract pure pixels from high spatial resolution satellites, as well as to implement atmospheric fluxes measurements.
The main crops are wheat (32%), sunflower (20%), maize (9%), and grassland (16%). A detailed and exhaustive classification was achieved over the test site (Figure 2). The measurements over the site started in October 1996, and were completed in November 1997.

5.1.2 Satellite data

5.1.2.1 Satellite sensors and images acquired

The satellite images were acquired during the whole experiment according to the scheme presented in Figure 8. They thus include SPOT, Landsat TM, NOAA/AVHRR, ERS 2, ATSR2, and Radarsat and cover the whole wavelength spectrum and most of the growing season for winter and spring crops. Table 3 shows the characteristics of the satellite sensors used.

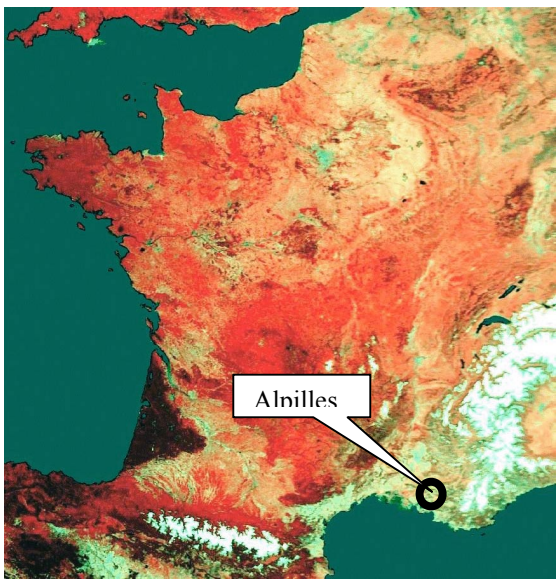

Figure 7. Situation of the Alpilles/ReSeDA Site.

	Sensor	Spectral domain	View angle	Swath (width)	Spatial Resolution	Polarization	Revisit Frequency
µ-wave sensors	ERS	C-band	23°	100 km	20 m	VV	
	Radarsat	C-band	23° 38°	150 km 50 km	25 m 9 m	HH	
Solar & Thermal sensors	Landsat TM	0.45-0.52 µm 0.52-0.60 µm 0.63-0.69 µm 0.76-0.90 µm 1.55-1.75 µm 10.4-12.5 µm 2.08-2.35 µm	0°	185 km	30m	non appl.	18 days
	NOAA-AVHRR	0.58-0.68 µm 0.72-1.10 µm 3.55-3.93 µm 10.3-11.30 µm 11.5-12.50 µm	± 55°	2400 km	1.1 km	non appl.	1 day
	SPOT XS	0.50-0.59 µm 0.61-0.69 µm 0.79-0.89 µm	0°	60 km	20 m	non appl.	26 days

Table 3. Characteristics of the satellite sensors used during the ReSeDA experiment.

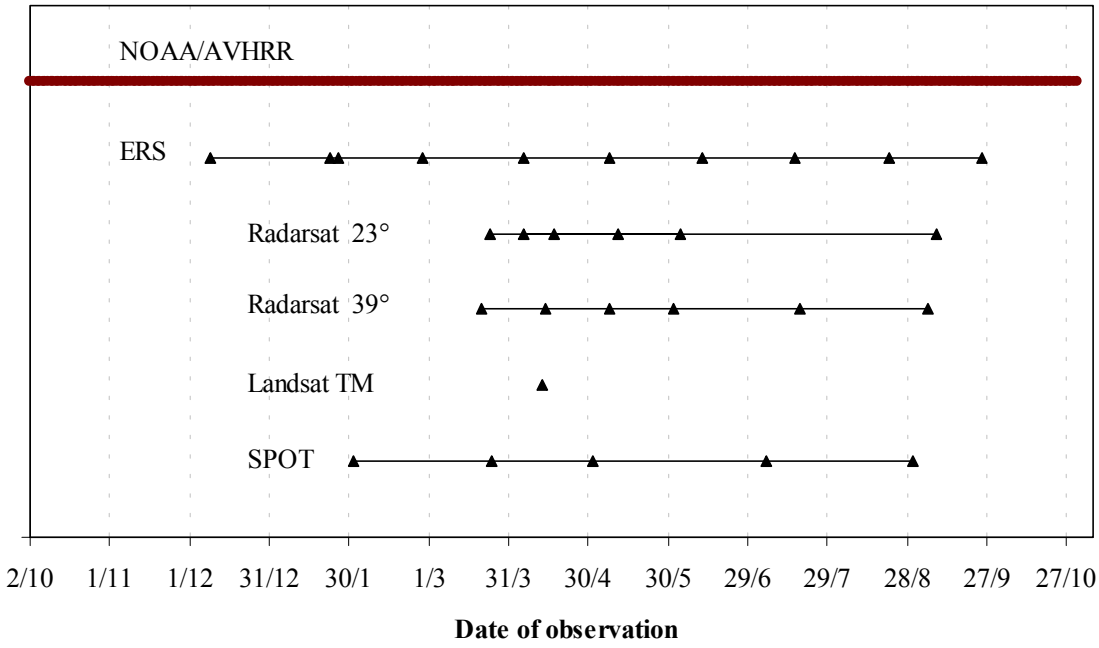

Figure 8. The satellite images acquired during the ReSeDA experiment and available on the server.

5.1.2.2 Processing of the images

The geometric correction was performed for all satellite images as well as airborne sensors thanks to a reference SPOT image. The geometric correction was mainly made thanks to a network of ground control points. This reference image was then precisely transformed to match a raster image of the topographic map at a scale of 1/25000. The Projection system adopted here is the extended Lambert II.

- For **SPOT** series in XS mode and **TM** image. Prior to geo-correction, the data were corrected from the MTF. The data were then radiometrically corrected. Atmospheric correction (MODTRAN) was applied, based on the ground level measurements of the atmospheric characteristics continuously acquired during the experiment.
- **Radar** images: the geo-coding uses a DEM (BRGM) and the description of orbit. An important point is to be emphasised : the size of pixel in the corrected image is the same as the DEM. To avoid an important degradation of the radar resolution, a sub-sampling of the original DEM has been artificially extracted: 25m for ERS and Radarsat mode standard, and 12,50m for Radarsat in fine mode. This choice keeps relatively high spatial resolution of the corrected images by comparison with the raw data, while saving computer time and minimising the size of the saved image

files. Calibration and filtering (gamma map filter) were finally applied to the data in order to get the proper physical value of the back-scattering coefficient σ^0.

- **NOAA/AVHRR** raw data are simply stored on the data base. No particular corrections or transformations have been applied.

5.1.2.3 The data base

- **Copyrights.** Copyrights have been obtained so that the data corresponding to the 5*5km² zone are available for free to any users. The use of the whole image must generally be made with agreement with ReSeDA partners. In addition, it is asked to the people who use these data to acknowledge the ReSeDA people who acquired and processed the images.
- **Data format.** Three export formats are archived for each image: ERDAS (*.img), TIFF (*.tif) for 8 bit images, and binary (*.dat). In addition to these imagettes, an EXCEL synopsis file provides the average and standard deviation values of a selection of 43 plots within the test site. This will facilitate the use of satellite data when the spatial arrangement is not required.
- **Data base architecture.** The data are available at the ReSeDA server at INRA that is fully accessible to the scientific community. The files are organised in directories per sensor. Each directory is organised in three sub-directories corresponding to the three formats used.
-

	SENSOR	Waveband	View angle	Swath	Resolution	Altitude	Polarisation	Data type
µ-wave sensors	ERASME	C-band	20° and 40°	-	20 m	300 m	VV/HH/HV	profiles
		X-band	20° and 40°	-	20 m	300 m	VV/HH	profiles
	RENÉ	S-band	20° and 40°	-	18 m	300 m	Full polar.	profiles
	IROE	6.8GHz	20° and 40°	-		150 m	H and V	profiles
		10GHz						
Optical sensors	POLDER	443 nm 550 nm 670 nm 865 nm 910 nm	± 50°	± 3 km	30m	3000m 1500m	N/A	images
	CIMEL	540 nm 640 nm 840 nm	0°	-	20m	300m	no	profiles
	DAIS	0.45-2.45 µm 72 bands	0°	± 2 km	7 m	2900 m	no	images
Thermal sensors	Heinman	8-14 µm	0°	-	20m	300 m	no	profiles
	Inframetrics	9-13 µm	± 40°	± 3 km	60 m 30 m	3000m 1500 m	no	images
	DAIS	8-12µm 6 bands	nadir	± 2 km	7 m	2900 m	no	images

Table 3. Characteristics of the airborne sensors used during the ReSeDA experiment.

5.1.3 Airborne data.

The objective here was to acquire data that will be provided by future space systems already scheduled or that represent a very high potential with regards to the characterisation of vegetation or soils.

5.1.3.1 Sensors and vectors used

Four types of vectors were used:

- **Small plane**. This plane (PIPER PA28) was operated from Aix en Provence by INRA and CESBIO. POLDER and INFRAMETRICS sensors were mounted on it and connected to a device acquiring continuously the position (GPS) and the attitude of the plane. This is one of the routine measurements, the plane being operated at least once per month.
- **Helicopter.** It was operated by CETP and INRA. ERASME and RENE were mounted on it, with a CIMEL and a thermal infrared radiothermometer. All the instruments are profilers (except RENE). A video camera was used to identify the fields actually sampled.
- **ARAT.** This FOKKER 27 operated by INSU (CNRS, France) was used for the passive microwave measurements thanks to the STAAARTE program. The IROE sensor was mounted on it. Additional thermal infrared data (8-14 µm) were acquired at the same time from the same vector. This sensor was used only at two dates during the experiment.
- **DLR plane.** The Dornier plane from DLR was used for the DAIS instrument. It was used only once during the campaign.The main characteristics of the sensors are presented in table 3. The sensors can be split according to the frequency of the flights.

1. **Routine sensors** that provide at least monthly data sets with two imaging instruments covering the visible, near infrared (POLDER) and thermal infrared (INFRAMETRICS) domains and a profiler scatterometer (ERASME).

- ***POLDER*** The Polarised and Directional Earth's Reflectance (POLDER) instrument measures the intensity of the sun light reflected by the Earth/atmosphere system in five spectral bands and under different viewing directions. Further, the polarisation of the light reflected is measured in two bands. The flight lines were designed in order to get a pertinent directional sampling of the test site. (Figure 9)
- ***INFRAMETRICS***. This thermal infrared camera is equipped with a wide angle field of view providing directional measurements in the 8-13 μm domain in the same way as POLDER does. The thermal camera was most of the time coupled with POLDER. However, additional flights were performed using the thermal camera only. In this case, the altitude of the flights was 1500m rather than the regular 3000m altitude. This provides a better spatial resolution although the directionality is poorly sampled.

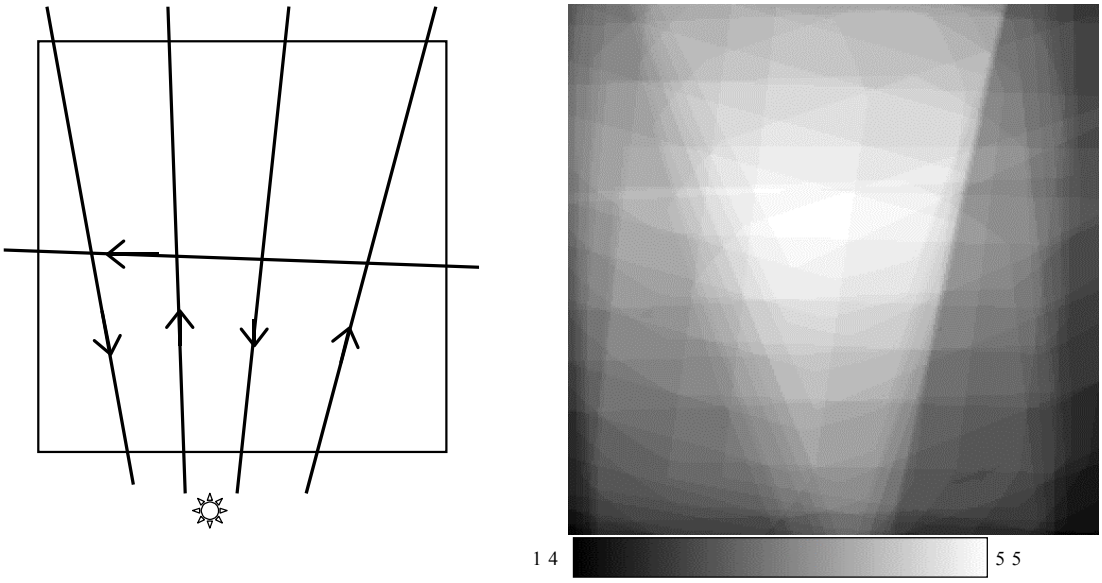

Figure 9. POLDER schematic flight plan: four tracks are oriented roughly parallel to the solar direction, and one track perpendicular to that direction (left figure). The square represents a 5 km x 5 km area around the Alpilles site. The typical corresponding number of observation for a given pixel in 5 km x 5 km study area is given (right figure).

ERASME C and X band, HH and VV. These instruments were operated concurrently with CIMEL and Heinman radiometers to cover the whole spectral domain. The flight lines were chosen to get a good sampling of a selection of plots on which intensive ground measurements were made. The time and frequency of the flights were governed by the growth of the vegetation, and possible variation in soil moisture and roughness conditions. For this purpose, we defined two intensive campaigns one in April and the other in June, where we concentrated the flights and the concurrent ground measurements. ERASME was mainly in its C and X band, in VV and HH polarisation configuration.

2. **Additional measurements.** Additional measurements were acquired, depending on national or other European funding opportunities. They allow to investigate some complementary instrument configurations. This includes
   - ***ERASME C band HV.*** Five flights of ERASME in cross polarisation configuration were scheduled. They were always associated to the routine ERASME configuration during the intensive campaigns, in order to make the comparison possible.
   - ***RENE S polarimetric radar.*** RENE was set-up in S band (3.25 GHz), and HH polarisation. It flew once in each intensive campaign. RENE provides images unlike ERASME.
   - ***IROE sensor.*** Passive microwave measurements were acquired using the IROE sensors aboard the ARAT thanks to the E.C. STAAARTE program. It measures the brightness temperature in the 6.8GHz and 10GHz bands within about 1K accuracy. The flight lines were defined to sample the fields that were actually characterised with the other profiling sensors such as ERASME.
   - ***DAIS sensor.*** The DAIS flew once the site thanks to the E.C. DAIS large scale facility program set up by DLR. The DAIS provides high spectral resolution images in the visible/near infrared domain and six bands in the thermal infrared (8-12μm). The flight lines were designed to get a full cover of the site.

5.1.3.2 Flight schedule

The acquisition scheme is shown in Figure 10 where the configuration for ERASME is detailed. It shows that the objective of getting a regular monitoring with the routine sensors (POLDER, INFRAMETRICS and ERASME) was achieved. The two intensive campaigns in April and June were also achieved in good conditions with complementary RENE μ-wave images in S band and concur-

rent multiple INFRAMETRICS thermal infrared data. An other interesting period with almost all the sensors (and configuration for ERASME) available is centred on the 8th of July with the DAIS spectro-imaging systems.

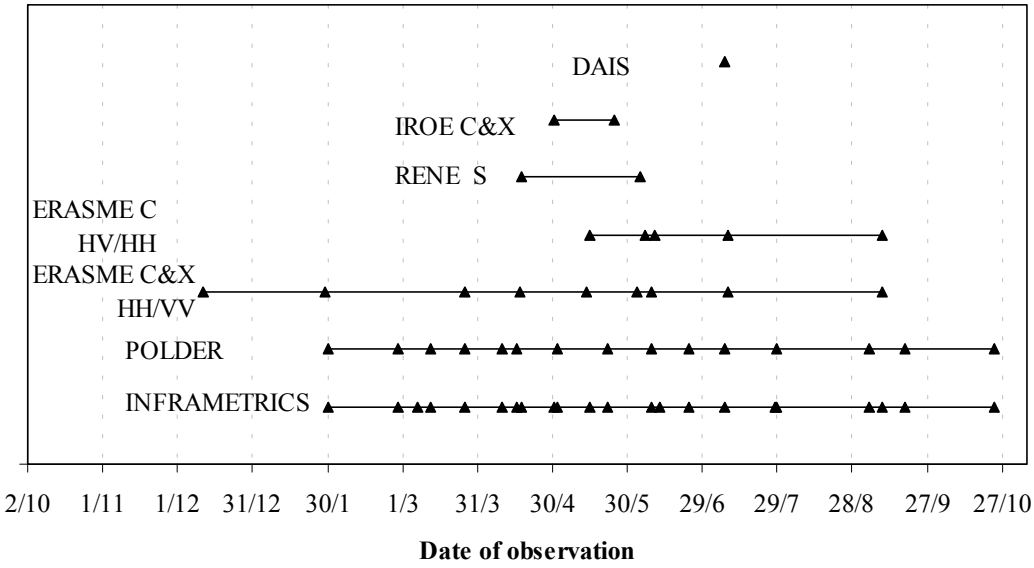

Figure 10. Distribution of the airborne remote sensing observations along the experiment (1996-1997)

5.1.3.3 Processing of the data

The data have been processed in order to get "take and play" data. This includes geometric correction, radiometric calibration and atmospheric correction for solar and thermal sensors. The quality of the processing depends on the type of sensor:

- ***POLDER:*** all the images acquired at 3000 m have been processed. The geometric correction achieved an accuracy around ±1.5 pixels, except for few images where it can reach up to 4 pixels. In these cases, better registration can be achieved locally by correlation techniques. The absolute calibration was performed thanks to three calibration experiments performed at LOA using an integrative sphere. The accuracy might be close to usual figures in these conditions, i.e. around 2% relative. The radiometric noise was very low. The atmospheric correction was performed using SMAC and measured aerosol optical thickness and water vapour. The uncertainties associated to these values are in the range of ±0.03 for aerosol optical thickness at 550nm and ±0.2g.cm^{-2} for water vapour.
- ***INFRAMETRICS***: The 19 dates of observation at 3000m, and 7 dates at 1500m have been processed. The geometric correction was performed thanks to ground control points scattered on the images. The accuracy achieved is similar to that of POLDER. The absolute radiometric calibration was performed over a large number of combination of black body and ambient temperature. The accuracy is close to ±0.3K. Atmospheric correction was applied using MODTRAN code and water vapour and temperature profile measurements provided by the radiosoundings. However, because of stability problems of the camera, the data were recalibrated using the ground measurements over the surface temperature contemporaneously to the INFRAMETRICS flight.
- ***ERASME***: The ERASME data have been processed by CETP. The registration was achieved thanks to the video camera aboard the helicopter. The radiometric calibration was performed by external calibration. Validation of the results were performed by comparison with ERS and Radarsat data when possible, as well as by correlation with soil moisture. All these tests demonstrate high consistency and accuracy of ERASME data around ±1dB. Both in like and cross polarisation.
- ***RENE***: The data have been recently processed and are now available in the data base.
- ***DAIS***: The DAIS data have been processed by DLR. The geometric registration shows quite good performances. However, radiometric calibration shows stability problems both in the solar and thermal domains, and instrumental noise was quite high. Local calibration was applied using well identified targets

5.1.3.4 The data base

- **Copyrights.** No copyrights are covering these data. Therefore, they are free for use to the whole community. However, when people out of the consortium will use these data, we would like them to acknowledge those who spent a lot of time and energy in acquiring and processing the data. This information is found in the data base.
- **Data base architecture.** The data are available at the ReSeDA server at INRA that is fully accessible to the scientific community. The files are organised in directories per sensor. In the main sensor directory, and information file describes the type of data and the format associated.

5.1.4 Ground measurements

5.1.4.1 The selection of fields

Four types of crops were investigated: wheat, alfalfa, sunflower and maize (Figure 2). This ensures enough variability between crops to test the robustness of the models developed. We defined several levels of field instrumentation. Calibration and validation sites were termed "permanent sites" because instrumentation was installed during several months. They mainly aim at the understanding and modelling of the detailed processes. The remote sensing sites are sampled mainly during the airborne flights and the intensive periods. They aim at the evaluation of retrieval algorithms for canopy and soil biophysical variables through radiative transfer models.

1. **Calibration fields.** These fields correspond to the highest level of instrumentation to satisfy the calibration requirements for SVAT and canopy functioning models as well as those for the test of remote sensing data inversion techniques. The calibration fields were equipped with a fixed set of instruments measuring the surface energy balance components, some climatic parameters, the daily soil water balance, the surface temperature and the albedo. Observations of the root system and a detailed description of soil physical properties were performed.
2. **Validation fields.** The instrumentation and the characterisation of the crops is lighter than those of the calibration fields. The measurements were dedicated to the evaluation of SVAT and crop models and for the test of the inversion of remote sensing data. Beside the required data for pure remote sensing purposes, the measurements were limited to the components of the energy balance, a weekly water balance and the surface temperature. Additional characterisation of the crops and the soils were performed.
3. **Remote sensing fields.** A selection of fields was monitored to provide the surface parameters required to test the inversion procedures. All the soil and the vegetation measurements mentioned above were collected concurrently to each aircraft campaign and for some important satellite data acquisition.

Table 4 shows the measurements performed on the different type of fields.

The main emphasis of the experiment is its temporal dimension. However, scaling problems will also be addressed. The spatial sampling strategy was designed to allow a good characterisation of :

- **the field scale** that reveals the variability between fields. This variability is to be used to evaluate the robustness of the algorithms proposed.
- **the km scale** as observed by large swath satellite. The individual fields sampled at the local scale can be used to estimate the corresponding km scale characteristics.

Some problems occur in some fields due to the internal variability. A specific interpretation of the data is required in such situations. Figure 8 shows the time distribution of the measurements. This campaign was mostly organised and actually conducted by INRA. However, significant help was provided by the several partners during the two intensive campaigns.

Measurements	Calibration	Validation	Remote Sensing
Radiative balance (R_n, $a.R_g$, T_{rad} (20°))	✔	✔	
Bowen ratio (T_a, p_v, H, LE, $u(2h)$, $u(3h)$)	✔	✔	
Soil Heat Flux (G(0;05m))	✔	✔	
Soil Temperature profile (0.005, 0.01, 0.025, 0.075, 0.15, 0.25, 0.50, 1.00m)	✔	✔	
Moisture profile (3 neutron probe tubes)	✔	✔	
Surface moisture (2 capacitance probes at 0.025 m)	✔	✔	
Surface moisture (5 TDR at 0.025 m)	✔	✔	
Moisture profile (2 capacitance 0.025, 0.075, 0.125, 0.175, 0.25, 0.40, 0.65, 1.00m)	✔		
Tensiometers (2 sets at 0.10, 0.20, 0.30, 0.50, 0.80, 1.10, 1.30 m) (2 sets at 0.20, 0.50, 0.80, 1.10, 1.30 m)	✔	✔	
Rain gauges	✔	✔	
Wet and dry mass of the organs	✔	✔	✔ F
Height of the crop	✔	✔	✔ F
Leaf area index (direct and LAI 2000)	✔	✔	✔ F

Table 4. Measurements performed routinely on the calibration, validation and remote-sensing fields. F means that these measurements are mainly performed during the flights.

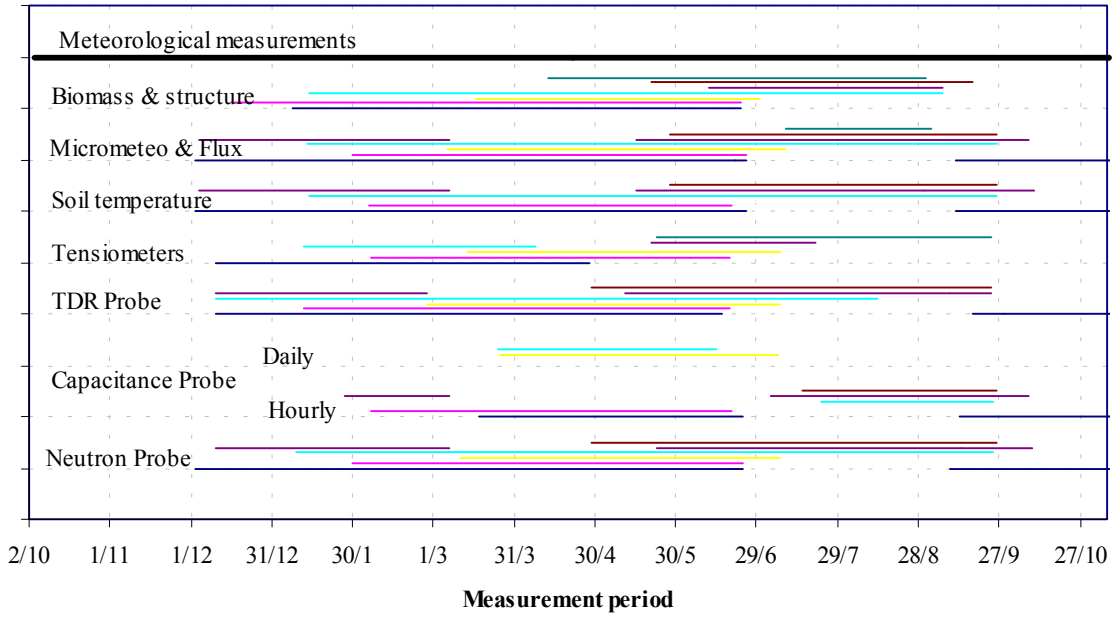

Figure 11. Temporal distribution of the measurements on the main calibration and validation fields. Each colour bar corresponds to a particular field, from bottom to top for each set of measurement: 101, 120, 214, (wheat),203 (alfalfa), 102, 121, 501 (sunflower).

5.1.4.2 Soil measurements

5.1.4.2.1 Soil permanent characteristics.

Soil permanent characteristics were measured over the calibration and validation fields. This includes physical, chemical analysis. Additionally, other soil functioning variables were measured and considered stable during the growth period. It includes density, retention, hydraulic and thermal conductivity curves.

5.1.4.2.2 Soil dynamics measurements.

- ***surface moisture.*** Soil surface moisture was measured at specific dates corresponding to the µ-wave instrument overpasses (either ERS, radarsat, or ERASME/RENE). They were acquired using either the gravimetric procedure, or using the capacity gauges providing a good temporal sampling and TDR devices providing a good spatial sampling.
- ***Soil roughness***. The roughness profiles were measured using either an automated non contact laser profiler, 1.5 m long, with a sampling interval of 1.7mm, or contact needles over 1-2m long with a sampling interval between 5 to 10mm.The measurements were carried out over 12 fields including wheat, sunflower, alfalfa and maize validation and calibration plots. They were performed after the main cultural practices (tillering, sowing, harvest) over five to eight profiles orthogonal and parallel to the row or tillage directions. The processing provides the standard deviation of height, the correlation length and the calibrated digitised profiles.
- ***Soil moisture and tension profiles***. Frequent moisture profiles and tensiometer measurements were performed over the calibration and validation fields. Figure 12 shows the good agreement between the several methods used for soil moisture measurements.
- ***Temperature profiles***.
- ***Soil heat flux***. Heat transducers were used.

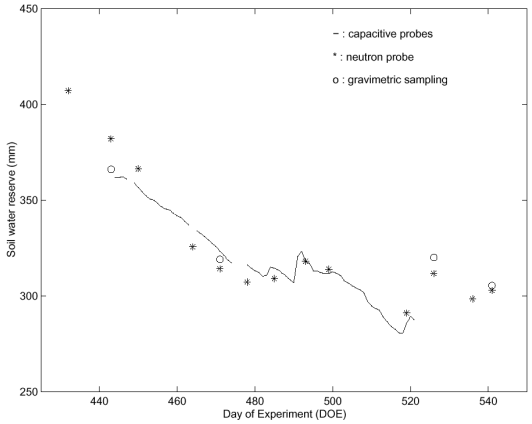

Figure 12. Comparison of water storage in the 0-120 cm soil layer as obtained by different methods of measurement on field 101.

5.1.4.3 Canopy measurements

5.1.4.3.1 Canopy structure and biomass

The ground data collected throughout the growing season were processed to provide values representative of the fields. They include the leaf area index (direct measurements) canopy height and the fresh and dry biomass per organ. An example of the output is shown in figure 10. No particular problem is to be noticed, except that in some plots the heterogeneity was important.

5.1.4.3.2 LAI2000 gap fraction and leaf area index.

LAI2000 measurements were performed frequently over a selection of plots during the growing season. Ten random places were sampled using ten measurements to get a good representation of the field value. The data were processed to get estimates of the leaf area index, and the average leaf angle. Figure 13 shows the relatively good agreement between both types of measurements. The scatter could be explained mainly by spatial heterogeneity, and the biases by the fact that LAI2000 estimates accounts for the area of other components than just green leaves, i.e. senescent organs, stems and ears that could represent a significant fraction of the total area index, particularly at the end of the growth cycle.

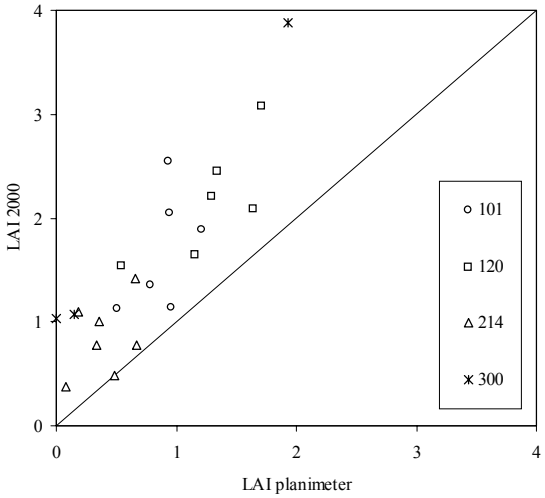

Figure 13. Comparison between LAI2000 estimates of *LAI* and direct *LAI* measurements. Results over wheat fields.

5.1.4.3.3 Ground Reflectance measurements

Bi-directional reflectance measurements were performed mainly during intensive campaign using the CROPSCAN radiometer. The instrument used has the following bands: 490, 550, 670, 700, 740, 780, 870 and 1090 nm. A wheat field and a sunflower fields were sampled.

5.1.4.3.4 Emissivity measurements

Emissivity measurements were performed for alfalfa and wheat crops in April, and for sunflower and corn crops in July. The box method with one-lid or two-lids was used. For both methods (one-lid and two-lid) emissivity calculations have been corrected from effects due to the non-ideal nature of the box according to the procedure of Rubio et al. (1997). Depending on the nature of the crops, measurements were taken for pure samples (soils and plants) and for mixed samples (plants over the natural soil background).

In addition to emissivity measurements, the cover fraction and spatial distribution of plant elements over the plots were measured.

5.1.4.4 Atmosphere measurements

5.1.4.4.1 Meteorological station

It measured the main climatic variables on a 20 minutes frequency basis during the whole experimental campaign. The meteorological instruments were located in the centre of the test site. It was maintained over a natural vegetation (bare soil in winter, and natural grass developing during the season). The height of the vegetation was kept below 0.20m. The measurements included:

- Global, diffuse, long-wave and PAR radiation
- Air temperature at 2m height
- Vapour pressure at 2m height
- Wind speed and direction at 2m height
- Soil temperature at 0.1, 0.5 and 1.0m depth
- Rain
- Atmospheric pressure

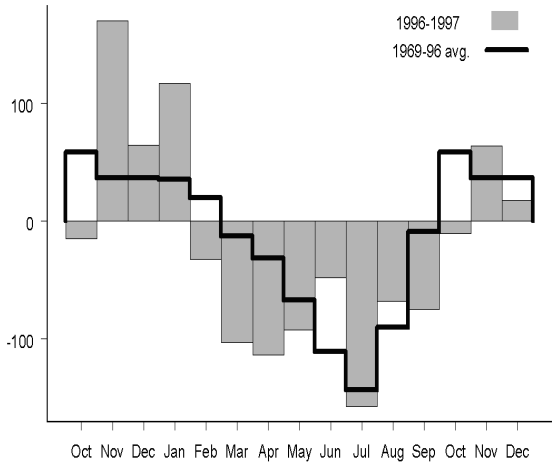

Figure 14. Temporal profile of the difference between monthly rainfall and evapo-transpiration (P-ETP) during the ReSeDA campaign as compared to the average values observed in Avignon.

The data from the meteorological station have been processed and evaluated. This includes test of consistency

- with the station from Avignon,
- the temporal consistency
- the consistency with the data available over the calibration and validation fields.

During the ReSeDA experiment, the winter was particularly wet, and the spring very dry (Figure 14). Other periods show quite regular patterns. These climatic conditions influenced largely the growth of wheat crops and the installation phase of summer crops.

5.1.4.4.2 Atmosphere characteristics

Three sets of measurements were performed:

- The ***CIMEL sun-photometer*** was permanently installed within the meteorological site. It provided the optical depth in various directions and in several wavebands. This CIMEL device was running automatically. Additional measurements

with a manual sun-photometer were performed to check the outputs of the automatic instrument.

- The ***direct and diffuse global radiation*** of the meteorological station allows to estimate quite accurately the aerosol optical thickness when sun photometer measurements were not available (Figure 15)
- The ***radio-sounding*** data from the Nîmes Courbesac airport which is about 40 km from the experimental site were systematically recorded during the flights. Additional radio-soundings were performed by Meteo-France during intensive campaigns to better characterise the atmosphere both for the correction of thermal infrared and optical observations and for a better characterisation of the planetary boundary layer used in the modelling of the fluxes between the soil, vegetation and atmosphere.

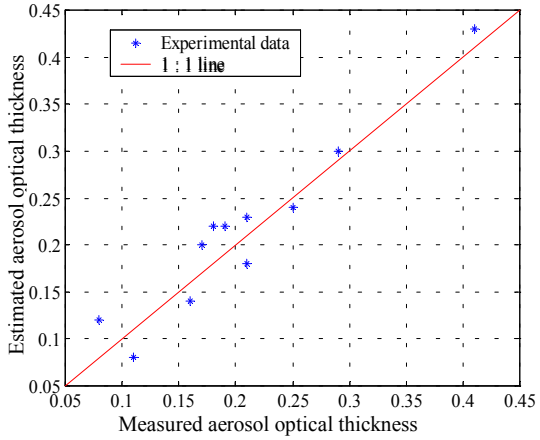

Figure 15. Comparison of Aerosols optical thickness at 550 nm measured by solar photometer and that estimated by equivalent direct solar pyranometer measurements.

5.1.4.4.3 Energy balance and flux measurements

Micrometeorological measurements were performed over calibration and validation fields with a time step of 15 seconds and an averaging period of 20 minutes. The instrumentation was installed at least at 100 m of the upwind edge of the fields. It consisted in air temperature, relative humidity and wind speed measurements. All the instruments were calibrated and inter-compared before and after the experiment. The measurements were performed at two levels above the canopy (at about 1.5 times and 3 times the canopy height) to be able to compute heat fluxes by means of the Bowen ratio method or the ***combined aerodynamic method***. However, frequent failures in the instrumentation did not allow to use these data with a good confidence. Moreover, a misconception of the system for measuring vapour pressure and temperature gradients did not allow to compute the fluxes with a good accuracy: at least half of the measurements were rejected. However, additional flux measurements were performed as a backup of the previous system:

- ***Mono-dimensional eddy-correlation*** systems were performed as often as possible and generated a significant set of data over the three wheat fields;
- ***Three dimensional sonic anemometers*** measurements were also performed for some days in June over a wheat field;
- ***commercial Bowen ratio*** systems based on dew point hygrometer measurements or on direct gradient measurements also provided data on wheat fields.

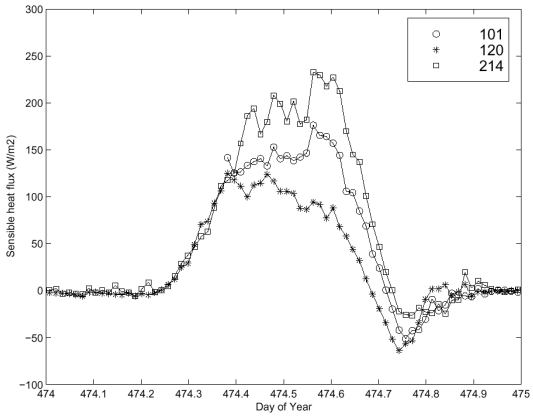

Figure 16. Comparison of sensible heat flux based on the eddy-correlation method over three wheat fields during a particular day.

5.1.4.4.4 Spatial heterogeneity of fluxes.

To investigate the effect of spatial heterogeneity of the fluxes, two systems were used:

- ***The unmanned plane*** from Cranfield University (Figure 17) was launched with a payload including sensors for temperature, humidity and position. Extensive data processing has been performed to check data quality and provide a consistent dataset with common time and position references. Results show the expected general features of the surface layer profiles of temperature and humidity and also give details of structure near field boundaries.
- ***Scintillometer measurements*** were performed in June 1997 over a transect including an important contrast between fields. Simultaneous eddy correlation flux sensors measurements were taken for the individual fields within this transect. Figure 18 shows the installation of the devices over the scintillometer transect.

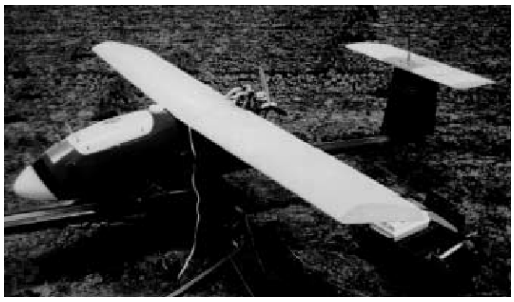

Figure 17. The Cranfield University unmaned aircraft used.

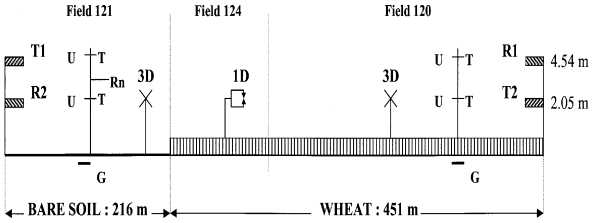

Figure 18. The scintillometer measurements performed in the center of the Alpilles site.

5.2 The data base

The data base is one of the important output of the ReSeDA project because it will provide input for testing radiative transfer, SVAT and canopy functioning models, as well as the associated inversion and assimilation techniques. This will obviously be used for the ReSeDA scientific objectives themselves, but it will also be available to the whole scientific community. For this reason, it should be very easy to access and to use. The data base is hosted at INRA at the following address: www.avignon.inra.fr/reseda where a dedicated hard disk was installed.

5.2.1 Structure of the data base and diffusion

5.2.1.1 The data base

The structure described in Figure 19 was implemented. Directories were created for the main categories of data. These directories can be divided into subdirectories according to specific sensors or measurement type. In the last level sub directories, there are three types of files:

- The ***documentation file*** that provides information on the type of measurements, protocols and implementation of the measurements during the experiment. This is generally a RTF, PDF or ASCII format
- The ***update file*** that provides information on the last changes. It is an ASCII file.
- The ***data files*** that contain a header with a description of the data format and the data them selves. They are also ASCII files.

The consistency of the data base was checked by combining several tests. Further, the first exploitation of the data that is described in the following sections was also a good opportunity to evaluate the quality of the data. However, it is possible that in places, errors and uncertainties are embedded. That is the reason why we would like any problem encountered to be reported in order to take the proper actions for correction. The data base will therefore evolve and improve in the next years. Therefore, the web server appears as the most convenient media for distribution of the data and was preferred to CD-ROM or DVD at this stage.

When data will be used by scientists outside the consortium, it will be asked to acknowledge the people and institutions who directly collected and processed the data as well as the funding organisations, i.e. the European Commission and the French Programme National de Télédétection Spatiale.

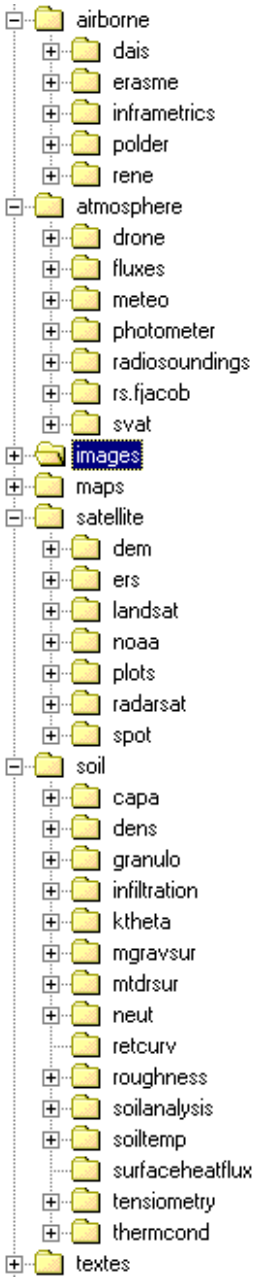

Figure 19. General structure of the Reseda data base.

5.2.1.2 The web server

The web server originally hosted by Synoptics was transferred to INRA Avignon. It includes three main components:

1. A ***general description*** of the ReSeDA project, the partners with proper links and the funding organisations.
2. A ***list of the papers*** that have been published from the project. Most of the papers will be accessible fully in electronic version (PDF) except when copyrights are active.

3. A ***description of the data base*** with links to the corresponding directories and files for downloading.
The maintenance of the web server for the next years will be under the responsibility of INRA Avignon.

5.3 Development and evaluation of inversion methods

The inversion of radiative transfer models from remote sensing data as illustrated by figure 14 can be defined by four main aspects :

1. *The choice of the biophysical variables to be retrieved.* These variables had to be very intimately related both to the radiative transfer process within the canopy and to the vegetation processes to be described. We focussed on the 9 following variables that were already listed in Table 1 as a function of the spectral domain where it is accessible:

- ***albedo***, the bi-hemispherical reflectance of the canopy integrated over the 300-3000nm spectral domain
- f_{Cover}, the cover fraction that corresponds to the gap fraction for nadir direction,
- f_{PAR}, the daily fraction of photosynthetically active radiation absorbed by the canopy
- ***LAI,*** the leaf area index that defines the size of the main interface for exchange of energy and mass between the canopy and the atmosphere
- h_c, the height of the canopy that is very important for the determination of the resistance to transfer used in SVAT models.
- W_c, the canopy water content
- W_s, the surface soil water content
- h_{rms}, the roughness of the soil surface
- ***Ts,*** the surface temperature of the canopies (soil and/or vegetation)

2. The type of remote sensing data used. The spectral, directional and polarisation features of the radiometric response can be used to extract canopy characteristics. The ReSeDa has put some emphasis on the directional dimension, particularly in the thermal and solar domains.

3. The choice of the radiative transfer model. Radiative transfer models differ mainly by the way they consider canopy structure and the way the radiative transfer equation is approximated. The model had to be relatively general although realistic. Both constraints appear however to be antagonist because of the diversity of canopy structure. Further, for routine application, the model is desired to run fast, particularly when using iterative optimisation techniques. The choice of the radiative transfer model is therefore a critical question to minimise uncertainties in the inversion process. The several radiative transfer models used in ReSeDA are presented in Table 5. The operational models that can be used for applications are distinguished from reference models that attempt to describe the best both canopy structure and the radiative transfer.

	Model type	Physical				Semi-empirical
	Radiative transfer computation	Turbid medium		Geometric	Ray tracing	
	Representation of the scatterers	Continuous	Discrete	Geometric	Realistic	
Solar domain	PROSPECT (leaves)		Oper			
	SOILSPECT (soil)	Oper				
	CGI		Oper			
	SAIL/KUUSK/IAPI/NADI	Oper				
	CLAIR					Oper
	BRDF (MRPV, Walthall, FLIK)					Oper
Thermal Infrared	SAIL-T	Oper				
	Prévot	Ref				
µ-wave active	IEM (soil)	Oper				
	MIMICS		Ref			
	KARAM		Ref			
	ACT		Ref			
	CLOUD					Oper
µ-wave passive	TSA	Oper				
	MEV		Ref			
	[ω,τ]					Oper

Table 5. The radiative transfer models used over the spectral domains in ReSeDA. Operational (Oper) and reference (Ref) models are distinguished.

4. ***The choice of inversion techniques***. Two main approaches are classically used by the geophysical and thus the remote sensing scientific communities as illustrated by Figure 20:

- **Minimisation of the distance over radiance.** This is generally achieved through various optimisation techniques where, starting from an initial set of input variables, these values are iteratively updated up to the point where a good match is reached between the radiance field simulated by the models and that measured by the sensors. The use of look up tables is a special case of these iterative techniques.
- **Minimisation of the distance over the variable of interest.** This is generally achieved through approximation of the surface response, using mathematical methods such as neural networks that learn to approximate the inverse relationship between the radiance field and the variables of interest. Simpler relationships such as vegetation indices used to estimate several variables such as *fAPAR* have been investigated extensively. The split-window technique for atmospheric correction in the thermal infrared belongs also to that category of approach. The minimisation is performed here in a first step, the learning or calibration phase.

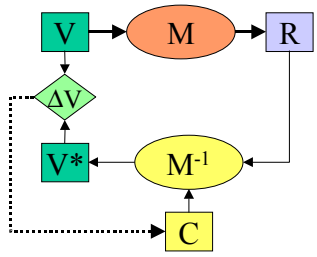

Canopy variable driven approaches: minimising on canopy variables
(vegetation indices, neural networks, …)

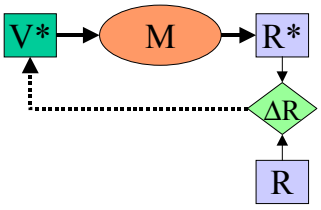

Reflectance driven approaches : minimising on reflectance
(iterative optimisation, look up tables)

Figure 20. The two main approaches used to estimate canopy characteristics from remote sensing data. V, R and M respectively represent the variables of interest, the reflectance and the RT model. M^{-1} is the inverse model with coefficients C. V* represents the estimated value of V, and R* the corresponding simulated reflectance. Δ represents the distance between either R (ΔR) or V (ΔV).

We will review here the work achieved up to date about model inversion. This includes studies on:

- the modelling of radiative transfer models,
- comparison of radiative transfer models
- comparison of inversion approaches
- investigation of the optimal spectral and directional sampling
- and obviously investigation on methods of canopy biophysical variable estimation using the actual ReSeDA data.

We will present the studies by wavelength domains, since the sensors and radiative transfer models are quite different. We will start from the lower wavelengths in the solar domain, then address the thermal infrared domain, and finally go to the µ-wave.

5.3.1 Inversion in the solar domain

5.3.1.1 Investigation about inversion techniques

Three main inversion techniques have been compared, based on a simulation experiment:

- **LUT:** The look up table (LUT) is the simplest approach, although not straightforward to implement. The LUT was generated by randomly drawing the model input variables within a distribution law designed to better sample regions where reflectance is more sensitive to the variable. Each variable were considered independent. A set of 280 000 cases was generated, and the corresponding reflectance values were simulated thanks to SAIL +PROSPECT models. The median value and the standard deviation were computed over the 50 best solutions found in the table .
- **OPT:** The optimisation technique is one of the mostly used at this time for radiative model inversion. The initial guess was derived from a simple look up table. The quasi Newton search algorithm was used. The cost function was designed to impose constraints on the variables to be estimated and takes also into account the uncertainty associated to the measurements and the models. The distribution of the solutions were obtained by inversion of the model over the distribution of the measured reflectance for each case, taking into account the uncertainty of each measurement. Again the median value and the standard deviation were used to characterise the solution.
- **NNT.** The neural network technique (NNT) is rapidly developing for the estimation of biophysical variables. In this case, a 2 layer back-propagation network was used, trained with the Levenberg-Marquart procedure. The learning data set was made of 50000 cases taken among the 280000 cases simulated for the LUT approach. A set of 30 parallel networks for each of the four biophysical variables considered was used to form

the solution. The median value of the ten best neural networks was retained as the solution. When the noise associated to the reflectance values was known, it was introduced in the learning data set.

The three inversion techniques were compared over a reference data set made of ray tracing model simulation applied on a 3D realistic maize architecture (Figure 21). The LUT performs generally similarly to the OPT method although the NNT gets generally better results.
Figure 21 shows that the f_{APAR} and f_{Cover} are the variables the better retrieved with a relative *RMSE* close to 10% which is very encouraging. Then, estimates of the chlorophyll content C_{ab} is retrieved within 15% relative accuracy. Finally, *LAI* is retrieved with the worse accuracy, close to 25% relative *RMSE*. This shows clearly the advantage of using secondary variables that exploits the possible compensations between variables and could reduce the saturation problem such as in the case of f_{APAR} and f_{Cover}.

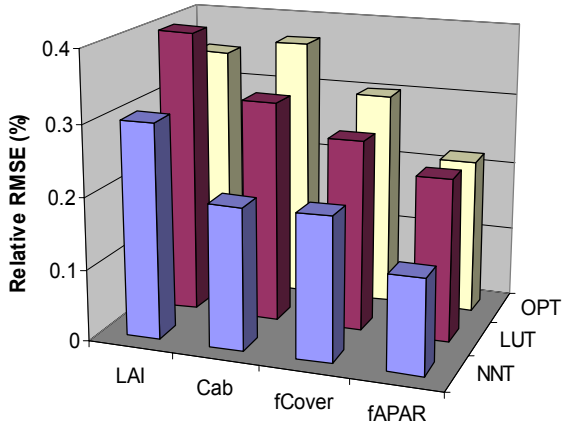

Figure 21. Comparison of retrieval techniques for the biophysical variables considered. Case with 2.5% radiometric noise and 2% biase.

5.3.1.2 Optimal spectral and directional sampling

The variables considered were *LAI*, C_{ab}, *fAPAR* and *fCover*. We used a simple inversion technique based on look-up-tables as implemented previously. The reflectance data were simulated in 9 wavebands in the visible and near infrared domain for 32 directions chosen in the principal and perpendicular plane. The sun position was fixed to 45° zenith angle.

5.3.1.2.1 Spectral sampling

Starting from the classical combination of red and near-infrared bands, the band providing the best estimation performances among the 7 remaining bands was selected. The same process was repeated until all the nine bands were selected.
Results (Figure 23) showed that, when the number of bands used increased, the absolute *RMSE* value was decreasing until a minimum is reached. This demonstrated that only a limited number of wavebands were required for canopy biophysical variable estimation. The estimation of *fAPAR* and *fCover* required less bands than for *LAI* and C_{ab}.
The *RMSE* value difference computed over the biophysical variables of interest between the best and the poorest band selection demonstrated that the choice of the bands was obviously important, particularly for the first bands selected. The other bands were generally selected in the red-edge domain (680-740nm) where the dynamics of the vegetation spectrum is the largest.
As a conclusion of this step, we decided to keep the band combination that gave the lowest *RMSE* for each variable : For these optimal band sets, the optimal directional sampling was then investigated.

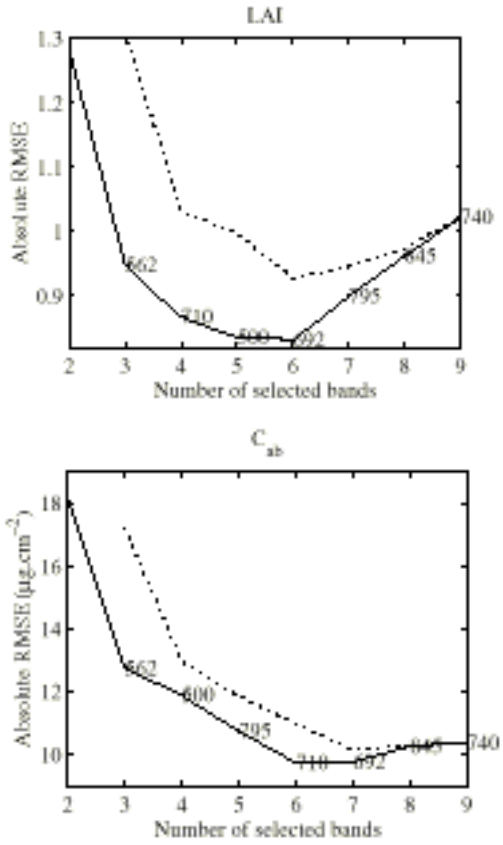

Figure 22 Absolute *RMSE* value between actual and estimated canopy variables (*LAI* and C_{ab})as a function of the number of bands selected for each canopy biophysical variable of interest. The solid line corresponds to the best band combination and the dotted line to the worst combination.

5.3.1.2.2 Directional sampling

Considering the best set of bands for each variable as derived for nadir viewing, the same procedure as the one used previously for the spectral sampling was applied to select the optimal directional combination.
Results showed that for each of the four biophysical variables considered, less than six directions were required (Figure 23). The other directions contained redundant information and thus, their use as additional bands induced noise in the retrieval process. The first selected direction was able to reduce significantly the uncertainty on the retrieval of the four biophysical variables considered. For this direction,

the difference between the optimal and the worst view angle was large. The first directions were always located in the principal plane, either close to the hot spot direction, or in the forward direction to high zenith angles.

For the leaf area index estimation, only one direction, the hot spot, was required to obtain the lowest *RMSE* value, confirming the importance of that direction for canopy structure estimation. Moreover, the following selected angles were very close to the hot spot, except the second one which was located in the forward direction with high zenith angle. The leaf chlorophyll content estimation required more directions (6), mainly located in the backward and forward directions at high zenith angles, and in the hot spot feature. One direction in the perpendicular plane was also needed. Considering *fAPAR* and *fCover*, about six directions were required and only the first one was actually discriminating. Moreover, for *fCover* estimation, the first selected direction was the nadir which was fully consistent with the fact that it corresponds to the gap fraction in the nadir direction. For *fAPAR*, the first selected direction was located in the perpendicular plane (zenith angle of 30°) and the second one close to the hot spot direction. This was again consistent with the fact that *fAPAR* could be approximated by the gap fraction in the solar direction.

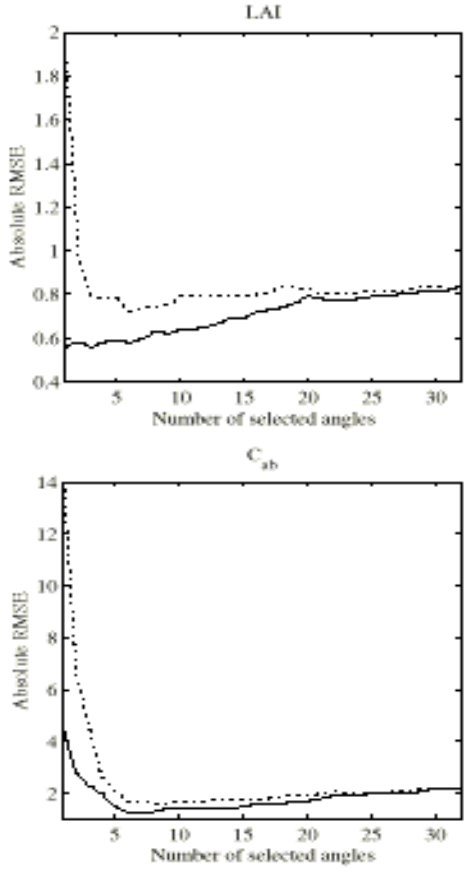

Figure 23 Absolute *RMSE* value between actual and estimated canopy variable (*LAI* and C_{ab}) as a function of the number of selected directions. The solid line and the dashed line corresponds respectively to the best and worse sets of directions.

5.3.1.3 Comparison of the inversion performances of three operational radiative transfer models

Operational models are based on different assumptions and approximations on canopy architecture and the computation of the radiative transfer. It is therefore required to compare the performances of the models when used in the inverse mode for estimation of canopy biophysical variables. This was achieved over three 1D turbid medium operational radiative transfer models, all coupled to the PROSPECT model for description of the optical properties of the leaves:

- ***PROSAIL***, the classical 1D turbid medium model developed by Verhoef (1984)
- ***PROKUUSK***, the model developed by Kuusk (1995),
- ***PROIAPI***, the model developed by Iaquinta and Pinty (1994).

The main differences between these models come from the description of the leaf angle distribution, the hot-spot effect, and the multiple scattering computation. The soil background was described by MRPV BRDF model fitted over bare soils. The POLDER data over the 16 flights were used to extract the BRDF for all the fields for which *LAI* was measured. It includes wheat, alfalfa, sunflower and maize. The 3 bands of POLDER were used (550, 670 and 865nm) for all the directions available. The inversion technique is based on a quasi-Newton optimisation algorithm implemented with a cost function that measures the relative distance between measurements and simulations. Among the variables (*Cab*, *Cw*, *Cm*, *N*, *S*, *LAI*, *ALA*, *hot*), three were set to a priori fixed values. The inversion was therefore concentrating on the other 5 variables: *LAI*, *ALA*, *Cab*, *S* and *N*.

All three models allow to get a good fit of the spectral BRDF as measured by POLDER, with RMSE values in the range 0.02 – 0.04. Figure 24 shows that the three models are actually estimating *LAI* in a quite consistent way. The same applies for chlorophyll estimation.

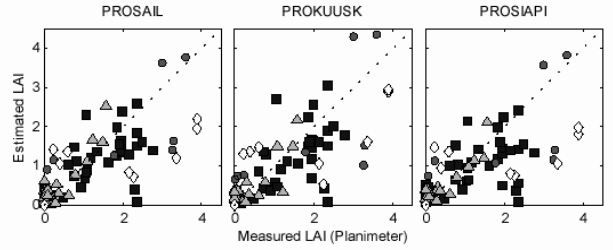

Figure 24. Comparison of measured *LAI* and values estimated by inversion of three radiative transfer models using POLDER data in three wavebands during the ReSeDA experiment.

It can therefore be concluded from this investigation that *LAI* could be retrieved with a quite good accuracy by radiative transfer model inversion. The slight differences between the three 1D turbid medium radiative transfer operational model tested have only marginal influence on the retrieval performances.

5.3.1.4 Validation of a neuronal technique for LAI and fCover estimation

The neural network technique is based on the minimisation of the distance over the variables to be estimated, conversely to the previous model inversion technique (OPT). A learning data set (1500 cases) was generated thanks to SAIL canopy model coupled to PROSPECT leaf optical properties and SOILSPECT soil reflectance models. The range of variation and distribution of the input variables were chosen to embrace the actual distribution over crops. The reflectance simulated were the nadir and the hemispherical reflectance in the three POLDER bands. The networks were trained as described earlier in §5.3.1.1 using 50 parallel nets from which the median of the output is computed.

The MRPV BRDF model was adjusted on the same POLDER data as previously. It allos to estimate the nadir and hemispherical reflectance values. As we will see latter, the MRPV model has very good interpolation capacity for nadir reflectance estimation, and reasonable extrapolation performances for hemispherical reflectance estimation. For *fCover* estimation, the input of the neural networks were the nadir reflectance in the three POLDER bands and the sun zenith angle. For *LAI* estimation, the hemispherical reflectance was required in addition. Figure 25 shows that the accuracy of the estimation is quite good.

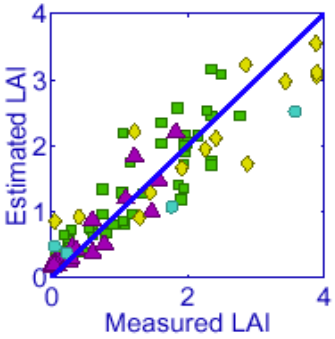

Figure 25. Comparison between measured *LAI* to the values estimated by the neural network.

Method	OPT	NNT	NDVI
RMSE	0.78	0.44	0.49

Table 6. RMSE values obtained over the Alpilles data set by using three inversion techniques (OPT: optimisation as implemented in §5.3.1.3; NNT: this neural network implementation; NDVI: NDVI estimation when calibrating the NDVI-LAI relationship on the same data base as the one used fortraining the nets).

Table 6 shows that the neuronal network outperforms the optimisation technique. For comparison, the NDVI estimation when the relationship between NDVI and *LAI* is calibrated over the same data set as the one used for the neural nets training, appears quite performing in these conditions.

The cover fraction (*fCover*) is generally better estimated than the *LAI*, with a RMSE value close to 0.08, as compared to 0.13.

These results are very consistent with the previous theoretical investigations presented in §5.3.1.1. It proves that model inversion is now very close to be an operational technique that could be used routinely for applications.

5.3.1.5 Robustness of the WDVI-LAI relationship for wheat crops.

The WDVI (Clevers, 1991) vegetation index was computed from the SPOT images over the wheat fields: $WDVI = \rho_{nir} - (C \times \rho_{red})$. The slope of the soil line (C=1.26) was calculated by using reflectance derived from the SPOT images for a bare field during the first half of 1997 and for the harvested wheat fields on August 30th, 1997.

A semi-empirical model was used to relate the *WDVI* to *LAI* according to Clevers (1991):

$LAI = -1/\alpha \times \ln(1 - WDVI/WDVI_{\infty})$

Clevers (1991) obtained for α a value of 0.252 at the vegetative phase and for $WDVI_{\infty}$ a value of 68.6 if the WDVI is based on NIR and red reflectance. At the reproductive phase he obtained for α a value of 0.530 and for $WDVI_{\infty}$ a value of 57.9. Using this equation and the above coefficients obtained over crops under Netherlands' conditions, Figure 26 shows the good agreement and robustness of the approach.

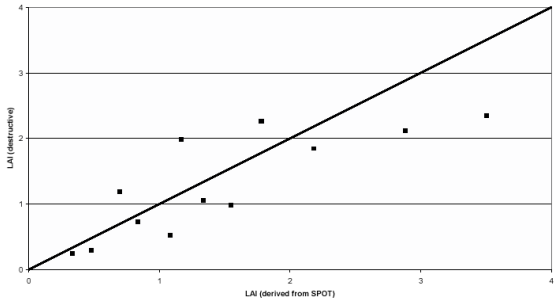

Figure 26. Comparison between measured *LAI* values to those estimated using *WDVI* applied to SPOT data over wheat and Clevers (1991) semi-empirical model.

5.3.1.6 Using BRDF and hybrid models for canopy height estimation

Estimation of canopy height could be very interesting because it is one the main driver of the heat exchange between the canopy and the atmosphere. A 3D radiative transfer model is thus mandatory to be able to extract canopy height from the BRDF signature. For this purpose, the hybrid geometric-turbid medium CGI model was implemented (Figure 27).

The variables of the models were tuned for wheat crops. Figure 28 shows that CGI allows to get a good representation of the BRDF of wheat crops as measured by POLDER during the growing season. The CGI model was then inverted by using a look up table technique based on simulation of hot-spot and nadir *WDVI* values ($WDVI = R_{865} - \alpha . R_{670}$ where α is the soil line slope). The *WDVI* allows to account for soil background reflectance variation.

Application of this technique to the ReSeDA POLDER data over wheat fields appear to provide poor estimates of canopy height. As a matter of fact, a detailed sensitivity analysis showed that the illumination conditions during the experiment (sun position) did not allow to get enough handles on the BRDF to extract accurately canopy height.

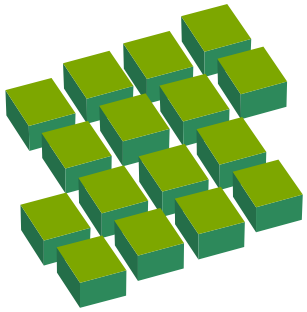

Figure 27. Typical canopy structure representation by the CGI model. The geometric protrusions are considered turbid medium object. This view corresponds to the hot-spot (no shadow).

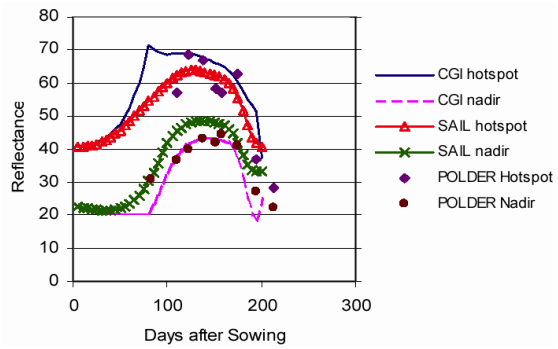

Figure 28. Comparison between CGI simulations and actual canopy reflectance as measured by POLDER during the growth season over wheat.

5.3.1.7 BRDF models and albedo estimation

BRDF models are developed to describe (rather than explain) the directional variation of reflectance. They are very useful for the normalisation of reflectance data acquired under different viewing conditions, as well as for the derivation of the hemispherical reflectance used to compute albedo. We will first show the results obtained on the comparison of classical BRDF models, and then address the problem of albedo estimation.

5.3.1.7.1 Comparison of BRDF models

Linear kernel models are now classical to describe the BRDF as:

$$\rho(\theta_o,\theta_s,\phi) = \sum_{i=1}^{k} \alpha_i . K_i(\theta_o,\theta_s,\phi)$$

where $\rho(\theta_o,\theta_s,\phi)$ is the bi-directional reflectance, k is the number of kernels i used, $K_i(\theta_o,\theta_s,\phi)$ are kernel functions, and α_i the associated kernel coefficients. We considered 10 models:

- ***Walthall*** et al. (1985) which is mostly an empirical model, with 3 parameters but without hot-spot description. Further it is not reciprocal
- ***MRPV*** (Engelson et al., 1996) which a semi-empirical model, with 3 parameters, reciprocal, ith a hot-spot feature. It is originally not linear, bit it could be linearised.
- ***Roujean*** et al. (1992), which is a semi-empirical model with 3 parameters, reciprocal and with a hot-spot feature.
- **Li-Ross** (Wanner et al., 1997). Which is based on simple geometric-optic model. It has 3 parameters, is reciprocal and has a hot-spot feature.
- ***Nadir*** Which is the simplest BRDF model, assuming that the canopy is lambertian with reflectance equals to that at nadir. It has no parameter.
- ***GEN*** that stands for generic BRDF model. It has a generic shape based on average MRPV functions. The BRDF is adjusted to the measured reflectance by offset and gain. It has therefore 2 parameters and is reciprocal and has a (generic) hot-spot feature.
- **FLIK3-FLIK6** which is based on the adjustment of empirical kernels over a BRDF data base generated by radiative transfer simulations. It can have in principle any number of kernels. In practice, this number was limited to 6. Figure 29 shows that the directional variation could reasonably be represented by a small number of kernels. FLIK is reciprocal and has a hot spot feature.

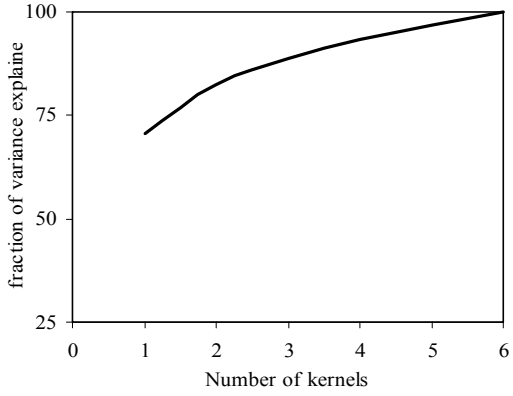

Figure 29. Fraction of the variance in the BRDF explained, as a function of the number of kernels used.

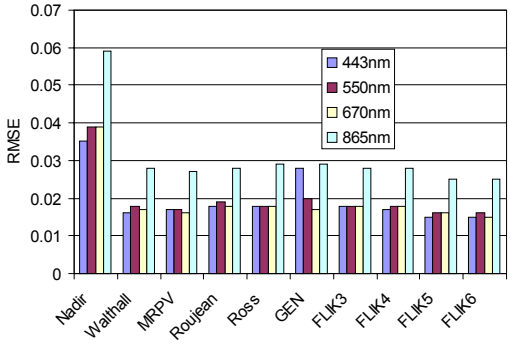

Figure 30. Goodness of fit of the 10 BRDF models investigated on the POLDER data acquired over the whole growing season on a selection of fields.

The results were analysed in two ways:

- ***Fitting capacity***. It measured the goodness of fit of the models to the POLDER BRDF data. Figure 30 shows that, except the lambertian assumption (nadir), and to a lesser degree GEN, all models are performing reasonably well, with a RMSE close to 0.015 in the visible and 0.025 in the near infrared. Because of the good fitting capacity of most of the BRDF models, reflectance at nadir which is a privileged direction sampled by current polar orbiting sensors will always be accurately estimated.
- ***Extrapolation capacity***. It describes the capacity of a BRDF model to estimate the reflectance in directions outside directions used for adjusting the model. This criterion is very important when estimating the hemispherical reflectance. Results show (Figure 31) that most models are reasonably well reconstructing POLDER data when adjusted in the principal plane. However, when adjusted in the perpendicular plane, the situation is more complex. For the models with the larger number of parameters, the results are very poor. The directional signature in the perpendicular plane is not sufficient to get enough constraints on the BRDF model. In this case, the generic model performs the best.

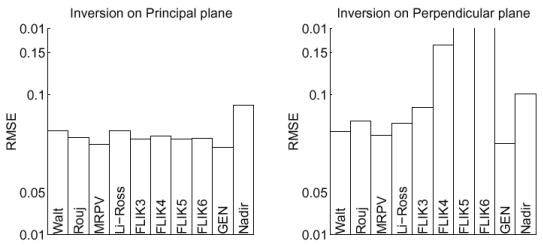

Figure 31. Extrapolation performances of the BRDF models. The models are adjusted either over the data close to principal plane (left) or close to the perpendicular plane (right). They are then tested over all the POLDER data.

5.3.1.7.2 Albedo estimation

Albedo is one of the main variables governing the radiation balance and thus the energy balance. We will restrict the problem to the estimation of the instantaneous albedo, i.e. the bi-hemispherical reflectance integrated over the 300-3000nm spectral domain, as it could be observed concurrently to remote sensing data acquisition. The estimation of albedo values from remote sensing data poses at least two main problems:

Directional: the estimation of hemispherical reflectance from a limited number of directions sampled by the sensor. This was investigated previously. We mainly selected Walthall model for its robustness and MRPV model for its performances when sufficient directions are sampled with accurate reflectance data.

Spectral: the estimation of albedo from a limited number of hemispherical reflectance. We tested three sets of coefficients proposed by Weiss et al. (1999) and shown in Table 7.

	445	560	665	865
Set #1	0.000	0.000	0.570	0.460
Set #2	0.000	0.680	0.080	0.350
Set #3	0.060	0.690	0.001	0.350

Table 7. Spectral coefficients used to extend to the whole spectral domain the hemispherical reflectance observed in few wavebands.

The validation was performed over field measurements of albedo in the validation and calibration fields. It shows an overestimation that should mainly result from the spectral coefficients that were derived over 400-2500nm spectral domain as compared to the 300-3000nm spectral region considered by albedo measurements. Further work should be directed to address this issue, particularly considering the fact that very little data is available on the spectral properties of leaves and soils at these extremities of the solar spectrum. However, an empirical correction performed over the experimental points (Figure 32) shows that the relative accuracy achieved this way is close to 8%. Possible improvements could be gained by considering the diffuse radiation at the time of the measurements.

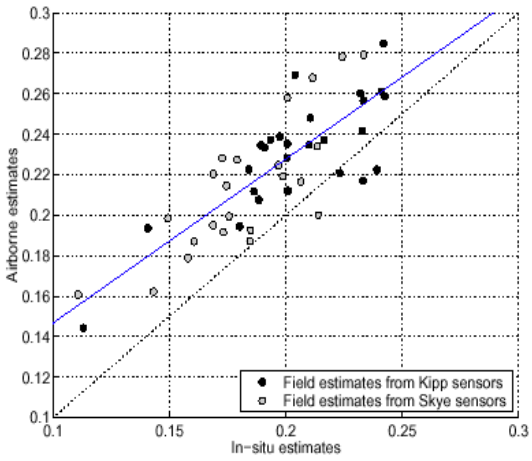

Figure 32. Comparison beween measured values of albedo and the values estimated using POLDER data and MRPV model with the set #3 of spectral coefficients.

5.3.1.8 Scaling issues

The scaling effect when observing heterogeneous landscapes is certainly one of the main problems when estimating canopy biophysical variables from remote sensing data. This is obviously linked to non linearity in the relationship between the radiometric data and biophysical variables.

This question was investigated both from the theoretical and the experimental aspects.

5.3.1.8.1 Theoretical investigation.

A simulation study was developed to evaluate the error associated to the estimation of biophysical variables over heterogeneous pixels. Pixels with the same value of biophysical variable such as *LAI* and *fCover* were generated under a range of spatial distribution. The corresponding reflectance value was

computed. An index of heterogeneity was built that reflects the spatial heterogeneity of the pixel. It ranges from 0.0 for homogeneous pixels, up to 1.0 for the most heterogeneous pixel made of equal fraction of bare soil and vegetation cover. Results (Figure 33) show that the *LAI* estimation is strongly dependent on the degree of heterogeneity of the pixel. Relative errors up to 40% can be observed in the case of heterogeneous pixels with the largest *LAI* values. Moreover, the *LAI* value is generally underestimated over heterogeneous pixels. The same was observed for chlorophyll content estimation. Conversely, the estimation of the cover fraction is little sensitive to the pixel heterogeneity. The same applies for *fAPAR*. This is mainly due to the fact that *fCover* and *fAPAR* are flux variables that are almost linearly related to radiometric data conversely to *LAI* and chlorophyll content that express strong curvature.

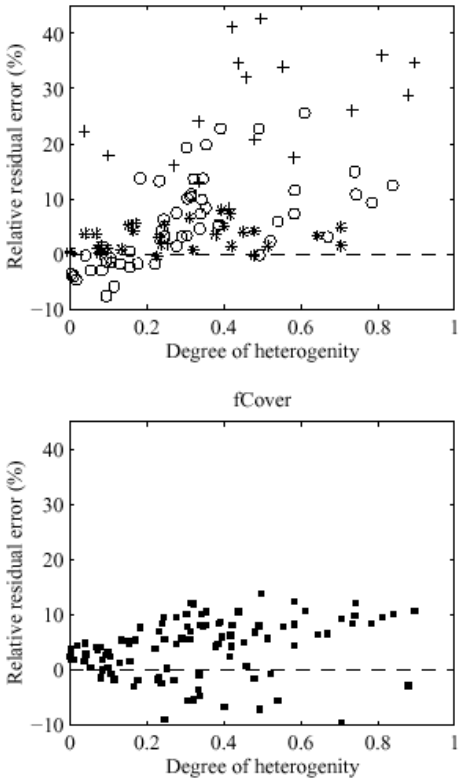

Figure 33. Relative error when estimating *LAI* (top) and *fCover* (bottom) from remote sensing data over heterogeneous pixels. Results from a simulation experiment. The retrieval technique used here is based on look up tables.

5.3.1.8.2 Experimental evidence

The POLDER data were used to validate the previous findings. The 16 POLDER flights were used to compute the radiometric data over a single 1km² pixel. The neural networks trained as explained in §5.3.1.4 were fed with the 1km² averaged reflectance value. This estimation was compared to that obtained when averaging over the 1km² pixel the output of the neural nets fed with the POLDER resolution reflectance data. Results (Figure 34) confirms the theoretical findings, with a significant systematic error for *LAI*, and little effect for *fCover*. These findings indicate that the estimation of biophysical variables such as *LAI* and chlorophyll content derived from large swath satellites with a low spatial resolution should be corrected from the a priori knowledge of the spatial heterogeneity.

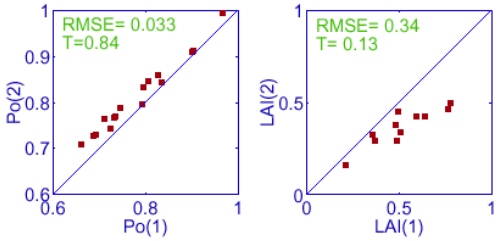

Figure 34. Impact of the spatial resolution over heterogeneous pixels for the estimation of *fCover* (1-Po, figure on the left) and *LAI* (figure on the right). The comparison is made when feeding the neural net for the estimation of biophysical variables with (1) the reflectance values averaged over a 1 km² pixel, against (2), when using the original POLDER spatial resolution and averaging the estimated biophysical variabes over the same 1km² pixel.

5.3.2 Inversion in the Thermal Infrared domain

Three main issues were addressed in this domain. First, the atmospheric correction problem in order to retrieve ground brightness temperature from that observed at the sensor level. This will be illustrated using the NOAA/AVHRR data. Then, the decoupling between emissivity and temperature, mainly using the DAIS data that provides enough spectral features in the thermal infrared. Finally, we will address the problem of the directionality of canopy temperature as observed by the INFRAMTRICS camera.

5.3.2.1 Water content estimates from NOAA/AVHRR

The total atmospheric water vapour content is estimated by a statistical analysis of the brightness temperatures at two wavelengths where water vapour is the principal absorber. The split window channels of AVHRR instruments (11 and 12 μm) are thus good candidates. The split-window variance-covariance method (Sobrino et al., 96; Ottlé et al., 97) consists in relating the atmospheric water content to:

$$\overline{R} = \frac{\sum_{k=1}^{N}(T_k^{11} - T_0^{11})(T_k^{12} - T_0^{12})}{\sum_{k=1}^{N}(T_k^{11} - T_0^{11})^2}$$

where the superscript and subscript refer respectively to the split window band and to a pixel within a window of analysis. All the AVHRR database was processed and the retrieved water vapour values were compared to the ARPEGE model outputs. The ARPEGE model is a numeric weather prediction model designed by Météo-France to work at regional scale. It is based on assimilation techniques of radiosounding data among other input

data. Results (Figure 25) show a very good correlation (R^2=0.91 ; RMSE=0.25cm). This method is thus quite interesting both for the estimation of the atmospheric water content, and for its use to correct the atmospheric effects in the shorter wavelengths from the water absorption.

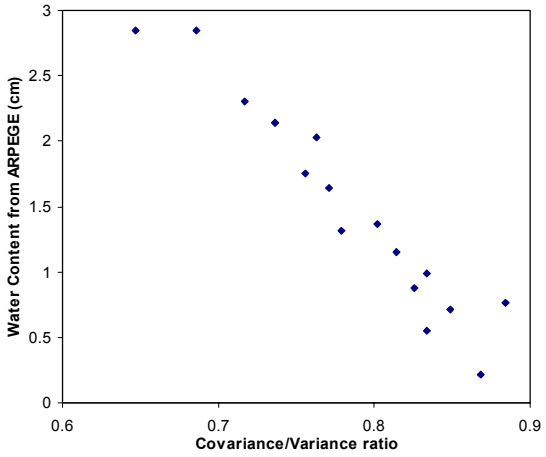

Figure 35 Atmospheric water content derived from the ARPEGE model compared to the Covariance-variance ratio for channel 11 and 12 of NOAA/AVHRR. 15 days selected for clear sky conditions.

5.3.2.2 Estimating temperature and emissivity from the spectral variation of DAIS data.

The Digital Airborne Imaging Spectrometer (DAIS 7915), acquired images over the ReSeDA test site on July 8, 1997 (Figure 36). Simultaneously, emissivity measurements were performed at the field level. The atmospheric correction was performed with a radiosounding as input to the MODTRAN radiative transfer code.

Using the surface radiances for a view angle θ, $L_j^{surf}(\theta)$, the NEM algorithm (Gillespie, 1986) has been applied. If an emissivity value, $\varepsilon_{NEM}(\theta)$, is assumed for all channels, then the previous equation can be solved for temperature for the N channels of the sensor as:

$$B_j(T_j^{NEM}) = \frac{L_j^{surf}(\theta) - (1-\varepsilon_{NEM}(\theta))L_j^{sky}}{\varepsilon_{NEM}(\theta)}$$

and T_j^{NEM} is calculated through inversion of the averaged Planck function while L_j^{sky} is obtained from MODTRAN calculations. This provides a set of N values of temperature (one per channel) from which the maximum value, is selected. The maximum temperature selected $T_{\max}$ is now used to obtain the N emissivity, through,

$$\varepsilon_j(\theta) = \frac{L_j^{surf}(\theta) - L_j^{sky}(\theta)}{B_j(T_{\max}) - L_j^{sky}(\theta)}$$

This provides a first estimate of the surface temperature and emissivity. The accuracy of these estimates depends on the assumed $\varepsilon_{NEM}(\theta)$. To minimise the error, we have selected $\varepsilon_{NEM}(\theta)$ according to the emissivity measurements. The NEM algorithm has been applied to arrays of 5×5 pixels extracted for selected fields.

Figure 36. Image of radiance at the sensor (no atmospheric correction) for DAIS channel 76, showing part of the ReSeDA test site with some selected plots indicated. North is up. Radiances range approximately from 0.92 to 1.51 mW/cm^2 sr μm (23 to 58 ºC).

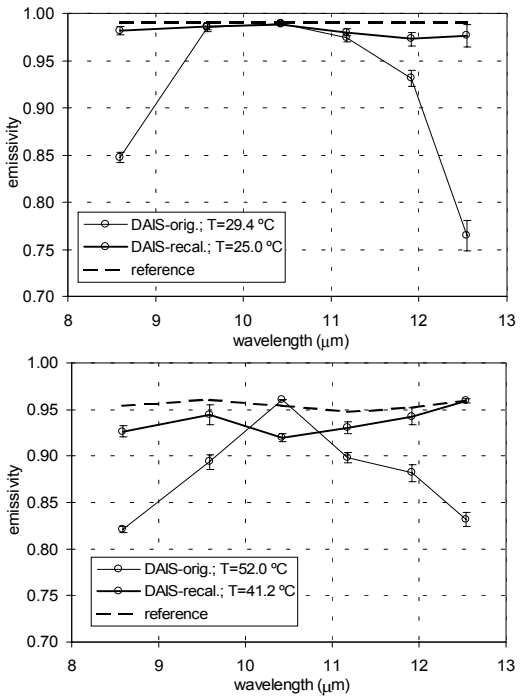

Figure 37. Corn and soil+stubble emissivity values derived from the DAIS instrument before and after re-calibration. The values are compared to ground emissivity measurements.

Results (Figure 37) show that The DAIS instrument has some calibration problem. This was corrected

according to ground measurements of surface temperature performed over two fields. The re-calibrated DAIS data were then used for estimation of emissivity over a selection of fields. The comparison with reference emissivity derived from ground measurements (Figure 37) shows a reasonable agreement between both values. The differences observed could be explained mainly by the poor stability of the calibration of the DAIS sensor in the thermal infrared.

5.3.2.3 Brightness temperature directional effects observed with the INFRAMETRICS camera.

Directionality of brightness temperature has received up to now little attention. However, few studies show the importance of these effects, both for normalisation of the data, but also for the exploitation of this information to allow the retrieval of the temperature of canopy components, i.e. the soil and the vegetation.

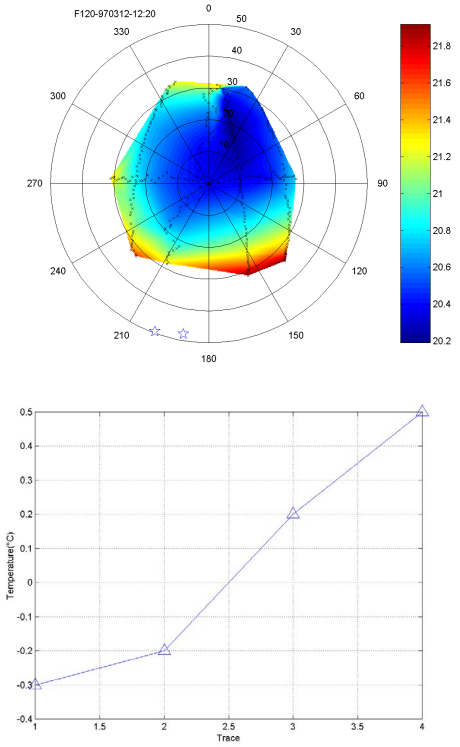

Figure 38. Schema showing the directional sampling achieved by the INFRAMETRICS camera (top in polar representation), and the temporal trend observed between the flight lines when looking at the cross points (bottom). The polar representation on the top shows the directional distribution of brightness temperature after temporal normalisation and smoothing.

The INFRAMETRICS camera equipped with a wide field of view angle was operating the same way as POLDER. Figure 38 shows the polar representation of its directional sampling for a particular field. However, conversely to the solar domain, the brightness temperature may vary significantly with time due to climatic conditions such as wind, turbulence cells, and radiation. Significant differences are therefore expected between observation of a single pixel from different directions for which the observations are separated by up to 20 minutes interval (Figure 38). Therefore, a simple procedure was applied to reduce this artefact on the directional effects. It consists in normalising the several observations to those acquired along the flight axis that crosses the four other axes close to the principal plane.

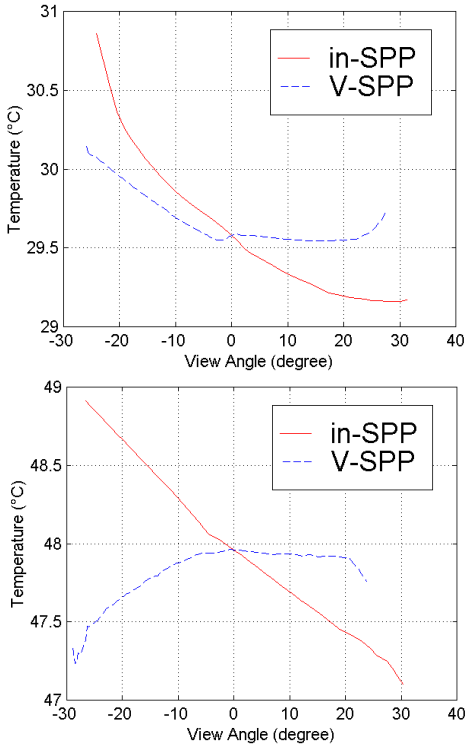

Figure 39. Directional variation of the brightness temperature in the principal (in-SPP) and perpendicular (V-SPP) planes for a bare soil (top) and corn (bottom) fields.

Results show a significant directional effects with an increase in the hot-spot direction corresponding to the maximum viewing of (hot) illuminated soil and vegetation. The perpendicular plane shows generally patterns symmetric to the nadir direction. The amplitude of variation is around 1 or 2°C in this limited directional sampling (roughly ±30°). In places it can reach up to 4°C in the hot-spot direction. This investigation shows prospects for exploiting this information if the hot-spot direction is sampled and if larger view angles are available.

5.3.3 Inversion in the µ-wave domain

Two main issues related to µ-wave data applications have been investigated. First, a qualitative one corresponding to land use classification. Then, a quantitative one corresponding to canopy and soil biophysical characteristics estimation. Similarly to the solar domain, radiative transfer models have been used for this second issue, and therefore, improvement of these models was also investigated.

5.3.3.1 Land use classification based on µ-wave

5.3.3.1.1 Using active µ-wave and multi-temporal data.

Land use classification is quite an important application of remote sensing. It is classically performed using the solar domain. However, because of the cost of the images and their often limited availability due to cloud occurrence, µ-wave could contribute significantly to this application.

The performances of land use classification based on ERS and Radarsat multi-temporal data were evaluated based on exhaustive ground survey. Three sets of time series of SAR data have been compared in the perspective of operational assessment:

- 3 dates of ERS2,
- 3 dates of Radarsat,
- 6 dates of bi-angular ERS and Radarsat.

The data were properly calibrated and masks were applied to non agricultural zones. Filtering was applied to the images in order to reduce the speckle. Three filtering techniques were tested

- no filter
- multitemporal filter from Lopez
- multitemporal + gammaMap filters
- Nagao filter

Sensor	Filter	Wheat (8 plots)	Maize (7plots)	Sunflower (11 plots)
ERS	No filter	45.0	26.9	0.0
	multitemporal	44.9	27.5	**33.8**
	Gamma Map	47.0	**33.9**	24.6
	Nagao	**48.7**	29.1	0.1
Radarsat	no filter	23.8	31.4	0.1
	multitemporal	33.6	34.2	**17.3**
	Gamma Map	**46.6**	**43.3**	15.3
	Nagao	30.4	42.7	0.0
ERS+ Radarsat	no filter	45.7	29.7	0.1
	multitemporal	58.4	**41.6**	17.7
	Gamma Map	**73.9**	38.3	**18.8**
	Nagao	55.3	25.7	0.1

Table 8. Results of the classification for various combination of senors and filters for the three main crops. Results evaluated over the validation segment.

The results evaluated on the validation segment (Table 8), are relatively poor. This is mainly explained by the limited number of plots available within the 25km² Alpilles site area. However, indications are given on the influence of the filtering method and on the combination of ERS and Radarsat data to exploit their variation in the viewing angle. Results (Table 8) show that the gamma map and the multi-temporal filters are performing the best. Additional investigations based on the full series of ERS data (10 images) confirmed that filtering improves classification accuracy in most cases.

The combination of ERS and Radarsat data did not always provide improvements of the classification. Because of the small number of fields available further investigations should be conducted to confirm these findings.

5.3.3.1.2 Combining active and passive µ-waves

Several combinations of active and passive µ-waves were evaluated for their discrimination performances. Results (Figure 40) show that combining two frequencies and two incidence angles provides a good way to discriminate between most of crops and soils over the ReSeDA site during the IROE flight.

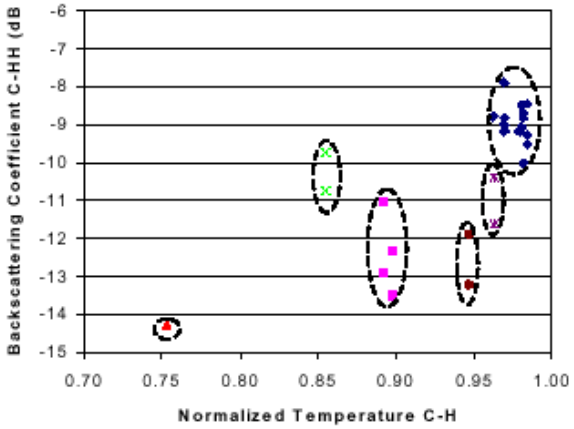

Figure 40. Discrimination performances of passive (normalized temperature, band C, polarisation H, 40° incidence) combined with active µ-wave (band C, polarisation HH, 20° incidence). (◆ wheat; ✷ alfalfa; ● grass; ■ sunflower; × dry soil; ▲ wet soil).

5.3.3.2 Modelling the µ-wave signal

The modelling activity is required to ensure that the models to be inverted are providing a good description of the radiative transfer within the ReSeDA context. It consists both in the development of new or improved models, and on the calibration and validation of these former models or of already available models. The models used are preferentially physical. However, due to the complexity of the radiative transfer in the microwave, semi-empirical and empirical models will also be used. Both active and passive microwave models will be investigated.

5.3.3.2.1 ACF soil model

Recent studies have shown that statistical parameters such as the *hrms (*height root mean square error), and the correlation length are not efficient descriptors of soil surfaces, since the latter are not purely random and possess multi-scale geometry. An interesting alternative approach is to model the surface by a continuous fractal function. Indeed fractals are suitable tools for describing mixtures of deterministic and random processes.

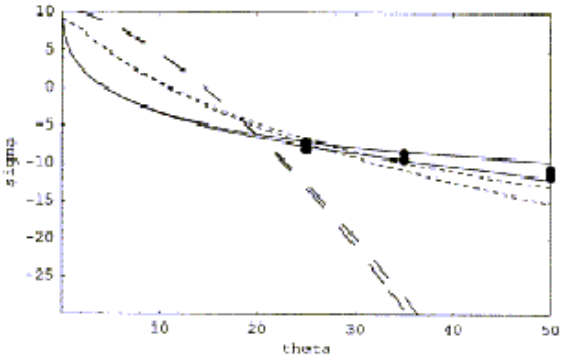

Figure 41 Simulated (dotted: Exponential ACF, dashed: Gaussian ACF, continuous: IROE's model) and measured (black circles) backscattering in C band as a function of incidence angle

In our research the surfaces have been characterised by a semi-empirical spectrum with an exponent related to the fractal dimension. A comparison of simulations with experimental results shows that this approach gives more accurate results with respect to the spectra corresponding to both Gaussian and Exponential ACF (Figure 41).

5.3.3.2.2 Adaptation of the IEM soil model

The Integral Equation Model (IEM) (Fung, 1994), is one of the most widely used model to describe soil backscattering as a function of roughness and moisture. However, the relation between the correlation length used by the model and the actual roughness is not straightforward. Further, measurement of the correlation length is difficult and associated to uncertainties.

The aim of this study is to propose an empirical calibration of an effective correlation length to obtain a good agreement between model simulations and observed data. Then, the effective correlation length is related to the measured root mean square of the surface height (*hrms*). This approach was applied to ERS and Radarsat configuration over the European FLOODGEN campaign in 1998 (Pays de Caux). Figure 42 shows the very strong correlation between the effective correlation length and the actual *hrms*.

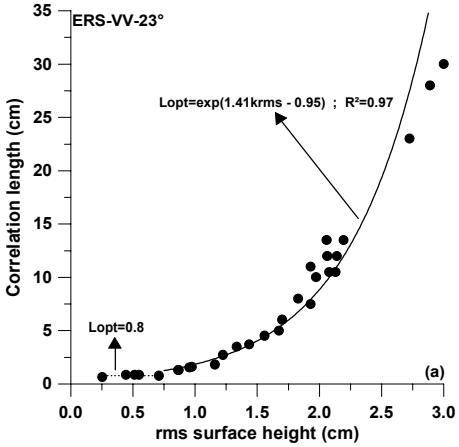

Figure 42. Relationship between the effective correlation length and the actual root mean square surface height for ERS configuration.

The reliability of this empirical relationship has been validated using the ReSeDA database (two radar configurations: ERS-23° and Radarsat-39°). A good overall agreement was observed between the calibrated IEM (using the optimal correlation length) and the measured data of the studied radar configurations (Figure 43).

The good correlation between space-borne SAR data and the calibrated IEM indicates the feasibility of retrieving *hrms* and/or soil moisture from SAR observations. These results are very promising because this empirical calibration of the IEM can be used to develop an inversion technique for predicting soil characteristics.

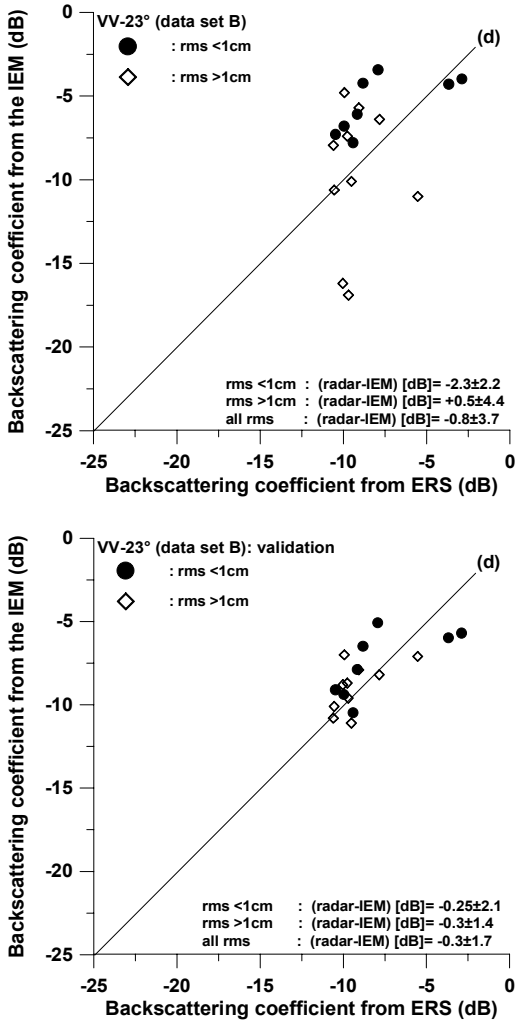

Figure 43. IEM performances for ERS configuration when using the measured correlation length (top) compared to the use of the efective hrsm deduced from the actual root mean square of surface height (bottom). Validation data set from ReSeDA.

5.3.3.2.3 A linear model for soil moisture

The relationship between soil moisture, w_s, and the backscattering coefficient as a simple linear one:

$\sigma°_S = C + D\, w_s$

where C and D depend on soil roughness and texture. However, we observed over the whole bare soil data set, that the slope, D, could be considered

as constant as observed earlier by (Ulaby et al. 1978). The coefficients were adjusted for ERS or ERASME data for band C and 20° incidence and VV polarization (Figure 44). Good performances were obtained for most of the fields.

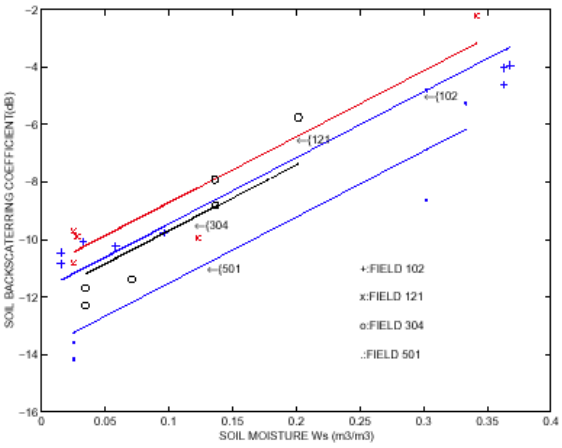

Figure 44. Best fit linear relationship between volumetric 0-1cm soil moisture w_S ($m^3.m^{-3}$) and soil backscattering σ_0 (dB).

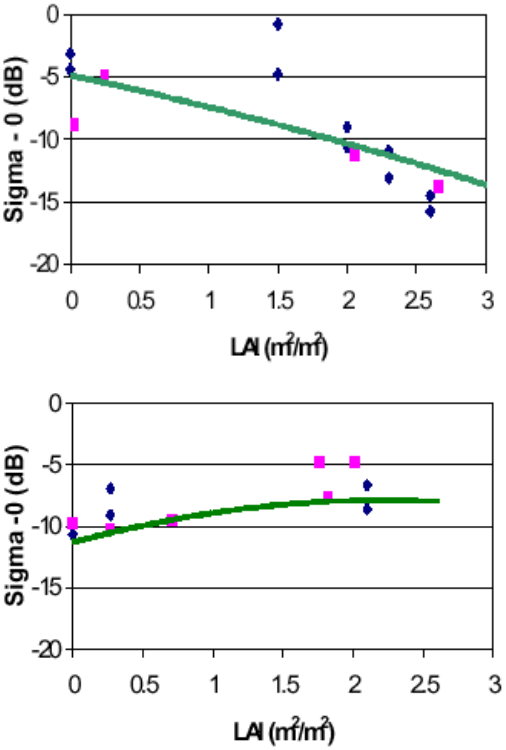

Figure 45. Comparison between model simulation (solid line) and ReSeDA experimental data (ERS:squares, ERASME: diamonds) for C band at 20° over wheat (top) and sunflower canopies.

5.3.3.2.4 A discrete canopy radiative transfer model

A model was developed, based on the radiative transfer theory, and representing the vegetation elements as an ensemble of randomly oriented disks and almost vertical cylinders over a rough surface. The model describes the single scattering, the interaction between the soil and vegetation (double scattering) and the soil-vegetation-soil contribution. The simulations were compared to the ReSeDA experimental measurements over two very contrasted canopies: wheat and sunflower. Results (Figure 45) shows a reasonable agreement. Further, it confirms the very different behaviour of the two canopies: wheat for which the backscattering coefficient decreases when LAI increases, and sunflower that experiences an opposite behaviour.

5.3.3.2.5 Validation of the water cloud model

To represent the influence on the backscattering coefficients of the surface variables such as canopy water content w_c and soil water content w_s, the semi-empirical water cloud model of Attema and Ulaby was evaluated. This model is a good candidate for inversion, thanks to its simplicity and low number of variables and parameters. The cloud model writes:

$\sigma^o = A.(1-t^2) + t^2.\sigma^o_{soil}$, where t^2 is the two-way attenuation by the canopy expressed as:

$t^2 = \exp(-2.B.w_c / \cos\theta)$.

where θ is the incidence angle. The soil contribution σ°_{soil} is expressed as a linear function of the surface soil moisture as seen in §5.3.3.2.3:

$\sigma^o_{soil} = C + D.w_s$

The parameters *A*, *B*, *C* and *D* are assumed to have the following properties:

- *A,* related to the scattering albedo of the canopy, and *B*, related to its optical depth, are varying only with the frequency (C or X bands) and the polarisation (HH or VV);
- *D,* the sensitivity of the soil back-scatter to soil moisture, is assumed to be constant (Ulaby, Batlivala et al. 1978);
- *C,* the intercept of the linear relationship between the soil moisture and the soil back-scatter is assumed to be specific of the radar configuration (frequency, polarisation and incidence angle) and of the field considered, thus implicitly accounting for the effect of the soil roughness;

all four parameters are assumed to be constant during the growing season. This last assumption might be difficult to be met, especially for the roughness parameter *C*, but it must be kept in mind that during the ReSeDA experiment, strong rainfalls occurred during the fall and the beginning of winter, leading to very smooth surface on wheat fields.

The Cloud model was calibrated on ERS and Radarsat data (C-band only) then on Erasme data (C and X bands), using multi-angular configurations. In both cases, the leaf area index (*LAI*) was also tested as the vegetation variable but the total plant water content w_c was always found to be a better explanatory variable than *LAI* on wheat canopies.
Results (Table 9) shows values of the parameters in good agreement with the literature. Further the fitting is quite accurate, with a *rmse* value close to the *rmse* characterising the within field variability. However, we observe that Radarsat gets generally lower *rmse* values than ERS and Erasme (Figure 46).

Sensor	Frequency	Polarisation	Incidence (°)	*A*	*B*	*C*	*D*	*rmse* (dB)
ERS	C	VV	23	-	0.32	13.0-11.0	18.16	1.36
Radarsat	C	VV	23	-	0.098	10.2-9.7	18.16	0.95
	C	HH	39	-	0.098	15.2-13.8	18.16	1.14
Erasme	C	VV	20	-18.3	0.215	12.9-11.4	17.8	1.48
	C	VV	40	-18.3	0.215	16.0-14.4	17.8	1.48
	C	HH	20	-14.6	0.000	12.7-11.3	17.8	1.52
	C	HH	40	-14.6	0.000	15.3-14.2	17.8	1.52
	X	VV	20	-14.4	0.590	10.9- 9.1	17.8	1.39
	X	VV	40	-14.4	0.590	16.0-12.7	17.8	1.39
	X	HH	20	-12.0	0.184	10.8- 9.4	17.8	1.20
	X	HH	40	-12.0	0.184	15.0-12.9	17.8	1.20

Table 9: parameters of the CLOUD model calibrated on the SAR (ERS and RADARSAT) data, along with the *rmse* error (in dB). The value of the parameter *C* being field-specific, only its range is given for each radar configuration.

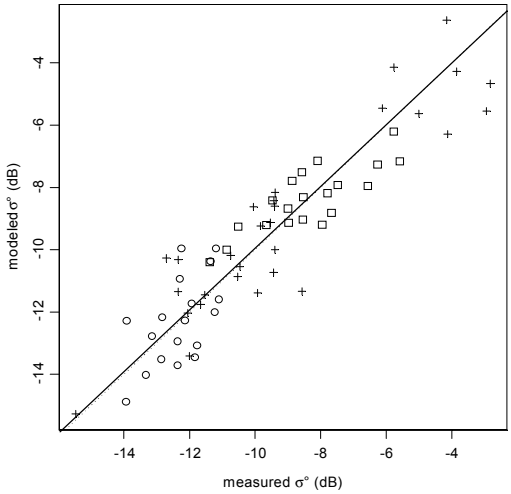

Figure 46 fitting the CLOUD model on ERASME data: modeled vs. measured σ°. Data acquired at 20°: plus, at 40°: open squares. (a) C-HH, (b) C-VV, (c) X-HH, (d) X-VV. The solid line is the 1:1 line.

Similarly, the cloud model was adjusted for sunflower canopies using ERS and ERASME band C, 20° incidence and HH polarisation. Instead of canopy water content, the LAI was used to describe the canopy status. Results (Figure 47) show quite good agreement between the model simulations and the actual µ-wave backscattering coefficient.

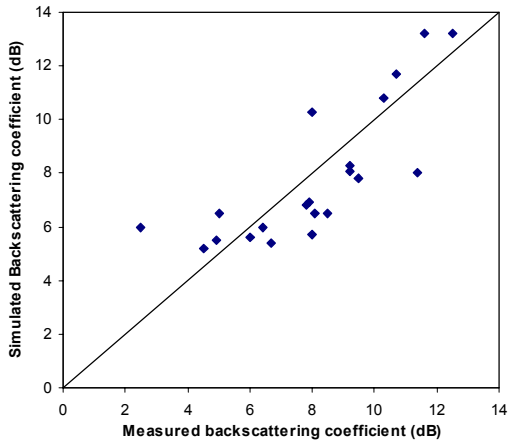

Figure 47. Comparison between modeled and measured backscattering coefficient for sunflower fields as observed by ERS and ERASME, band C, 20° incidence, VV polarisation.

5.3.3.3 Biophysical parameter estimation from µ-wave data

5.3.3.3.1 Soil moisture retrieval

5.3.3.3.1.1 Active µ-wave

ERS data over the whole season have been used to evaluate their interest for soil moisture estimation. When each field is taken individually, a very nice similarity is observed between the back-scattering coefficient and the top cm soil moisture (Figure 48). However, when all the fields are used to draw a single correlation between ERS data and soil moisture, an important scatter is observed (Figure 49 top). This is mainly due to the effect of roughness that differs strongly from one field to an other. This effect could be minimised when considering larger areas where the roughness variations are smoothed out. Figure 49, bottom, shows the improvement of the accuracy of the correlation between radar data and soil moisture when averaging over 10 fields. This shows that it could be possible to monitor quite accurately surface soil moisture at regional scales from active µ-wave observations.

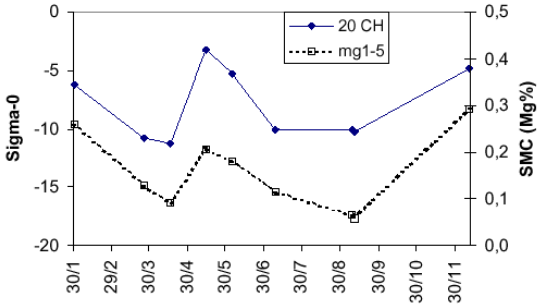

Figure 48. Time course of the backscattering coefficient and soil moisture in the first cm over a single field from 30/01/97 to 30/11/97. ERS data, band C, HH, 20° incidence.

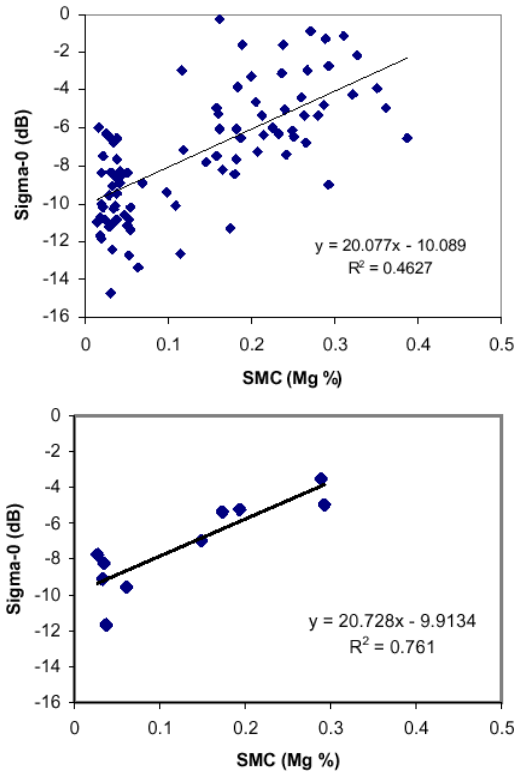

Figure 49. Relationship between back-scattering coefficient (Sigma-0) and soil moisture in the first cm (SMC). All the fields (top), and average of 10 fields for all the dates (bottom).

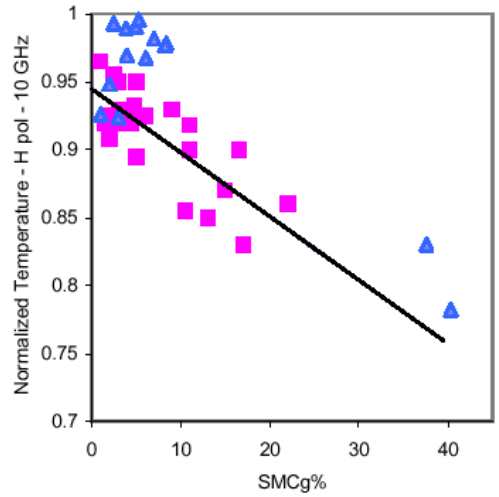

Figure 50. Normalized temperature at 10 GHz, 20° incidence as a function of soil moisture (first cm). Solid line: semi-empirical model; triangles: ReSeDA data; squares: other data.

5.3.3.3.1.2 Passive µ-wave

The X band (10GHz) data acquired from 20° incidence from the IROE radiometer were correlated to the corresponding soil moisture (top cm) and compared to previous results. Figure 50 shows a very good agreement between the ReSeDA data, other data and the semi-empirical model. This provides evidence of the interest of such observations for soil moisture estimates at the local to the regional scales. We observe here that the roughness appears to have less influence of the moisture signal than previously in band C, HH, 20° incidence with the active µ-wave.

5.3.3.3.2 Leaf area index and biomass estimation from µ-wave data

5.3.3.3.2.1 Active µ-wave

Previous investigation had pointed out that the retrieval of biomass or related variables (*LAI* or canopy water content) was ambiguous when using only one configuration. However, for a given species, with its limited range of variation of canopy structure, this appears feasible. A semi-empirical polynomial fit was adjusted on simulations of the discrete model developed previously as a function of *LAI* for wheat and sunflower separately. Results show a reasonable agreement (Figure 51) with ReSeDA ERS data. However, a slight overestimation is observed for both crops.

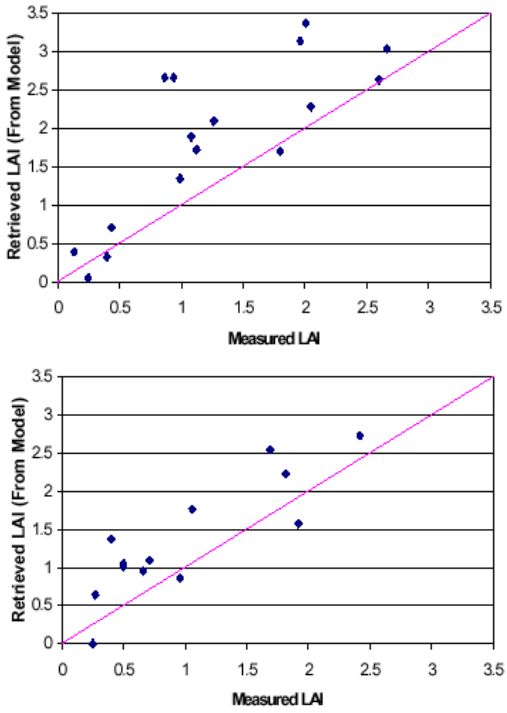

Figure 51. Comparison between measured LAI values of wheat (top) and sunflower (bottom) and those estimated from a semi-empirical polynomial model.

5.3.3.3.2.2 Passive µ-wave

The polarisation index (*PI*) was found to be quite efficient for the estimation of canopy variables. The following equation was developed to relate *PI* and *LAI* values as a function of wavelength λ and incidence angle θ: $PI(LAI,\theta) = PI(0,\theta)\cdot e^{-K\cdot LAI\cdot\frac{\lambda}{\cos\theta}}$

Where $PI(0, \theta)$ stands for the bare soil *PI* value. The application of this simple model (Figure 52) shows a quite good agreement with observations of wheat fields with the IROE radiometer in band X, 20° incidence.

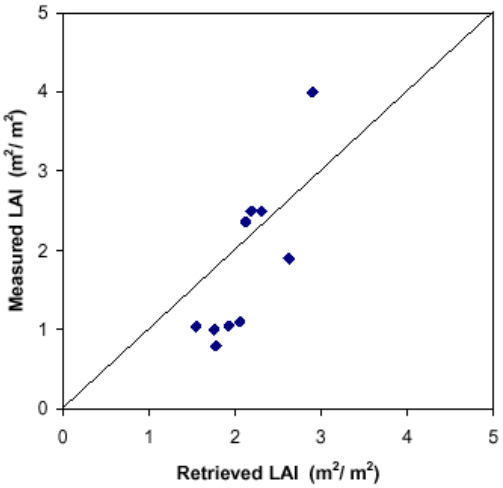

Figure 52. Comparison between measured *LAI* values and those estimated from the polarisation index computed from passive µ-waves (band X, 20° incidence).

5.3.3.3.3 Concurrent estimation of soil and canopy water content

Since the wheat canopy back-scatter depends on two canopy variables w_s and w_c, it is possible to estimate these two variables when at least two radar configurations are available (Attema 1984, Prévot et al. 1993). This was tested based on the bi-angular Radarsat data set. Results showed that this inversion algorithm failed (Prévot et al. 1998) presumably because on the non simultaneity of the two Radarsat observations. Therefore, we investigated the Erasme data that present many possible simultaneous configurations. The inversion technique used here is based on iterative optimisation and tested with all the possible couples of Erasme configurations (28 couples). The residual errors of inversion (*rmse*) are given in Table 10 for w_s and w_c. Reasonable estimates of w_s are obtained when one of the two radar configurations is C20HH (Table 10), that is when the attenuation by the canopy is low. The best estimates of w_s is achieved with C20HH & X40HH combination. whereas accurate estimates of w_c requires a dual-frequency configuration (C20VV & X20VV). The couple of radar configuration C20HH & C20VV appears as an interesting compromise between configuration complexity (single frequency, single incidence angle and dual polarisation) and quality of retrieval for both for w_s and w_c, as can be seen on Table 10.

	w_s: soil moisture							**w_c: Canopy water content**						
	C20VV	C40HH	C40VV	X20HH	X20VV	X40HH	X40VV	C20VV	C40HH	C40VV	X20HH	X20VV	X40HH	X40VV
C20HH	0.084	**0.081**	**0.080**	0.082	0.083	**0.077**	**0.081**	**0.50**	0.65	0.94	0.65	**0.41**	1.07	1.13
C20VV		**0.081**	*0.122*	0.103	0.089	0.103	0.119		0.86	*1.20*	1.01	**0.46**	*1.16*	1.02
C40HH			0.091	**0.081**	0.084	0.090	0.092			0.72	0.86	**0.44**	0.98	1.09
C40VV				0.112	*0.138*	*0.129*	0.113				*1.33*	0.67	0.94	0.84
X20HH					0.087	0.104	0.103					0.58	*1.28*	1.09
X20VV						0.115	*0.168*						0.55	0.59
X40HH							0.097							0.95

Table 10: *rmse* on soil moisture (w_s, in $m^3.m^{-3}$) and canopy water content (w_c, in $m^3.m^{-2}$) estimation by inversion of the cloud model using two configurations; lower values are in bold, higher values are in italics.

5.4 Development of the assimilation technique

The assimilation of remote sensing data into process models was investigated separately for the SVAT and for the canopy functioning models. They will thus be described separately.

5.4.1 Assimilation into SVAT models.

We will first describe and evaluate the SVAT models investigated, then assimilation of remote sensing data will be presented. Additionally, the role of heterogeneity of the surface on the distribution of the fluxes will be addressed.

5.4.1.1 Comparison and improvement of SVAT models

5.4.1.1.1 Comparison of SVAT models

Assimilation of remote sensing data will only be efficient if the process models used are representing adequately the mechanisms involved. It was therefore critical to evaluate and compare the SVAT models within the framework of assimilation of remote sensing data, i.e. including an evaluation on variables such as surface soil moisture and canopy or soil temperatures. A rigorous approach was developed to quantify the performances of the models according to a range of criterions:

Criterion 1: Accuracy of processes description. For this purpose, the models were run using all the measurements available that could be used to characterise directly (without model tuning) some internal variables or parameters.

Criterion 2: Portability of the models. The models will be run with the values of the variables and parameters extracted from the literature. Here again, no model tuning is tolerated.

Criterion 3: Robustness of the calibration. The models are calibrated on the calibration fields and their performances are evaluated on the validation fields. In this case model tuning (calibration) is the rule, but limited on the calibration fields.

Table **11** presents briefly the models investigated. It corresponds to a range of complexity, from the simplest one, MAGRET, to the more complex and physically based one, SISPAT.

Model	Reference	year
MAGRET	Courault etal.,	1995
ISBA	Noilhan and Planton,	1989
TEC	Chanzy and Bruckler,	1993
SOIL	Janssen	1998
SiSPAT	Braud et al.,	1995

Table 11. The SVAT models investigated in the ReSeDA project.

The results suggest some general comments:

- model simulations were close despite the large range of model parameterisation and complexity;
- except for SISPAT, better results were obtained in scenario 2 compared to scenario 1, which may be surprising considering scenario definition. However, this was mainly due to the minimum stomatal resistance;
- for the more complex model (SiSPAT) scenario 2 did not gave better results; this was explained by the less adequate hydraulic properties obtained by using pedo-transfer functions; this was less sensitive in the case of simple models in which only field capacity and wilting point were required as input;
- on the calibration fields, scenario 3 results were better than for the two other scenarios; however, application to the validation fields did not always provided good results for turbulent heat fluxes, while better results were always obtained for the soil heat flux and quite always for soil moisture;
- the use of SiSPAT considering an homogeneous soil column generated a lot of troubles showing that it is not pertinent to apply such type of complex model without taking into account soil layering.

5.4.1.1.2 Improvement of SVAT models

5.4.1.1.2.1 Influence of soil hydraulic properties on SISPAT model performances.

Richards' equation describing water movement in soil requires knowledge of the soil water retention curve, and the hydraulic conductivity function. Uncertainties in soil hydraulic characteristics affect the performance of land-surface schemes used in SVAT models. A series of numerical experiments were performed to assess the sensitivity of the SISPAT model to soil parameters and compare the results with Alpilles-ReSeDA data set under bare soil conditions. The simulations, using the simplest version of SISPAT with a single horizon (i.e. homogeneous soil), show that water content and land surface water and energy fluxes are very sensitive to these parameters when soil moisture is lower than approximately 90% of the water content at saturation. It is found that, for bare soil condition, latent heat flux is the most sensitive factor to soil hydraulic properties. For wetter soils the energy fluxes are totally independent from the soil water content. It is therefore concluded that SISPAT has to be implemented with more than a single layer to describe accurately surface soil water moisture.

5.4.1.1.2.2 Effect of aerodynamic resistance scheme on SISPAT performances

The aerodynamic resistance scheme used in the two-layer SVAT model such as SISPAT, affects strongly the surface fluxes and temperatures simulation. A large review of existing schemes has been conducted and 6 parameterisations based on the first approximation of turbulence theory (the K-

theory) have been considered. These parameterisations were implemented in the SISPAT scheme already calibrated on the experimental sites of the ReSeDA experiment. Results show that the different parameterisations lead to similar simulations of total surface fluxes but to different soil and vegetation temperatures. This is due to the change in the partition of energy between the soil and vegetation layers considered in the model. These differences are critical for the description of the radiative temperature as observed by remote sensing in the thermal infrared.

5.4.1.1.2.3 Estimation of the aerodynamic characteristics over the ReSeDA experiment

As stated previously, the description of the aerodynamic characteristics is critical for an accurate representation of the surface fluxes and the associated remote sensing variables such as temperature and surface soil moisture. Therefore, emphasis was put on this issue. The displacement height, roughness length for momentum, the stability correction terms and the scaling parameters ($u*$ and $T*$) can be determined by using the measurements of wind speed and air temperature at two heights and the sensible heat flux above the canopy through a two-concentric-loop iterative (TCLI) method. Application of this method to a wheat field shows that estimation of d and z_0 were possible only if the temperature gradients were measured differentially. nevertheless, consistent estimation of the scaling parameters, and therefore the Monin Obhukov length and the stability correction terms was found.

5.4.1.2 Estimation of surface fluxes using the SEBAL algorithm

The SEBAL algorithms proposed by Bastiansen et al. (1998) is based on a surface energy balance model using the Monin-Obukhof theory for the boundary layer description. The algorithm provides instantaneous estimates of evapotranspiration using spatially distributed measurements of surface albedo, the normalised difference vegetation index (*NDVI*) and surface temperature. The vegetation and soil characteristics are not explicitly described in the SEBAL algorithm. They are retrieved from empirical relationships with the former input variables.

The SEBAL algorithm requires to have both completely dry and wet pixels to compute the spatial distribution of the fluxes. The wet pixels are used to estimate air temperature at the reference level. The dry pixels are used to estimate the resistance to transfer at the canopy surface through wind speed estimates at the reference level. The selection of dry and wet pixels is based on the distribution of albedo and surface temperature (Figure 53)

The SEBAL inputs were derived from the POLDER data for albedo and *NDVI*, and INFRAMETRICS camera for surface temperature. Special procedures were used to get improved values of SEBAL input:

- ***Albedo.*** The method developed in §5.3.1.7.2 was used here.
- ***NDVI.*** The *NDVI* values were computed from nadir, thanks to the MRPV BRDF model (§5.3.1.7.1) applied on atmospherically corrected POLDER data.
- ***Surface temperature.*** To minimise the directional effects, the selected T_s measurements were restricted to view zenith angles lower than 25° and outside the hot-spot region. The pixels values were averaged over 2 minutes period. All the site was covered within approximately one hour.
- ***global radiation.*** The ReSeDA meteorological station global radiation measurements were used. They were averaged over one hour.
- ***Atmospheric long wave radiation*** was derived from ground measurements averaged over one hour.

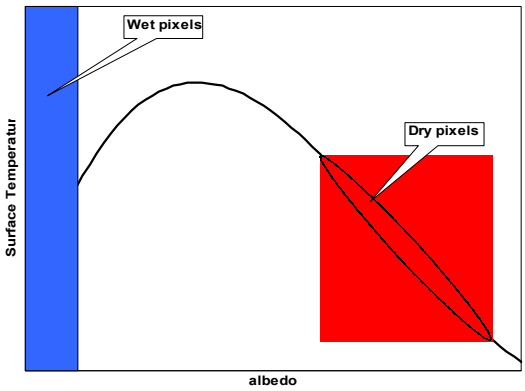

Figure 53. Procedure used to select the wet and dry pixels using the co-distribution of albedo and surface temperature.

Fluxes	Absolute RMSE ($W.m^{-2}$)	Relative RMSE (%)
Net radiation	60	10%
Soil heat flux	40	30%
Sensible heat flux	50	25%
Latent heat flux	50	25%

Table 12. Results of the validation of the SEBAL algorithm observed over seven points located on alfalfa, wheat and sunflower crops.

The Results (Table 12) show that the SEBAL net radiation estimates were close to field measurements. Comparison between soil heat flux from SEBAL simulations and field measurements were not satisfactory although the *rmse* was corresponding to the field data accuracy. Due to inconsistencies in the Bowen ratio and aerodynamic methods for convective flux estimation, it was not possible to get final conclusion. Only few eddy correlation data were available and reliable. However, maps of surface energy fluxes (Figure 54) were generated. They show a strong spatial variability inside some fields that can reach up to 50 Wm^{-2} although the variability between fields could reach up to 500$W.m^{-2}$.

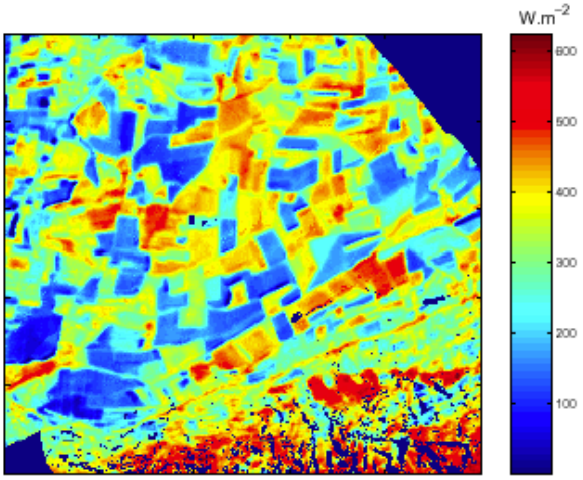

Figure 54 Map of the evapotranspiration (latent heat flux) derived from the SEBAL algorithm using POLDER and INFRAMETRICS data over the ReSeDA site, April 10th at 20m spatial resolution and averaged over 45 min.

5.4.1.3 Spatial heterogeneity of fluxes

The atmospheric surface layer couples processes in the atmosphere with those at the land surface. However, the effect of spatial heterogeneity is not fully understood. Therefore these investigations were aiming at a better description of the heterogeneity of fluxes with consequences on the scaling of fluxes.

5.4.1.3.1 Boundary layer structure over heterogeneous surfaces

The small remotely piloted aircraft flown during the ReSeDA experiment measured profiles of heat and humidity in the atmosphere's surface layer near boundaries between different land cover types to study atmospheric surface layer structure over heterogeneous terrain.

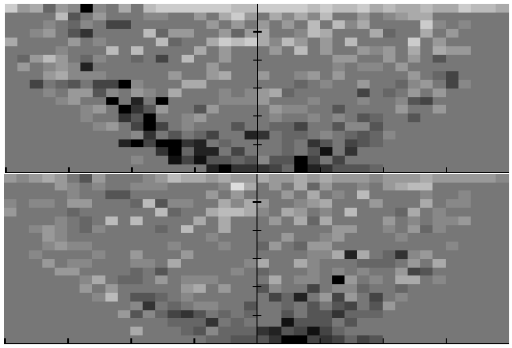

Figure 55. Mean air temperature (top) and huidity (bottom) distribution as a function of height and distance from the boundary. Darker shading represents values above the mean (mid-grey). Horizontal axis ticks are at 100 m intervals and vertical axis ticks are spaced by 10m; the vertical line shows the surface boundary position.

Figure 55 illustrates the typical structure of the atmosphere at a boundary between two contrasted fields for neutral stability conditions. In this case the surface to the right of the boundary was irrigated meadow, with dry fallow land to the left, and the wind was blowing from the meadow to the fallow (about 4 ms^{-1}). The contrast near the surface on either side of the boundary is apparent, with cool moist air over the meadow and warm dry air over the fallow; by 30 m above the surface the contrast has practically disappeared. However, the sharpest structures were observed in unstable conditions with contrasting surface. This provides a first estimation of the blending height with values up to about 30 m for these conditions, which is again consistent with expectations.

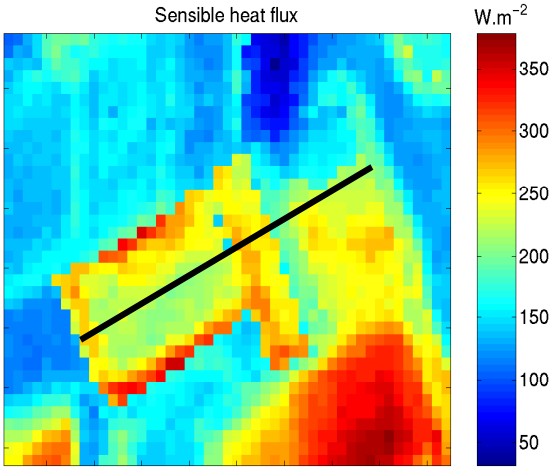

Figure 56. SEBAL derived sensible heat flux around the scintillometer optical path (the black line).

5.4.1.3.2 Heat flux scaling

Two methods for retrieving sensible heat flux over a bare soil/wheat composite surface are compared (Figure 56):

- The first method is based on field measurements using large aperture scintillometers. The comparison against reference fluxes obtained from eddy correlation technique shows that scintillometry-derived fluxes are overestimated by about 10% (Figure 57). A numerical experiment demonstrates that this is induced by aggregation problems resulting both from non linearity in the relationship between the structure parameter for refractive index and the sensible heat flux, as well as from non uniform sensitivity of the scintillometer along the path-length.
- The second method is based on the use of the SEBAL algorithm (§5.4.1.2). A comparison against scintillometry derived fluxes shows important discrepancies (Table 13). They mainly result from large errors in the estimation of the roughness length z_0 in the model. This demonstrates that the use of an empirical relationship based on NDVI only is inadequate for inferring this key parameter in SEBAL.

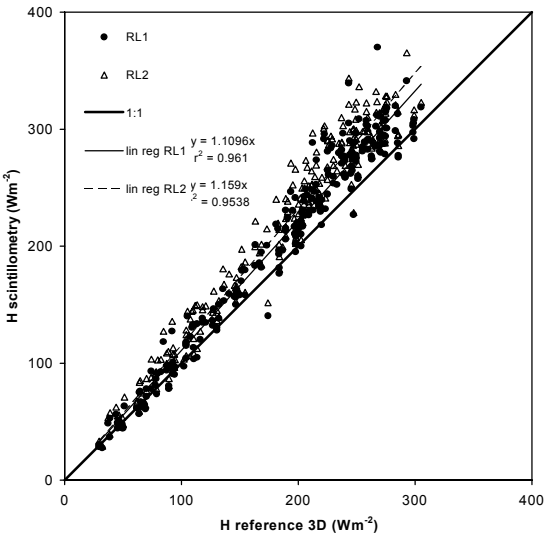

Figure 57. Comparison between spatially-averaged sensible heat flux derived from eddy correlation measurements and from scintillometry, using 2 aggregation schemes for roughness length.

Sensible heat flux ($W.m^{-2}$)	Wheat	Bare soil	Optical path
Eddy correlation	303	189	273
Scintillometer	-	-	297
SEBAL (initial version)	122	175	141
SEBAL (z_0 prescribed)	243	206	241

Table 13. Comparison between reference eddy correlation, scintillometry, and SEBAL estimates of sensible heat flux for individual fields (wheat and bare soil) and integrated over the scintillometer path-length.

5.4.2 Assimilation into canopy functioning models

Similarly to the SVAT models, performances of the assimilation into canopy functioning models are strongly linked to the accuracy of the canopy functioning models themselves. A range of canopy functioning models have been investigated (Table 14). All these models have first to be calibrated over the particular crops considered within the ReSeDA project. Special emphasis was put on wheat canopies for which the largest range of ground measurements and remote sensing data are available. We will therefore present first the performances of the models after calibration, and then address the assimilation issue itself.

MODEL	Reference	Year	Time step
V-S	Cayrol et al.	1999	hour
ROTASK	Jongschaap	2000	day
STICS	Brisson et al.	1998	day

Table 14. The several canopy functioning models used.

5.4.2.1 Calibration and evaluation of canopy functioning models.

The results of the calibration and evaluation of the three models considered here will be reviewed briefly. Similarly to the SVAT evaluation procedure, the calibration and evaluation procedures were kept as independent as possible to insure confidence in the robustness of the evaluation.

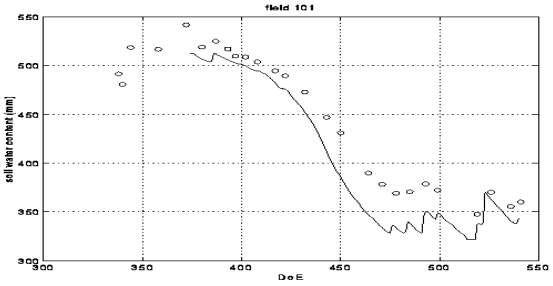

Figure 58. Comparison between the V-S model simulation of water storage in the 0-140cm layer to the actual measurements over a wheat field.

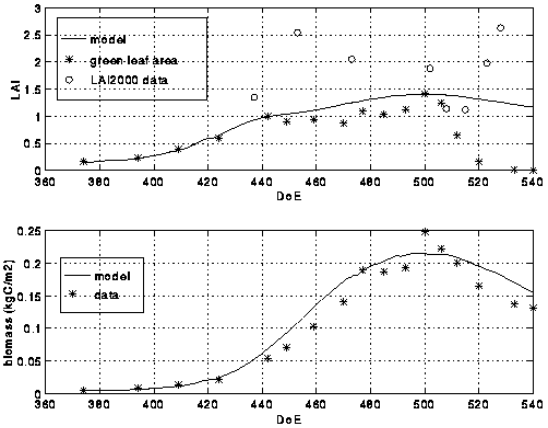

Figure 59. Comparison between V-S model simulations and actual *LAI* (top) and biomass (bottom) measurements over a wheat field.

5.4.2.1.1 The V-S model

The V-S model (for Vegetation-SVAT) was developed by Cayrol et al. (1999) for simulation of energy, water and carbon exchanges over the whole growing season. Indeed, this model couples a simple SVAT model to a canopy functioning model. This model was originally developed to describe sparse canopies as in the case of Sahel. The calibration was performed using either data from the literature or values of the variables measured during the experiment. This scheme corresponds to Criterion 1 scenario for SVAT. The evaluation shows some discrepancy between the latent and sensible heat fluxes and moisture in the rooting zone (Figure 58). This was mainly coming from a problem in the value of the rooting depth. However, the canopy functioning model, calibrated mainly with values extracted from the literature was performing quite satisfactorily. Nevertheless, some error is observed for *LAI* at the end of the cycle, presumably because of a poor description of senescence processes. Because of these deficiencies, and the large effort to spend for corrections from sparse Sahelian canopy to wheat crops, this model was not used later in the assimilation process.

5.4.2.1.2 Calibration of the ROTASK model

The ROTASK 1.5 model is a derivation of the SUCROS models (Spitters, 1990). It includes a tipping-bucket water balance without capillary rise (DRSAHE), a soil organic matter module (SOM), a crop growth module (WOFCROP), and a management module (MAN). The calibration was focussing on three modules:

- The ***water balance*** module (DRSAHE). The four parameters characterising the bucket storage (water holding capacity when air dry, at wilting point, at field capacity, and at saturation) were adjusted over the calibration ReSeDA wheat fields. The first layers up to 60 cm were quite well simulated by the original ROTASK model. However, below 60cm, this was not the case (Figure 60 top). The calibration of the bucket characteristics as well as the dynamics of the rooting system and water uptake potential resulted in clear improvement of the simulations (Figure 60, bottom).
- The ***temperature sums*** module (SOM°) was calibrated to describe the developmental stage more accurately. Additionally, the leaf life-span parameter was adjusted to better simulate the ceasing of the crop canopy.
- The ***dry matter partitioning*** towards roots (WOFCROP), shoots, leaves, stems and ears was calibrated for each development stage (Figure 61).

The resulting simulations show good performances for *LAI* dynamics as seen in Figure 62, which is critical for remote sensing assimilation purposes. Additional tests were performed to ensure the robustness of the calibration.

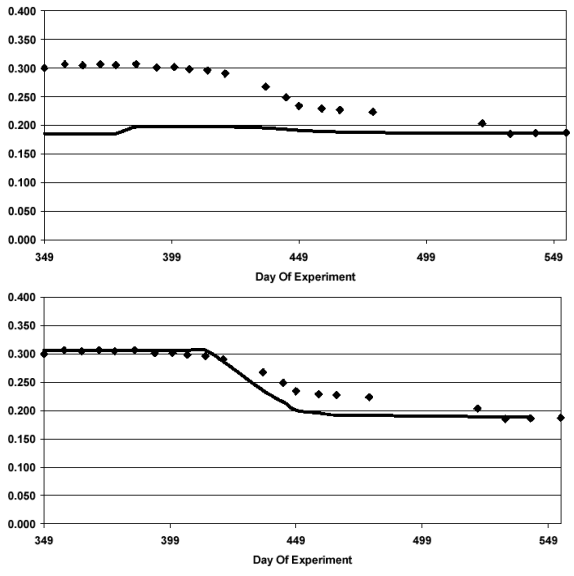

Figure 60. Dynamics of the soil moisture in the 60-80cm layer simulated (solid line) and measured (dots). The top figure corresponds to the initial ROTASK model; the bottom figure corresponds to the model simulation after calibration of soil and canopy parameters.

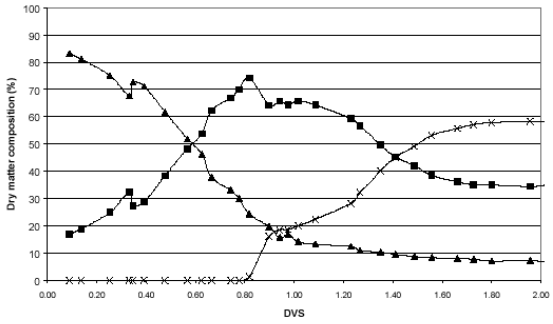

Figure 61. Dry matter partitioning coefficients used to calibrate the ROTASK model.

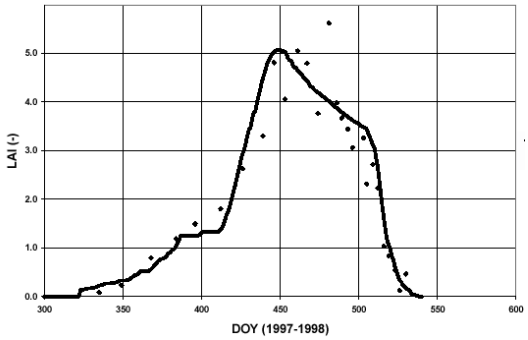

Figure 62. Comparison between measured (direct measurements) and ROTASK simulated LAI values after calibration.

5.4.2.1.3 Coupling STICS and radiative transfer models.

The STICS model is a generic model of canopy functioning capable to represent the behaviour of a large range of species. It was already calibrated on wheat crops (Brisson, 1998). However, the main effort was directed to the coupling of STICS to a multi-layer and multi-component version of the SAIL radiative transfer model. It allows to describe the structure according to the scheme presented in Figure 63. Therefore, the STICS model that originally outputs only the green leaf area index, has to simulate the dynamics of the organ are index (*OAI*) required for the detailed canopy structure description (Figure 63). In the same way, the optical properties have to be described according to the PROSPECT model, i.e. by developing a module that simulates the chlorophyll, the water, and the dry matter of the organs, as well as a characterisation of their internal structure.

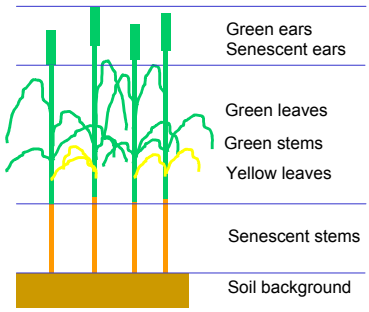

Figure 63. Schematic description of the wheat canopy structure used in the SAIL radiative transfer model.

Figure 64 shows the adaptations that were developed from the original STICS model to simulate the *OAI* and the composition (chlorophyll, water, dry matter) for all the organs considered, i.e. green and yellow leaves, green and senescent stems and ears. These additional characteristics were mainly derived from empirical relationships with the initial outputs of STICS, i.e. phenology, total dry matter, green *LAI*, nitrogen nutrition index and surface soil moisture. These relationships were calibrated over data sets independent from the ReSeDA experiment. They were then evaluated over ReSeDA.

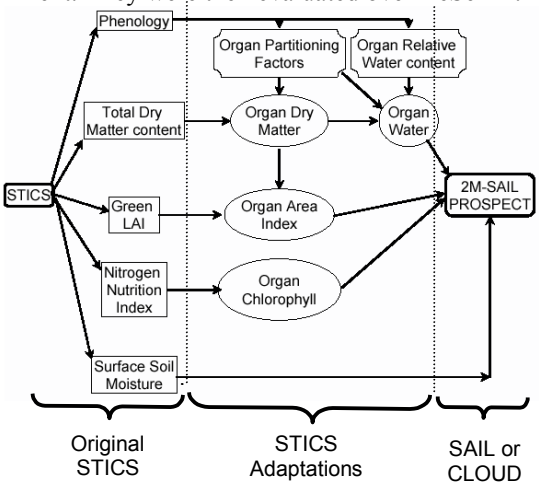

Figure 64. Schematic description of the coupling between STICS and SAIL+ PROSPECT models, and the necessary adaptations that have been developed for the STICS model.

Results show that generally, our parameterisation seems reasonable. However, for some variables such as the leaf water content, the agreement is relatively poor (Figure 65). This will have important consequences on the success of the assimilation, particularly when using µ-waves or reflectance in the short-wave infrared.

Figure 66 shows the resulting *OAI* dynamics simulated by our parameterisation. The agreement with actual ReSeDA experiment measurements is generally good. Other adaptations were implemented concerning the soil water balance in order to get a better representation of the moisture of the surface of the soil.

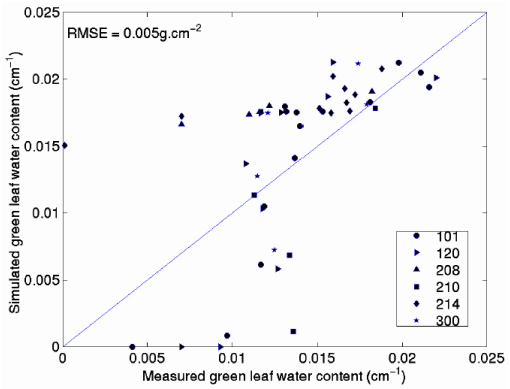

Figure 65. Comparison between the simulated leaf water content using our scheme, to the actual measurements over ReSeDA.

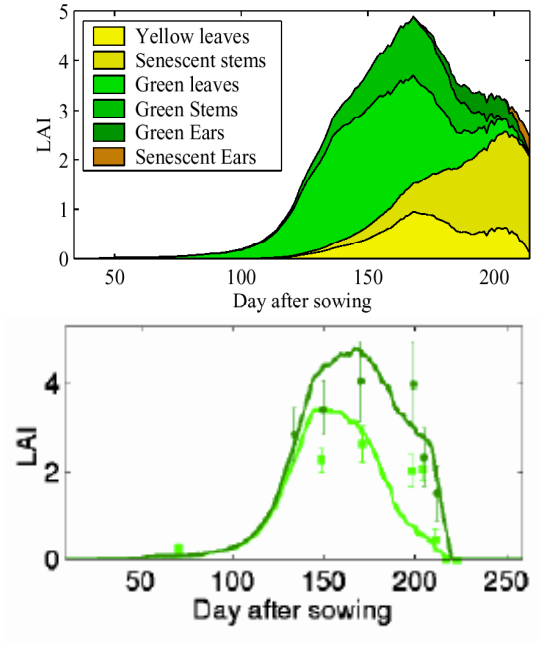

Figure 66. Simulation of the *OAI* for a wheat field in ReSeDA (top). The bottom graph shows the dynamics of the green LAI as measured by planimetry (dots) or simulated by our STICS adaptation (light green). Total green *OAI* is also compared to the LAI2000 measurements (dark green).

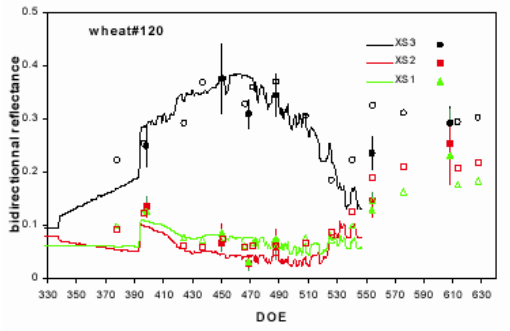

Figure 67. Comparison between our reflectance simulations (solid lines) based on STICS+SAIL to the actual ReSeDA POLDER (simple dots) and SPOT data (dots with vertical bars).

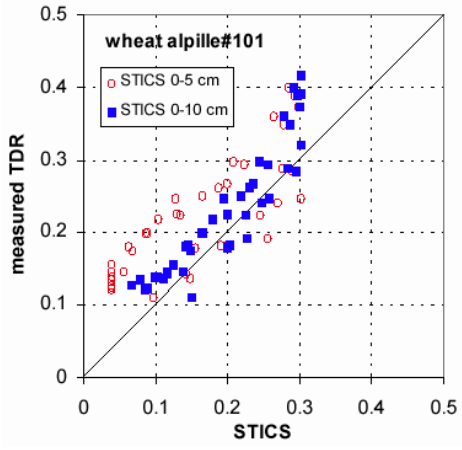

Figure 68. Comparison between the STICS simulations of the surface (0-5cm or 0-10cm) soil moisture to actual measurements (TDR) during the ReSeDA experiments.

Finally, the simulated reflectance (Figure 67) or surface soil moisture used in the µ-wave domain (Figure 68) were compared with actual measurements and show generally a good agreement. This will allow to investigate the last step of the project: remote sensing data assimilation.

5.4.2.2 Assimilation of remote sensing data into canopy functioning models

5.4.2.2.1 Yield estimation from assimilation in ROTASK model at the field scale

The ROTASK model after calibration (see §5.4.2.1.2) simulates the growth of wheat crops. It is capable of producing each day a *LAI* value. However, due to uncertainties in the values of some variables or parameters, as well as model approximation itself, it may deviate from the actual functioning. Remote sensing can be used to force the model to follow the right course by inputting the *LAI* values derived from satellites. In this case, the SPOT data were used to compute the *WDVI* and to estimate *LAI* according to results presented in §5.3.1.5. Three methods of remote sensing assimilation for yield estimates were compared:

1. Using the *LAI* simulated by ROTASK without exploiting remote sensing data
2. Resetting the *LAI* value at each date of image acquisition, and in the interval the ROTASK model provides the updated values.
3. Using ROTASK *LAI* up to the first image, and then using interpolated *LAI* values driving ROTASK.

Results show a small advantage to method 3, i.e. ROTASK forced with remote sensing estimates of *LAI*. However, the field variability and the fact that ROTASK was calibrated on part of the fields limits the validity of the results. Additional tests should therefore be conducted.

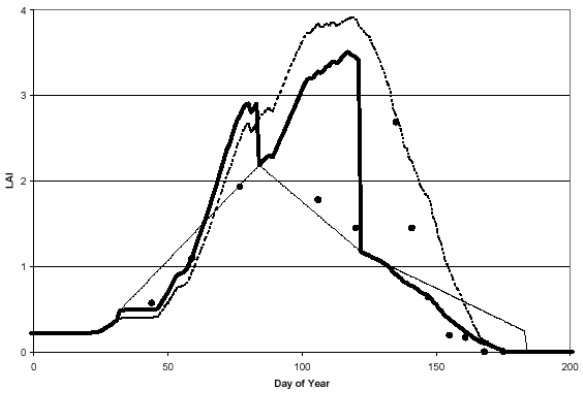

Figure 69. Comparison of the *LAI* time course corresponding to the three methods used to drive the ROTASK model over field 120 (method 1: dotted line; method 2: bold solid line; method 3: light solid line).

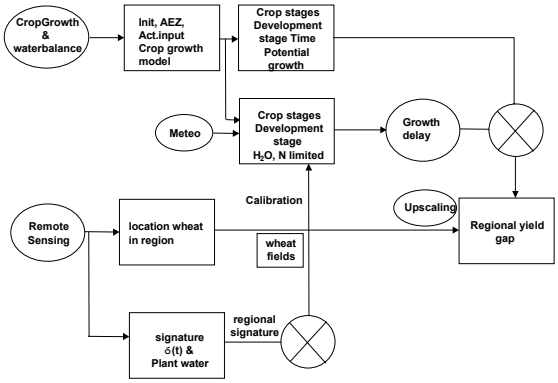

Figure 70. Combination methodology for the estimation of yield at the regional level using remote sensing and crop growth simulation. AEZ=Agro Ecological Zone, N=nitrogen.

5.4.2.2.2 Use of Remote sensing and the ROTASK model for regional yield estimation

This study aimed at extending wheat production estimates from field to regional scales concerning. Regional information available from the MARS project (Soil map, DEM, crop statistics, ancillary data, etc.), and field segment information acquired by the group of BRGM, were used to generate a land use map using optical satellite imagery. The locally calibrated Cloud-model (§5.3.3.2.4) was coupled to the ROTASK model to assimilate ERS time-series (Figure 70). ROTASK was initialized for the local growth conditions and fed with the actual meteorological data (temperature, rainfall, etc.) to predict wheat grain production.

The flowering stage corresponds to the transition between the vegetative and the generative growth cycles. This was used to adjust the crop growth model. As a matter of fact, this stage can be clearly recognized in the average time-series of the ERS data (Figure 71).

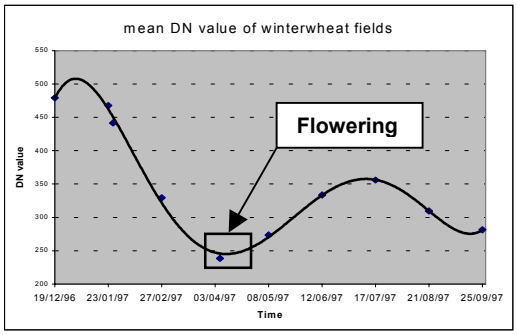

Figure 71. Typical evolution of ERS data over wheat fields, with the flowering date indicated.

A comparison was achieved between initial ROTASK production estimates and those using ERS data for adjustment of the flowering date. Table 15 shows that the use of ERS data changes slightly the yield estimation, and therefore the production. Although small, the difference ranges from 1% to 6% which is very important for large scale production estimation. Table 15 shows also the great importance of management practices for which only little

information is available at the regional scale. Remote sensing could therefore offer one way to get better estimates of the yield by implicitly accounting for these effects through the impact on phenology and *LAI* as demonstrated previously (§5.4.2.2.1).

Scenario	Soil type	Acreage (ha)	Yield without ERS	Yield with ERS	Relative difference
Potential	-	3000	11.4	11.5	-1%
H_2O limited	1	2700	6.1	5.8	5%
	2	300	5.3	5.0	6%
H_2O+ N limited	1	2700	4.7	4.5	4%
	2	300	4.2	4.1	2%

Table 15. Comparison of yield estimation ($t.ha^{-1}$) from ROTASK with or without ERS data for for determination of the flowering date.

5.4.2.2.3 Assimilation of solar and µ-wave data into STICS-RS model

The more advanced technique of remote sensing data assimilation consists in using coupled canopy functioning and radiative transfer models to be able to simulate the dynamics of radiometric data with the physical and physiological information embedded in the models, and ancillary data such as climate and soil variables. The STICS-RT model presented in §5.4.2.2.3 was used to assimilate concurrently the solar (POLDER data) and the µ-wave (ERS and Radarsat) data. The corresponding radiative transfer models used are the SAIL+PROSPECT model for the solar domain, and the CLOUD model for the µ-wave domain.

The assimilation scheme consists here in tuning a selection of parameters and variables of the canopy functioning model in order to minimise the distance between the simulated and measured radiometric data (Figure 72).

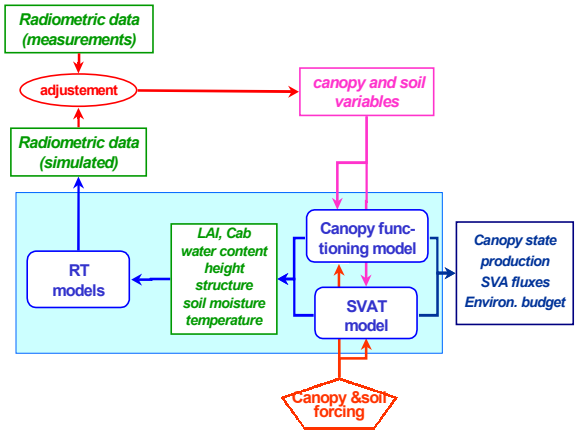

Figure 72. Schematic descrition of the assimilation of remote sensing data into coupled canopy functioning and radiative transfer models (STICS-RT).

Therefore, a preliminary sensitivity analysis was conducted to select the parameters and variables that could be tuned to change the dynamics of the STICS-RT model simulation of canopy reflectance (Table 16) and backscattering coefficient (Table 17). Results showed that the main variables selected were those driving the phenology of the canopy, plant density and some water characteristics of the upper soil layer.

param.	wave band	LEV	AMF	LAX	SEN	DRP	MAT
adens	RED	-	+++	+	+	+	-
	PIR	-	++	++++	++++	++++	-
	MIR	-	+	++++	++++	++++	-
stlevamf	RED	-	+	-	-	-	-
	PIR	-	+	+	-	+	-
	MIR	-	+	+	+	+	-
iplt	RED	-	++	-	-	-	++
	PIR	-	+	+	-	-	++
	MIR	-	+	-	-	-	++
hcc1	RED	+++	-	-	-	-	+
	PIR	+++	-	-	-	-	+
	MIR	+++	-	-	-	-	+

Table 16: Summary of the sensitivity of the reflectance in the red (*RED*), near infrared (*NIR*) and short wave middle infrared (*MIR*) to the parameters of STICS for the 6 main phenological stages (LEV: emergence to MAT: maturity). The sensitivity increases with the number of +. The parameters are: *adens*: compensation between stem number and plant density, *stlevamf*: sum of development units between the *LEV* and *AMF* stages, (*iplt*: sowing date, *density*: number of plants per m^2 at emergence, *extin*: extinction coefficient of PAR by the canopy, *hcc1* and *hcc3*: volumetric soil moisture at the field capacity for the first and third horizons, *h1*: initial moisture of the first horizon, *n1*: initial nitrogen content of the first horizon.

Parameter	DM	LAI	σ° ERS	σ° (23°) Radarsat	σ° (39°) Radarsat
iplt	++++	+++	+	+	+
density	++	++	+	+	+
extin	+++	+			
hcc1	++	+	++++	++++	++++
hcc3	++	+	+++	+++	+++
h1	++	+	+++	+++	+++
n1	++	+	++	++	++

Table 17: Same as **Table 16** but for the backscattering coefficient as observed by ERS and Radarsat.

These variables and parameters were finally adjusted in the assimilation process using the POLDER and ERS and Radarsat data over the whole growth season.

Figure 73 illustrates some results acquired over a wheat validation field. It clearly shows that the use of remote sensing observations allows to correct the values of the canopy functioning model variables and parameters identified in the sensitivity analysis step, leading to a better description of the actual processes and of the resulting variables of interest. The *LAI* dynamics is mainly corrected by shifting the time course by almost 20 days earlier (Figure 73). This induces an increase of the biomass pro-

duction (DM) as compared to the initial simulations and makes the final result closer to the actual ground measurements.

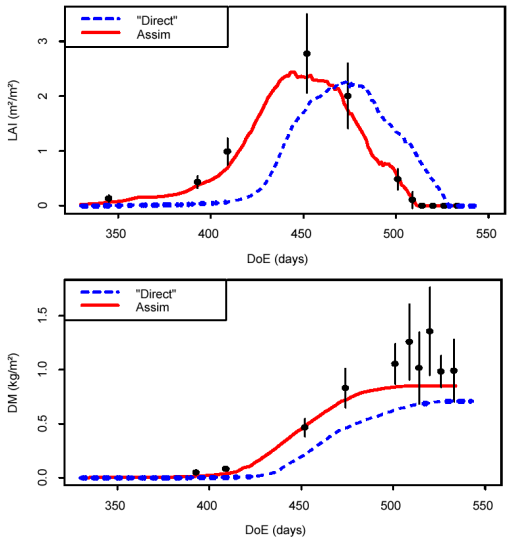

Figure 73. Comparison between simulations of the STICS-RT model before ("direct") and after assimilation of POLDER and ERS and Radarsat data (Assim) over field 300. Four variables are represented here, from top to bottom: *LAI*, total above ground dry matter (DM).

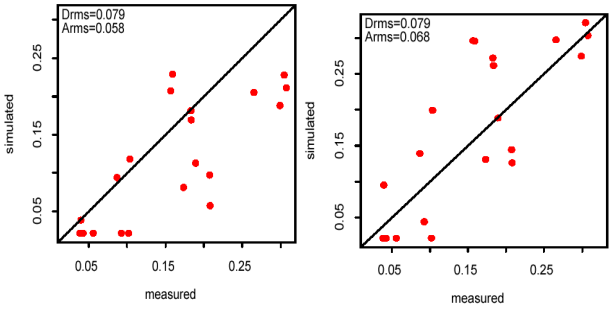

Figure 74. Comparison of measured top layer soil moisture values to those estimated by assimilation of POLDER and ERS and Radarsat data (left) and POLDER only (right) over field 300.

However, the situation is not so clear for the soil moisture in the top layer that is mainly determining µ-wave data (Figure 74). This reflects the difficulty in describing with a simple scheme as used in STICS the top surface water content, particularly because of the daily time step that may not be fine enough to account for the sometime large diurnal variation. Additional investigation shows that the µ-wave data did not contribute much to the improvement of canopy functioning description (Figure 74). It is mainly governed by the information in the solar domain.

6. Evaluation - user component

The ReSeDA project was mainly and directly oriented towards methodological objectives. Therefore, it is not obvious to identify direct and classical end users. However, the application objectives pursued within the project were addressing the following issues:

- Agriculture policy
- landscape management
- precision farming
- hydrology
- global vegetation monitoring

Therefore, three main categories of users could be identified:

1. ***The scientific community*** who is looking for issues such as those addressed by ReSeDA, i.e.
   - Canopy and soil functioning;
   - Estimation of canopy characteristics from remote sensing observations;
   - Scaling issued;
   - Assimilation of data into process models;
   - synergy between different spectral domains;
   - exploitation of the directional variation of reflectance and brightness temperature
2. ***Remote sensing data providers*** such as space agencies and industrial companies. The key issues to be addressed are:
   - The definition of the optimal configuration of sensors;
   - The prototyping and evaluation of algorithm for the generation of biophysical products.
   - The synergy between sensors. One issue appears obvious: there will be in the coming years a range of sensors, and it is necessary to exploit in synergy these sensors to improve the accuracy of the information on soil and vegetation surfaces. This project contributes significantly to the development of strategies of remote sensing data ingestion by several sensors using the algorithms that were proposed.
3. ***"true" remote sensing users*** such as service companies, agriculture bodies, national or European governmental organisation dealing with agriculture and environment, as well as the global change community.

Although ReSeDA was not close to the community of end users, except the two first categories listed, the project has initiated a momentum for developing studies exploiting the data base or the algorithms developed. Here is a list of the main studies initiated by the ReSeDA project and sponsored by third parties, proving their interest in the project.

- ***VEGETATION***: part of the data base was used to evaluate algorithms dedicated to derive biophysical products from VEGETATION sensor. The

scaling problem was also investigated for this application.

- ***HIBISCUS,*** the future generation of global monitoring instrument planned by CNES. The directionality of observations and scaling issues are critical for this mission.
- ***VALERI***: a project aiming at evaluating the biophysical products of large swath satellites. Within VALERI, an issue is devoted to the development of algorithms, and to the scaling effects. It is therefore largely inspired by the methods developed within ReSeDA.
- ***precision-farming***: studies are on going with CNES, ASTRIUM, AVENTIS, SPOT image and SCOT on the definition of products for precision farming. Here again, ReSeDA has served as a baseline for the assimilation part of this project.
- ***CROMA***, a European project on methodological aspects for precision farming
- ***ADAM***, a project funded by CNES in collaboration with Romania and aiming at the exploitation of multi-temporal data for agriculture applications including precision farming.
- ***Synergy between SAR and LSPIM missions***, a study sponsored by ESA for supporting LSPIM and its following, with important outputs from ReSeDA on data assimilation which is the main way to ingest data coming from different sensors.
- ***WATERMED***, a European project dealing with hydrology and remote sensing.
- ***EC-MARS***: evaluation of the Crop Growth Monitoring System (CGMS) developed by JRC Ispra within the MARS project and its future.
- ***Météo-France*** who is looking for improving the surface scheme description for weather prediction models. The ISBA model from météo-France was therefore included in the series of SVAT models investigated, for comparison to others and improvements.

7. Exploitation plan

The exploitation opportunity is mainly driven by the definition of the sensor specification and the actual use of current satellites. This data set offers the unique opportunity to investigate concurrently

- The spatial scaling problem
- The synergy between observations obtained in different spectral domains
- The temporal revisit frequency
- The functioning of soils and canopies for environmental issues

Space agencies as well as space industry companies could be potentially (and have been) interested in exploiting this data base and the results obtained.

National or European governments could be also (and have been) potentially interested in developing tools for the monitoring of crops and the evaluation of the environment

The exploitation plan will first consists in writing articles corresponding to the material presented at the EGS in Nice in April 2000, for publication in international journals and presentation in conferences. In parallel, the investigation will be pursued, including further use of the data base, as well as validation and improvements of the results over independent data sets. This will be described hereafter according to the same hierarchy as previously. We should note that what is listed here are the potential investigation to be undertaken. From this initial list, some investigations are already undertaken, while some others will start depending on external funding or availability of researchers within the consortium, or outside, but in collaboration with the ReSeDA partners. Most of the investigations that are already started are listed in the Technology Implementation Plan.

7.1 Radiative transfer modelling and model inversion

7.1.1 Solar domain

- ***Experimental validation of theoretical results obtained on model inversion.*** The investigation conducted on model inversion was mainly based on reference model simulations. Some approaches have been validated (neural network, optimisation, vegetation indices), but a more complete validation is required, where the contribution of the spectral and directional information could be analysed. Further, the importance of the a priori information put in the system, derived by the knowledge of the species should be also evaluated from this experiment.
- ***Improvement of spectral integration for albedo estimates.*** The validation of albedo estimation from PODLER data shows that a bias affects the retrieved values. This was identified as a spectral integration problem. This could be quite easily corrected for by developing an improved set of spectral coefficients to extend the few POLDER bands hemispherical reflectance to the whole solar spectral domain.
- ***Non linearity, spatial heterogeneity and scaling.*** In case of non linear processes relating a given surface variable to radiances observed by remote sensing sensors over heterogeneous scenes, the values of a the variable will depend on the scale of observation. This has been demonstrated for *LAI* over the ReSeDA site for VEGETATION spatial resolution. However, It should be possible to limit the problem by inputting a simple estimation of the spatial heterogeneity. This issue will be partly investigated within the VALERI project.

7.1.2 Thermal infrared domain

- ***Modelling the directional distribution of the brightness temperature***. The First results obtained on the directionality of brightness temperature demonstrated the range of variation of the effects, and also the difficulty encountered due to the temporal variation during directional sampling. Investigation on the modelling of the directional distribution of brightness temperature could now be initiated. Presumably, the similitude with the general BRDF patterns invites to test the classical BRDF models used in the solar domain.
- ***Estimation of the component temperature from combined solar and thermal domains.*** The determination of the component temperature (i.e. soil, vegetation, eventually illuminated and shadowed fractions) could be very pertinent for SVAT modelling and emissivity-temperature decoupling. The potential of the combination of thermal and solar domains is very strong for these issues. The ReSeDA experiment offers a unique opportunity for their evaluation.

7.1.3 µ-wave domain

- ***Improved land use mapping by per field discrimination***. One of the main difficulty in exploiting µ-wave for land cover mapping, is the important scattering associated to the data. Filtering is therefore required, and results indicate that some filters are more efficient than others. However, for agriculture landscapes, the organisation of space into field units that are latter associated to a particular crop, should be exploited and will therefore lead to improved classification results because the scatter in the data will be smoothed out over the field.
- ***Evaluation of alternative inversion techniques.*** In the present work presented, the inversion techniques used are either based on empirical relationships, or on optimisation algorithms. However, very little a priori information is used, and the uncertainties in the data and the model are not accounted for. Therefore, additional investigation should be directed to implement advanced inversion techniques that could exploit concurrently several configurations as demonstrated in §5.3.3.3.3.
- ***Solving the soil roughness problem***. The effect on soil roughness on the estimation of moisture or canopy characteristics from the backscattering coefficient is difficult to account for and was identified as a main source of inaccuracies of inverse algorithms. Passive µ-wave could be a solution to the problem. However, on an operational basis, it is associated to low spatial resolution (more than 10 kilometres). The use of several incidence, polarisation or frequencies should be investigated to minimise the roughness effect. For this purpose, the work conducted on the IEM model and the effective correlation length has to be exploited to simply eliminate the roughness effect when using concurrently several configurations.
- ***Choice of canopy biophysical variables depending on canopy structure***. In the µ-wave domain, the backscattering coefficient is generally not a simple function of a given canopy characteristics such as *LAI* or water content. However, for a given canopy that follows a genetically determined structure dynamics, the strong covariance between several structure characteristics could lead to choose the pertinent canopy characteristics as a function of the development stage and species. We should note that this could be a problem for classical operational applications where a single well identified variable is to be used in decision making. The assimilation is therefore quite promising for exploiting the µ-wave radiometric information.

7.2 Assimilation into process models

7.2.1 SVAT models

Two ways of exploiting remote sensing data have been investigated:

7.2.1.1 Using the temporal variation

Only part of the work was achieved during the ReSeDA project life time. This was mainly explained by the important underestimation of the time required for data processing, inducing significant delay in the data delivery and thus processing. Therefore, the SVAT assimilation, based on the temporal variation was mostly concentrating on the evaluation, comparison and improvement of SVAT models. Assimilation into SVATs based on optical, µ-wave and thermal data is thus still to be completed. This is to be accomplished for a selection of models within the WATERMED European project, with comparison of results acquired over other sites.

7.2.1.2 Using the spatial variation.

Assimilation with the SEBAL algorithm leads to interesting results and possible ways of improvement. These improvements, particularly regarding the estimation of the roughness, as well as the better retrieval of some inputs such as albedo will be also implemented within the WATERMED project, with comparison to other sites. This will be also tested using the ASTER images that provides both solar and thermal infrared data at a relatively fine spatial resolution.

7.2.2 Canopy functioning model

Canopy functioning models will be mainly exploited for agriculture and environmental applications. The coupling scheme implemented for wheat crops will be evaluated under different conditions within the ADAM project funded by CNES and

taking place in Romania. It will focus on the exploitation of concurrent use of the three SPOT satellites to get high temporal repetitivity. ERS and Radarsat data will be also acquired during the same period. Intensive ground truth is organised in order to be able to evaluate and improve the assimilation scheme developed within ReSeDA. The protocols and experience gained within ReSeDA was highly exploited. This project will allow the definition of the optimal revisit frequency.

The combination of μ-wave and solar observations will be investigated within a study initiated by the European Space Agency to further the Land Surface Processes Mission. ReSeDA data base and developments will serve as the main basis for this study.

The work achieved over wheat will be extended over maize and sunflower canopies of the ReSeDA experiment. This will be part of the CROMA European project. This will be also used within the CHRIS-ALIDE (CHRIS Assimilation of Land Information Data Experiment) project for which the CHRIS imaging spectrometer aboard the PROBA platform will be launched next spring. The ReSeDA site will serve as the experimental field.

8. List of related publications & deliverables

8.1 Publications

Bacour, C., Jacquemoud, S., Leroy, M., Hautecoeur, O., Prévot, L., Weiss, M., Bruguier, N., and Chauki, H. 2000. Estimation of vegetation characteristics by inversion of three canopy reflectance models on airborne POLDER data. Physics and chemistry of the Earth v. submitted.

Baghdadi, N., King, C., Chanzy, A., and Wigneron, A. 2000. An empirical adaptation of the IEM model for retrieving surface parameters from SAR observations. Physics and chemistry of the Earth v. submitted.

Baret, F. 1998. ReSeDA: Assimilation of Multisensor & Multitemporal remote sensing data to monitor vegetation and soil functioning,. INRA, Avignon (France).

Baret, F. 1999. ReSeDA: Assimilation of Multisensor & Multitemporal remote sensing data to monitor vegetation and soil functioning,. INRA, Avignon (France).

Baret, F., Knyazikhin, J., Weiss, M., Myneni, R., and Pragnère, A. 1999. Overview of canopy biophysical variables retrieval techniques. In ALPS'99, Meribel (France).

Baret, F., Weiss, M., and Pragnère, A. 1999. Evaluation of model inversion techniques. Application to the retrieval of key biophysical variables.,. INRA/ESA, Avignon (France).

Baret, F., Weiss, M., Troufleau, D., Prévot, L., and Combal, B. 2000. Maximum information exploitation for canopy characterisation by remote sensing. In Remote sensing in agriculture, Vol. 60, pp. 71-82. Association of Appied Biologists.

Braud, I., Chanzy, A., F., B., Calvet, J. C., E., G.-s., C., K., Prevot, L., Olioso, A., Ottle, C., Taconet, O., Thony, J. L., and Wigneron, J. P. 1998. Assimilation of remote sensing data in SVAT models: description of the alpilles experiment and first results. In European Geophysical Society, XXIII General Assembly,, Nice 20-24April 1998.

Cantelaube, P., Baret, F., Biard, F., and Clastre, P. 1999. Provision of thematic studies on agrometeorological Crop Growth Modelling. Calibration of CGMS physiological crop coefficients, Rep. No. report for contract n° 14165-1998-07. INRA-GEOSYS-SAI, Avignon, France.

Chanzy, A., King, C., Prévot, L., Remond, A., Wigneron, J. P., Calcagna, P., Mehrez, Z., and Desprats, J. F. 1998. Comparison of ERS and multi-angle RADARSAT measurements on bare soils : first results of the ReSeDA experiment. In 2nd International Workshop on Retrieval of Bio- and Geo-Physical parameters from SAR Data for land Applications, Noordwijk (Netherland).

Clevers, J. G. P. W., Vonder, O. W., Jongschaap, R. E. E., Desprats, J. F., King, C., Prévot, L., and Bruguier, N. 2000. Monitoring wheat growth by calibrating a crop growth model using optical satellite data. Physics and chemistry of the Earth v. submitted.

Coll, C., Caselles, V., Rubio, E., Sospedra, E., and Valor, E. 1999. Temperature and emissivity inversion using DAIS and ground measurements. Application to the ReSeDA test site. In ALPS99 Symposium, Meribel (France).

Coll, Caselles, Rubio, Sospedra and Valor, 2000, Analysis of thermal infrared data from the Digital Airborne Imaging Spectrometer, Int. J. Remote Sensing. accepted

Coll, C., Caselles, V., Rubio, E., Valor, E., and Sospedra, F. 2000. Field emissivity measurements during the ReSeDa experiment. Physics and chemistry of the Earth v. submitted.

Coll, C., Caselles, V., Rubio, E., Valor, E., Sospedra, F., and Baret, F. 2000. Estimating temperature and emissivities from the DAIS instrument. Physics and chemistry of the Earth v. submitted.

Coll, C., Schmugge, T. J., and Hook, S. J. 1998. Atmospheric effects on the temperature emissivity separation algorithm. In International Symposium on Remote Sensing, SPIE-EUROPTO, Barcelona, Spain.

Demarty, J., Ottlé, C., Braud, I., Mangeney, A., and Frangi, J. P. 2000. Effect of aerodynamic conductances modelisation on SISPAT-RS simu-

lated surface fluxes. Physics and chemistry of the Earth v. submitted.

Desprats, J. F., Borne, F., Bégué, A., King, C., Prévot, L., Baghdadi, N., and Bourguignon, A. 2000. ERS and Radarsat images for land use classification at a regional scale : possibilities for future A-SAR configuratio. Physics and chemistry of the Earth v. submitted.

Francois, C., Ottlé, C., and Olioso, A. 2000. Correction of silicon sensors albedo measurements using a canopy radiative transfer model. Physics and chemistry of the Earth v. submitted.

François, C., Ottlé, C., and Taconnet, O. 1998. Coupling SVAT model with multispcetral radiative transfer models into the canopy. First results with the Alpilles experiment. In EGS XXIII general assembly, Nice (France).

Gu, X. F., Jacob, F., Hanocq, J. F., Prévot, L., Yu, T., Liu, Q. H., Tian, G. L., Li, X. W., and Strahler, A. H. 2000. Measuring and analysing of thermal infrared emission directionality over crop canopies with an airborne wide-angle thermal infrared camera. Physics and chemistry of the Earth v. submitted.

Hobbs, S., Courault, D., Olioso, A., Lagouarde, J. P., Kerr, Y., Mc Anneney, J., and Bonnefond, J. M. 2000. Surface layer profiles of micrometeorological variables as measured from unmanned aircraft. Physics and chemistry of the Earth v. submitted.

Jacob, F. 2000. Utilisation de la télédétection courtes longueurs d'onde et infrarouge thermique à haute résolution spatiale pour l'estimation des flux d'énergie à l'échelle de la parcelle agricole. PhD, Université de Toulouse III, Toulouse (France).

Jacob, F., Olioso, A., Gu, X. F., Leroy, M., Hautecoeur, O., and Hanocq, J. F. 2000. Mapping surface fluxes using visible, near infrared and thermal infrared data and the SEBAL algorithm. Physics and chemistry of the Earth v. submitted.

Jacob, F., Olioso, A., Weiss, M., Francois, C., Leroy, M., Hautecoeur, O., and Ottlé, C. 2000. Albedo estimation from Polder data. Physics and chemistry of the Earth v. submitted.

Jongschaap, R. E. E. 2000. Calibration and validation of ROTASK 1.5 simulation model on field data of the ReSeDA project in southern France with special reference to winter wheat.,. AB-DLO, Wageningen (NL).

Lagouarde, J. P., Jacob, F., Gu, X. F., Olioso, A., Bonnefond, J. M., Kerr, Y., Mc Anneney, J., and Irvine, M. 2000. Spatialisation of sensible heat flux over heterogeneous landscapes. Physics and chemistry of the Earth v. submitted.

Lagouarde J.P., Chehbouni A., Kerr Y.H., McAneney J., Bonnefond J.M. and Irvine M., 1999 : Use of the scintillation method for the evaluation of surface fluxes at regional scale. In ALPS'99, Meribel (France), 4p.

Lagouarde J.P., Bonnefond J.M., Kerr Y.H., McAneney J. and Irvine M., 2000 : Estimation of the sensible heat flux integrated over a two surface composite landscape by scintillometry. Boundary layer Meteorol. submitted.

Leroy, M., Hautecoeur, O., Berthelot, B., and Gu, X. F. 2000. The airborne Polder data during the ReSeDA experiment. Physics and chemistry of the Earth v. submitted.

Macelloni G., Paloscia S., Pampaloni P., Ruisi R. and Susini S., Monitoring crop biomass and soil moisture with airborne microwave radiometers Proc. Int. Geosci. Remote Sensing Symp. (IGARSS=99), Hamburg, vol IV, 1999, pp. 2327- 2329.

Macelloni G., Paloscia S., Pampaloni P., Ruisi R., Dechambre M., Valentin R., Chanzy A., Wigneron J.P., Passive and active microwave data for soils and crops characterization," Proc. Int. Geosci. Remote Sensing Symp. (IGARSS 2000), Honululu, vol, 2000, pp. 2522-2524

Macelloni G., Paloscia S., Pampaloni P., Marliani F., Gai M., "The relationship between the backscattering coefficient and the biomass of narrow and broad leaf crops," To be published in IEEE Trans. Geosci. Remote Sensing.

Macelloni G.., Paloscia S., Pampaloni P., Ruisi R., Susini C. and Wigneron J.P. - AAirborne passive microwave measurements on agricultural fields,@ in Microwave Radiometry and Remote Sensing of the Earth' s Surface - P. Pampaloni and S. Paloscia Eds., VSP Press, The Netherlands, 2000, pp. 59-70.

Macelloni, G., Paloscia, S., Pampaloni, P., Ruisi, R., Dechambre, M., Valentin, R., Chanzy, A., and Wigneron, J. P. 2000. Active and passive microwave for soil and crops chazracterization. Physics and chemistry of the Earth v. submitted.

Macelloni, G., Paloscia, S., Pampaloni, P., Susini, C., and Ruisi, R. 1998. Airborne micro-wave radiometer measurements on an agricultural site: the IROE-STAAARTE mission. In EGS XXIII general assembly, Nice.

Macelloni, G., Pampaloni, P., Paloscia, S., and Ruisi, R. 1998. Microwave Emission Features of Crops with Vertical Stems. IEEE Transaction on Geoscience and Remote Sensing v. Ge-36, 332-337.

Maceloni, G., Paloscia, S., Pampaloni, P., Ruisi, R., Dechambre, M., Valentin, R., Chanzy, A., Prévot, L., and Bruguier, N. 2000. Modelling radar backscatter from crops during the growth cycle. Physics and chemistry of the Earth v. submitted.

Marliani F., Paloscia S., Pampaloni P.and. Kong J. A, "A coherent scattering model for interpreting InSAR data from vegetation," Proc. Int. Geosci. Remote Sensing Symp. (IGARSS 2000), Honululu, vol, 2000, pp.911-913

Marliani F., Paloscia S. and Pampaloni P., "A coherent scattering model for canopy covered soils", Proceedings AP2000, Davos, Switzerland, April 2000

Mangeney, A., Demarty, J., Ottlé, C., and Braud, I. 2000. Influence of soil hydraulic properties on surface fluxes, temperature and humidity in the one dimensional SISPAT model. Physics and chemistry of the Earth v. submitted.

Moulin, S., Kergoat, L., Cayrol, P., Dedieu, G., Prévot, L., Bruguier, N., Desprats, J. F., and King, C. 2000. Using coupled canopy functioning and SVAT model in the ReSeDA experiment. Assimilation of SPOT/HRV observations into the model. Physics and chemistry of the Earth v. submitted.

Moulin, S., Kergoat, L., and Dedieu, G. 1999. Coupling of a vegetation model and a SVAT model in the RESEDA experiment. In ALPS'99, Méribel (France).

Olioso, A., Autret, H., Bethenot, O., Bonnefond, J. M., Braud, I., Calvet, J. C., Chanzy, A., Courault, D., Demarty, J., Ducros, Y., Gaudu, J. C., Gonzales-Sosa, E., Gouget, R., Jongschaap, R., Kerr, Y., Lagouarde, J. P., Laurent, J. P., Lewan, E., Marloie, O., Mc Anneney, J., Moulin, S., Ottlé, C., Prévot, L., Thony, J. L., Wigneron, J. P., and Zhao, W. 2000. Comparison of SVAT models over the Alpilles-ReSeDA experiment. I Description of the framework and the data. Physics and chemistry of the Earth v. submitted.

Olioso, A., Autret, H., Bethenot, O., Bonnefond, J. M., Braud, I., Calvet, J. C., Chanzy, A., Courault, D., Demarty, J., Ducros, Y., Gaudu, J. C., Gonzales-Sosa, E., Gouget, R., Jongschaap, R., Kerr, Y., Lagouarde, J. P., Laurent, J. P., Lewan, E., Marloie, O., Mc Anneney, J., Moulin, S., Ottlé, C., Prévot, L., Thony, J. L., Wigneron, J. P., and Zhao, W. 2000. Comparison of SVAT models over the Alpilles-ReSeDA experiment. II Models and Results. Physics and chemistry of the Earth v. submitted.

Olioso, A., Prévot, L., Baret, F., Chanzy, A., Autret, H., Baudin, F., Bessemoulin, P., Bethenod, O., Blavoux, B., Bonnefond, J. M., Boubkraoui, S., Bouman, B. A. M., Braud, I., Bruguier N.(1), C. J. C., Caselles V.(7), Chauki H.(1), Clevers J.G.P.W.(8), Coll C.(7), Company A.(9), Courault, D., Dedieu, G., Delécolle, R., Denis, H., Desprats, J. F., Ducros, Y., Dyer, D., Fies, J. C., Fischer, A., François, C., Gaudu, J. C., Gonzalez, E., Gouget, R., Gu, X. F., Guérif, M., Hanocq, J. F., Hautecoeur, O., Haverkamp, R., Hobbs, S., Jacob, F., Jeansoulin, R., Jongschaap, R. E. E., Kerr, Y., King, C., Laborie, P., Lagouarde, J. P., Laques, A. E., Larcena, D., Laurent, G., Laurent , J. P., Leroy, M., McAneney, J., Macelloni, G., Moulin, S., Noilhan, J., Ottle, C., Paloscia, S., Pampaloni, P., Podvin, T., Quaracino, F., Roujean, J. L., Rozier, C., Ruisi, R., Susini, C., Taconet, O., Tallet, N., Thony, J. L., Travi, Y., Van Leewen, H., Vauclin, M., Vidal-Madjar, D., Vonder, O. W., and Wigneron, J. P. 1998. Spatial Aspects in the Alpilles-ReSeDA Pro ject. In Intermational worshop: Scaling and modelling in forest. Interest of remote sensing and GIS, Montreal (Canada).

Paloscia S., Macelloni G. and Pampaloni P., 1998, A The relations between backscattering coefficient and biomass of narrow and wide leaf crops, Proc. Int. Geosci. Remote Sensing Symp. (IGARSS=98), Seattle, USA pp 100-102.

Paloscia S., Macelloni G., Pampaloni P. and Sigismondi S., @The potential of C- and L- band SAR in estimating vegetation biomass: the ERS-1 and JERS-1 experiments@, IEEE Trans Geosci Remote Sensing, Vol 37, N. 4, pp 2107-2110,1999

Prévot, L., Baret, F., Chanzy, A., Olioso, A., Wigneron, J. P., Autret, H., Baudin, F., Bessemoulin, P., Bethenod, O., Blamont, D., Blavoux, B., Bonnefond, J. M., Boubkraoui, S., Bouman, B. A. M., Braud, I., Bruguier, N., Calvet, J. C., Caselles, V., Chauki, H., Clevers, J. G. P. W., Coll, C., Company, A., Courault, D., Dedieu, G., Degenne, P., Delécolle, R., Denis, H., Desprats, J. F., Ducros, Y., Dyer, D., Fies, J. C., Fischer, A., François, C., Gaudu, J. C., Gonzalez, E., Goujet, R., Gu, X. F., Guérif, M., Hanocq, J. F., Hautecoeur, O., Haverkamp, R., Hobbs, S., Jacob, F., Jeansoulin, R., Jongschaap, R. E. E., Kerr, Y., King, C., Laborie, P., Lagouarde, J. P., Laques, A. E., Larcena, D., Laurent, G., Laurent, J. P., Leroy, M., McAneney, J., Macelloni, G., Moulin, S., Noilhan, J., Ottlé, C., Paloscia, S., Pampaloni, P., Podvin, T., Quaracino, F., Roujean, J. L., Rozier, C., Ruisi, R., Susini, C., Taconet, O., Tallet, N., Thony, J. L., Travi, Y., Van Leewen, H., Vauclin, M., Vidal-Madjar, D., Vonder, O. W., and Weiss, M. 1998. Assimilation of Multi-Sensor and Multi-Temporal Remote Sensing Data to Monitor Vegetation and Soil: the Alpilles-ReSeDA project. In IGARS'98, Seatle (WA, USA).

Prévot, L., Chauki, H., Rémond, A., King, C., Wigneron, J. P., Chanzy, A., Calcagno, P., and Desprats, J. F. 1998. Comparison of ERS and multi-angular RadarSat measurements over agricultural canopies: first resukts of the Alpilles ReSeDA campaign. In 2nd International Workshop on "Retrieval of Bio- and Geophysical Parameters from SAR Data for Land Applications". ESA Publications, Noordwijk (The Netherlands).

Prévot, L., Chauki, H., Troufleau, D., Weiss, M., and Baret, F. 2000. Assimilating optical and radar data into the STICS model for wheat crops : Preliminary results. Physics and chemistry of the Earth v. submitted.

Prévot, L., Chauki, H., Troufleau, D., Weiss, M., Baret, F., and Brisson, N. 2000. Coupling the STICS canopy functioning model to radiative transfer models for assimilating remote sensing data in the solar and micro-wave domains. Physics and chemistry of the Earth v. submitted.

Prévot, L., Wigneron, J. P., Chanzy, A., Baghdadi, N., King, C., and Dechambre, M. 2000. Monitoring wheat development from radar observations during the ReSeDA experiment. Physics and chemistry of the Earth v. submitted.

Paloscia, S., Macelloni, G., Pampaloni, P., and Sigismondi, S. 1999. The potential of C- and L-band SAR in estimating vegetation biomass: the ERS-1 and JERS-1 experiments. IEEE Transaction on Geoscience and Remote Sensing v. accepted for publication.

Schouten, L., van Leeuwen, H., Desprats, J. F., King, C., Baghdadi, N., Prévot, L., Dechambre, M., and Valentin, R. 2000. Land use classification based on time series of microwave data. Physics and chemistry of the Earth v. submitted.

van Leeuwen, H., Scouten, L., Jongschaap, R., and King, C. 2000. Predicting wheat production at the regional scale by the assimilation of remote sensing data with the crop growth simulation model ROTASK v1.5. Physics and chemistry of the Earth v. submitted.

Vonder, O., Clevers, J., Desprats, J. F., King, C., Prévot, L., and Bruguier, N. 2000. Estimation of biophysical variables using multiple view angles. Physics and chemistry of the Earth v. submitted.

Weiss, M. 1998. Développement d'un algorithme de suivi dela végétation à large échelle. PhD thesis, Ecole des Mines de Paris, Avignon.

Weiss, M., Baret , F., Leroy, M., Hautecoeur, O., Prévot, L., and Bruguier, N. 2000. Validation of neural net techniques to estimate canopy biophysical variables. Physics and chemistry of the Earth v. submitted.

Weiss, M., and Baret, F. 1998. What canopy biophysical variables can be estimated from large swath satellite data. In EGS XXIII general assembly, Nice.

Weiss, M., and Baret, F. 2000. Evaluation of canopy biophysical variables retrieval performances from the accumulation of large swath satellite data. Remote Sensing of Environment v. in press.

Weiss, M., Baret, F., Leroy, M., Begué, A., Hautecoeur, O., and Santer, R. 1999. Hemispherical reflectance and albedo estimates from the accumulation of across track sun synchroneous satellite data. Journal of Geophysical Research v. 104, 22,221-22,232.

Weiss, M., Baret, F., Leroy, M., Hautecoeur, O., Prévot, L., and Bruguier, N. 2000. Validation of neural network techniques for the estimation of canopy biophysical variables from VEGETATION data. In VEGETATION preparatory programme. Final meeting. G. Saint, Belgirate (Italy).

Weiss, M., Baret, F., Myneni, R., Pragnère, A., and Knyazikhin, Y. 2000. Investigation of a model inversion technique for the estimation of crop charcteristics from spectral and directional reflectance data. Agronomie v. 20, 3-22.

Weiss, M., Jacob, F., Baret, F., Pragnère, A., Leroy, M., Hautecoeur, O., Prévot, L., and Bruguier, N. 2000. Evaluation of BRDF models on POLDER data. Physics and chemistry of the Earth v. submitted.

Weiss, M., Troufleau, D., Baret, F., Chauki, H., Prévot, L., Olioso, A., Bruguier, N., and Brisson, N. 2001. Coupling canopy functioning and canopy radiative transfer models for remote sensing data assimilation. The case of wheat. Agricultural and Forest Meteorology v. submitted.

Wigneron, J. P., Prévot, L., Chanzy, A., Baghdadi, N., and King, C. 2000. Monitoring summer crop development from radar observations during the ReSeDA experiment. Physics and chemistry of the Earth v. submitted.

Zhao, W., Olioso, A., Lagouarde, J. P., Kerr, Y., Mc Anneney, J., Bonnefond, J. M., Bethenod, O., and Gouget, R. 2000. Estimation of aerodynamic parameters from energy balance modelling and measurements. Physics and chemistry of the Earth v. submitted.

8.2 Deliverables

The main deliverables consist in

- the intermediate reports that are listed within the publications,
- the technology implementation plan
- The core report
- The articles presented during the EGS and that will be published in a special issue of Physics and Chemistry of the Earth
- The other articles already published or in the review process.
- the data base itself that is accessible by the web server: www.avignon.inra.fr/reseda

9. Conclusion

The ReSeDA project was a collaborative effort of 10 partners aiming at the development and evaluation of remote sensing data assimilation into process models. The project was also supported by the French Programme National de Télédétection Spatiale, and the Programme National de Recherche en Hydrologie .

The project was based on the ***development of an extensive experiment where the spectral, directional, temporal and spatial dimensions have been sampled***. It is therefore a very unique effort where the radiometric signal was monitored over a 5*5km² area, along the growth cycle using sensors observing under different directions and covering the whole spectral domain, from the with solar, thermal infrared up to the µ-wave. Ground measurements have been concurrently acquired to characterise the growth, energy and mass exchanges between the soil, the vegetation and the atmosphere.

A hierarchic ***data base*** was generated to make the observations available to the whole scientific community. It is under the form of a web server (www.avignon.inra.fr/reseda) containing the data files along the necessary documentation files. The generation of the data base captured significantly more effort than expected, particularly for the processing of the airborne sensors that all were prototype sensors. This resulted in delays in the delivery of calibrated and validated data. Nevertheless, this data base constitutes now a unique source of concurrent ground and remote sensing observations over the growth cycle of crops such as wheat, sunflower and maize.

Canopy biophysical variable estimation from remote sensing data was the preliminary step investigated before tackling assimilation. Intensive efforts have been put on this issue, leading to significant advances in the improvement of radiative transfer models and the development of model inversion techniques. The identification of the main biophysical variables accessible directly from remote sensing data is now quite clear. It includes albedo, *LAI*, *fCover*, *fAPAR*, leaf chlorophyll and water content for the solar domain, temperature and emissivity for the thermal infrared, *LAI* or canopy water content for the µ-wave. For the soil, emphasis was put on surface soil moisture in the µ-wave domain. Results show that

In the solar domain, quite accurate estimates of albedo, *LAI, fCover and fAPAR* could be retrieved from the spectral and directional variation of the signal. Because of the lack of sensor sampling sufficiently the spectral dimension, no attempt was directed to the estimation of chlorophyll or water content. For the same reason, atmospheric correction were applied based on atmospheric characteristics measured from the ground level. This issue needs further effort to be investigated and would constitute a major step in remote sensing data exploitation.

In the thermal infrared red domain, the main emphasis was put on the directional variation of the signal that was presenting a significant range of variation. However, the observation of the directional variation could not be instantaneous, and the temporal and directional effects have to be sorted out. However further work is needed for the exploitation of this directional variation of the temperature, to extract the component temperature that is required for more accurate energy balance estimation. This could be probably improved by concurrent use of the directional variation in the solar domain that will provide estimates of the fraction of soil and vegetation cover, with possible decomposition into the illuminated and shadowed parts. The spectral variation provided by the DAIS sensor was exploited to extract the emissivity. However the poor calibration and stability of the sensor limited the conclusions. Further attempts of emissivity estimation should be conducted with the ASTER sensor that is now on orbit.

In the µ-wave domain, classification using ERS and Radarsat images along the growth season provided fair results if the speckle effect is minimised with a Gamma map filter. However, for a single date, the potential of the combination of active and passive µ-waves was clearly demonstrated although the spatial resolution of passive µ-wave sensors aboard satellite will probably constitute a severe limitation to the application of this principle. For the estimation of canopy and soil characteristics, one of the main problem identified was the confounding effect of soil roughness. Several attempts were developed to solve this problem that shows possible solutions, both by a better modelling and by the use of multiple configurations. The passive µ-wave, by its little sensitivity to soil roughness could be a solution for low spatial resolution applications. Physical and semi-empirical backscattering models were tested and showed good performances in the inversion mode. The use of simultaneous observations in two different configurations appears mandatory. Optimal configurations were discussed based on this data set for wheat crops. However, because of the large sensitivity of µ-waves to canopy structure, these results should be evaluated over other crops. This could be a following study based on ReSeDA data base for sunflower and maize crops. However, one key issue still pending and that may be has no definite answer outside the assimilation approach, is the choice of the canopy biophysical variable to be retrieved.

The ***scaling issue*** was investigated. It shows that estimates of biophysical variables such as *LAI* could be seriously affected in case of heterogeneous landscapes. Flux variables such as albedo, fCover or fAPAR, because of their linear relationship with radiometric data, are very little sensitive to hetero-

geneity, thus to scaling. These issues have to be investigated for µ-wave domain, although strong effects are expected because of the non linear and highly variable effect of canopy structure, at least for the lower frequencies.

Investigation about the model inversion problem shows that techniques based on minimisation over the biophysical variables (neural nets, vegetation indices, …) appear performing better than those based on the minimisation over the radiometric signal (Look up tables, optimisation). However, this should be confirmed in the case of larger number of variables to be retrieved simultaneously, with due attention to the computer resources required for operational applications. The minimisation over biophysical variables techniques have also to be tested in the µ-wave domain. However, the, main factor to pay attention at is the ***amount of information*** actually used in the inverse problem. Therefore, better radiative transfer models that describe more accurately the physical processes, and overall the canopy architecture and optical or dielectric properties of the elements are required. Some advanced modelling have been proposed, mainly in the µ-wave domain. Additionally, a priori information on canopy variables and uncertainties both on measurements, models and variables and parameters have to be included in the inverse process. Ways to include this information in the range of inverse techniques have therefore to be developed.

Nevertheless, inverting radiative transfer models to retrieve canopy biophysical variables is sometimes a strong limitation in remote sensing data exploitation. As a matter of fact, some variables that are accessible by remote sensing observations could not be used directly for applications, because they are not directly involved in the processes of interest. This is the case of the canopy and leaf water content. The only way to get rid of this main limitation, is to assimilate directly remote sensing data into coupled radiative transfer and process models.

Assimilation of remote sensing data into process models was therefore the main objective of the ReSeDA project. Assimilation presents several advantages over radiative transfer model inversion that could be resumed hereafter:

Assimilation allows:

- to exploit our knowledge on the physical and physiological processes;
- to exploit remote sensing data provided by different sensors in a range of spectral domains;
- to exploit the multi-temporal information;
- to exploit ancillary information such as climate and soil variables;
- to get a more detailed description of canopy architecture and leaf properties that are derived from the dynamic canopy functioning and SVAT models;
- to retrieve higher level canopy and soil characteristics such as carbon (biomass), water, energy and nitrogen fluxes;

Assimilation is obviously based on process models and these process models have to be robust and accurate. The first task of the assimilation part was to focus on the ***evaluation and coupling of process models with radiative transfer models***. It shows that complex ***SVAT models*** such as SISPAT was not very robust when applied to the validation sites, while it performed the best on the calibration sites. Further, the required detailed description of soil characteristics might be too difficult to implement on an operational basis. More simple models such as MAGRET and ISBA were generally more robust and therefore performed better. They should be preferred for use in the assimilation process. However, one difficulty that has still to be solved in the coupling between SVAT models and radiative transfer models is the simulation of the surface temperature as a function of canopy structure and the aerodynamic temperature. The use of directional observations of surface temperature might help solving this problem, by providing access to the component temperature. The ***mapping of energy and water fluxes*** was investigated using the SEBAL algorithm. It shows that it provides a first approximation of evapotranspiration rates. However, improvements are foreseen by using the a better parameterisation of the aerodynamic resistance. Nevertheless it demonstrated that large variation between fields, and even within fields are observed. This heterogeneity of fluxes was highlighted by the use of scintillometer measurements as well as the 3D description of air temperature and humidity thanks to the unmanned plane.

A range of ***canopy functioning models*** were calibrated and evaluated over wheat crops. Canopy functioning models were adapted to provide a detailed description of canopy structure used for improving the accuracy of radiative transfer models. A sensitivity analysis allowed to select the variables to adjust during the assimilation process. The variables governing phenology, *LAI* dynamics, and top soil characteristics were the most important ones. Concurrent assimilation of solar (Polder) and µ-wave (ERS and Radarsat) data appears to improve significantly estimates of biomass production, but marginally the water balance. Closer inspection shows that the main limitation is the capacity of daily time step models to accurately model processes that may have significant diurnal variation such as top layer surface moisture. This also explains the marginal contribution of µ-wave data to the improvement of canopy functioning model simulations. A simpler version of assimilation scheme of ERS data was applied at the regional scale based on MARS project segments. It clearly shows the feasibility of the assimilation process at this scale, although results were not very conclusive in terms of yield estimation improvement.

The ReSeDA project demonstrated that the ***assimilation of remote sensing data was possible both at the field and regional scales***. It showed some limits of the models and indicated ways of improvement. This is certainly one of the main advances of this project, right in line with its main objectives. However, a lot of work is still to be accomplished, both at the extension of the technique to other crops, but also in the refinement and improvements of the process models and their coupling with radiative transfer models. This could be partly achieved over the large and unique data set acquired within this project. However, this has also to be investigated under different conditions. Projects have already started from the momentum initiated by ReSeDA (CROMA, WATERMED, ADAM, CHRIS-ALIDE, …). They aim both at a better exploitation of actual remote sensing data, but also at the preparation of the next generation of sensors, with improved capability in terms of spectral, spatial, temporal and directional sampling. The methodological component is still very important, showing that the developments are not yet enough mature to be exploited directly into operational applications. However, the distance to this application goal decreases significantly, and the user community starts to be highly interested by these techniques and shows it by significantly contributing to the funding of such projects.